ISBN 978-90-393-5000-3

**Cover:** Superposition of the X-ray structure (green) of rEDN with the structures of the conformers with *C*-linked mannose (pink) and without (blue) obtained after 200 ps of dynamics simulations.

# Investigations of prebiotics and of inter- and intra-molecular glycan-protein interactions

## Onderzoek aan prebiotica en inter- en intra-moleculaire glycaan-eiwit interacties

(met een samenvatting in het Nederlands en Italiaans)

**Proefschrift**

ter verkrijging van de graad van doctor aan de Universiteit Utrecht
op gezag van de rector magnificus, prof.dr. J.C. Stoof,
ingevolge het besluit van het college voor promoties in het openbaar te verdedigen
op 16 februari 2009 des middags te 2.30 uur

door

**Daniela Beccati**
geboren op 5 november 1971 te Milaan (Italië)

Promotoren: Prof.dr. J.F.G. Vliegenthart
Prof.dr. J.P. Kamerling

Het onderzoek beschreven in dit proefschrift werd mogelijk gemaakt met financiële steun van de Europesche Unie (EU project "Novel food additives and bioactive components from milk for innovative engineering" (NOFA) Contract Fair CT 97-3142; EC Marie Curie Training Site Grant HPMT-CT-2000-00045; CARENET 2 European network HPRN-CT-2000-000001)

## List of Contents

**List of Abbreviations**

2AB, 2-aminobenzamide
Arg, arginine
Asp, aspartic acid
ConA, Concanavalin A
COSY, correlation spectroscopy
CVFF, consistent valence force field
DFLNH, difucosyllacto-*N*-hexaose
DFLNH I, difucosyllacto-*N*-hexaose I
DFLNH b, difucosyllacto-*N*-hexaose b
DHB, 2,5-dihydroxybenzoic acid
DolP-Man, dolichol phosphate mannose
DSLNT, disialyllacto-*N*-tetraose
*E. coli*, *Escherichia coli*
EDN, eosinophil-derived neurotoxin
2'FL, 2'-fucosyllactose
3'FL, 3'-fucosyllactose
FSLNnH, monofucosylmonosialyllacto-*N*-neohexaose
Fuc, fucose
Gal, galactose
GDP-Man, GlcNAc-PP-dolichol mannosyltransferase
Glc, glucose
GLC-EI/MS, gas-liquid chromatography electron impact mass spectrometry
Hex, hexose
HMBC, heteronuclear multiple bond correlation
HPAEC-PAD, high-pH anion-exchange chromatography with pulsed amperometric detection
HPLC, high-performance liquid chromatography
HSQC, heteronuclear single quantum coherence spectroscopy
Ile, isoleucine
LNDFH II, lacto-*N*-difucohexaose
LNFP I, lacto-*N*-fucopentaose I

LNFP II, lacto-*N*-fucopentaose II

LNH, lacto-*N*-hexaose

LNnH, lacto-*N*-neohexaose

LNnT, lacto-*N*-neotetraose

LNT, lacto-*N*-tetraose

LSTa, sialyllacto-*N*-tetraose a

LSTc, sialyllacto-*N*-tetraose c

MALDI-TOF-MS, matrix-assisted laser desorption/ionization time-of-flight mass spectrometry

MBL-C, mannan-binding lectin C

MD, molecular dynamic

Met, methionine

MFLNH II, monofucosyllacto-*N*-hexaose II

MLEV, Malcolm Levitt's CPD sequence

NCN-R, $[C_6H_2(CH_2NMe_2)_2$-2,6-R-4$]^-$

Neu5Ac, *N*-acetylneuraminic acid

Neu5Gc, *N*-glycolylneuraminic acid.

NOE, nuclear Overhauser effect

NOESY, nuclear Overhauser effect spectroscopy

NMR, nuclear magnetic resonance

PFG, pulsed field gradient

Pro, proline

$RCA_{120}$, *Ricinus communis* agglutinin

RI, refractive index

RNA, ribonucleic acid

RNase 2, non-secretory ribonuclease 2

ROESY, rotating frame nuclear Overhauser enhancement spectroscopy

RU, response units

3'SL, 3'-sialyllactose

6'SL, 6'-sialyllactose

SPC, simple point charge

SPR, surface plasmon resonance

TBTU, *O*-benzotriazol-1-yl-*N*,*N*,*N*′,*N*′-tetramethyluronium tetrafluoroborate

TFLNH, trifucosyllacto-*N*-hexaose

Thr, threonine

TLC, thin layer chromatography

TOCSY, total correlation spectroscopy

TPPI, time-proportional phase incrementation

Trp, tryptophan

TSR, thrombospondin

Tyr, tyrosine

Val, valine

VLC, vacuum line column chromatography

WEFT, water eliminated Fourier transform

# 1

# Introduction

## Probiotics and prebiotics

The intestinal microbiota plays a crucial role in our health and well-being[1], and its activity extends beyond the intestine. Altered gut microflora has been associated with diseases such as rotavirus diarrhea[2], rheumatoid arthritis[3], allergic diseases[4], and possibly autism[5]. Probiotics, and more recently prebiotics, have been investigated in an attempt to modify in a favourable way the intestinal microflora. After preliminary definitions of the term probiotic by Lilly and Stilwell[6] (any substance or organism that contributes to the intestinal microbial balance) and Fuller[7] (a live microbial feed supplement), a recent, formal definition of probiotics was given by a working party of European scientists as 'a live microbial supplement that is beneficial to health'[8]. Prebiotics were instead defined as "a non-digestible food ingredient that beneficially affects the host by selectively stimulating the growth and/or activity of one or a limited number of bacteria in the colon, and thus improve host health"[9].

Little is known about the actual interactions that take place in the intestinal tract, but probiotics are believed to be able to compete with intestinal microbes and counter act some immunological disturbances[10,11], whereas prebiotics are believed to affect intestinal bacteria directly, since host cells cannot utilize prebiotic compounds.

## The gastrointestinal microbiota

The intestinal microbiota of humans is thought to be composed of more than 1000 different species, with the vast majority being obligatory anaerobic[12]. The stomach and the first two-thirds of the small bowel contain only relatively small amounts of microbes, but the population density and diversity increases from the proximal small intestine ($10^3$ microbes per milliliter of luminal contents) to the colon[13]. The large numbers of bacteria reside in the distal gut (ileum and colon), with densities of around $10^{11}$ microbes per gram of luminal contents. This vast collection of microbial species is acquired soon after birth and persists basically unmodified throughout life. The gastrointestinal tract of newborn is sterile, but it is rapidly colonized by bacteria[14,15] transmitted by the mother or by the surroundings. After well-adapted members of the microbiota have occupied all the niches of the gastrointestinal tract[16], the gut becomes resistant to further colonization[17,18]. During adulthood, perturbations of the gastrointestinal microflora are rare and mainly associated

with pathological conditions such as infections, antibiotics therapy, or immune suppression.

Principal sources of carbon and energy for the large bowel microbiota are simple sugars that have escaped digestion in the small bowel, and complex carbohydrates, which remain abundant in the distal part of the gastrointestinal tract. For this reason, bacteria such as *Bifidobacterium longum* or *B. thetaiotaomicron* that contain numerous genes involved in polysaccharide degradation, are better suited to survive in the lower compartments of the gastrointestinal tract. Besides contributing to the digestion of exogenous and endogenous substrates, such as fibers, mucins, sloughed epithelial cells, complex carbohydrates, proteins, and fats, that have escaped digestion in the small bowel, the intestinal microbiota provides a protective barrier against incoming potential pathogens. This colonization resistance is exerted through production of antimicrobial substances and competition for nutrients and binding sites[19]. The normal microbiota has considerable influence on host biochemistry, physiology, immunology, and low-level resistance to gut infections[20,21].

The indigenous bacteria can be classified as pathogenic, neutral, or health promoting. Probiotic activity has traditionally been associated with bifidobacteria and lactobacilli, but *Streptococcus*, *Enterococcus*, and non-pathogenic *E. coli* species, as well as *Saccharomyces boulardii* have also been shown to inhibit growth, metabolic activity and adhesion of enteropathogenic bacteria such as *Salmonella* and *Shigella*[22].

**Lactic acid bacteria**

Lactic acid bacteria (LAB) are gram-positive nonpathogenic bacteria capable of producing lactic acid as the main end-product of the fermentation of carbohydrates. *Streptococcus thermophilus* and *Lactococcus lactis* are among the most, commercially important lactic acid bacteria. In association with *Lactobacillus delbrueckii* subsp. *bulgaricus*, *Streptococcus thermophilus* is used as a starter culture for the production of yoghurts. Attribution of beneficial properties, such as alleviation of symptoms of lactose intolerance and other gastrointestinal disorders, to those two bacteria can be traced back to the pioneer of probiotics, Ilya Ilyich Metchnikoff (1907), as published in his book *The Prolongation of Life*. At present, in addition to yoghurt production, *S. thermophilus* is used in formulations together with bifidobacteria and other lactic acid bacteria (e.g.

*Lactobacillus casei*, *L. johnsonii*, *L. plantarum*, *L. rhamnosus*, *L. reuteri*) with positive results for prevention of diarrhea and shedding of rotavirus.[23]

*Lactobacillus* and *Bifidobacterium* also belong to the lactic acid bacteria. Lactobacilli are present in food (dairy products, fermented meat, sour dough, vegetables, fruit, beverages), in sewage and plant material, in respiratory systems and genital tracts of humans and animals, and throughout the gastrointestinal tract of humans. Bifidobacteria occur in animal and human habitats: in particular, they have been isolated from faeces, rumen of cattle, sewage, human vagina, dental caries, and honey bee intestine. Bifidobacteria strains that exhibit probiotic properties belong to the species *Bifidobacterium adolescentis*, *B. animalis*, *B. bifidum*, *B. breve*, *B. infantis*, and *B. longum.*

**Functionality of the gastrointestinal microflora**

Understanding of the features and functions of the intestinal microflora is a challenging task, since the majority of the gastrointestinal tract locations are inaccessible for sampling. Moreover, the majority of gastrointestinal tract microbes cannot be grown in culture[24]. A reason can be the necessity for strictly anoxic conditions, but also unknown growth requirements, the exposure to stress during the cultivation procedures, and eventually the need for specific interactions with other microbes and/or host cells[25]. In the past, the evaluation of gastrointestinal activity was based on analysis of faecal samples, but nowadays it is accepted that this sampling technique does not account for all parts of the gastrointestinal tract, since different niches within single individuals (faeces, GI tract location, lumen, mucosa) host different bacterial populations[26,27] including the colon[28,29]. The application of culture-independent approaches like the 16S rRNA method has provided novel insight into the gut ecology[30]. The features of predominant gastrointestinal tract bacterial communities seem to be host specific[31,32] and affected by the host genotype[33]. The microbiota is stable in healthy individuals[34], but unstable in individuals suffering from gastrointestinal tract disorders[35], and it changes during ageing of the host[36-38]. It is affected by antibiotics and certain diets[39-45], but not permanently altered by the consumption of pre- and/or probiotics.

**Probiotics**

The concept of probiotics dates back to the beginning of the past century when Metchnikoff[46] presumed that the bacterial community residing in the large bowel of humans was a source of substances, toxic to the nervous and vascular system of the host. He believed that administration of cultures of fermentative bacteria would 'implant' these 'beneficial' bacteria in the intestinal tract, and replace or diminish the number of putrefactive microbes that contribute to intoxication of the body and the ageing process. Lactic acid-producing bacteria were favored as fermentative bacteria to use for this purpose, since it had been observed that the natural fermentation of milk by these microbes prevented the growth of acid-intolerant bacteria, including proteolytic species. Moreover, Metchnikoff believed the longevity of Bulgarian peasants to be related to their elevated intake of 'soured milks', *i.e.* dairy-based drinks containing live bacteria.

Probiotic strains must have the following characteristics[47]: they should be normal inhabitants of the intestinal tract of human origin, since some health-promoting effects may be species specific; they should express high tolerance to acid of the stomach, digestive enzymes, and bile; they should survive and be metabolically active within the luminal flora; they must be safe for humans; they should maintain their viability and beneficial properties through processing, culture and storage[48]; they should be antagonists of pathogenic bacteria.

Much effort has been devoted to screen and characterize bacteria in order to identify a 'universal colonizer', which was supposed to survive passage through the stomach and small intestine and should colonize the intestinal tract of all consumers for a reasonable time. Nevertheless, several studies demonstrated conclusively that ingested strains do not become established members of the normal microbiota, but persist only during periods of dosing or for relatively short periods thereafter[49-52]. There is also evidence that common probiotic strains differ in their degree of persistence[53]. Theoretically, owing to the lack of a stable microbiota, probiotic treatment of infants should result in a more permanent colonization of the neonate gut and in a more pronounced effect on other bacteria[54]. Moreover, the passage of allochthonous lactobacilli through the human gut might constitute a stimulus for the immune system, especially in the early stages of life.

**Biological activities of probiotics**

***Colonization resistance***

One of the mechanisms of action of probiotics includes colonization resistance to the growth of pathogenic bacteria such as *Listeria monocytogenes*, *Escherichia coli,* and *Salmonella*[55-58]. This inhibition is due to various mechanisms. Besides the production of antimicrobial compounds such as organic acids, hydrogen peroxide, bacteriocin or reuterin[59-61], the competition for nutrients and for adhesion to intestinal surfaces plays an important role[62]. *Lactobacillus plantarum* 299v has been shown to enhance intestinal mucin gene expression to inhibit the adherence of enteropathogenic *E. coli* to HT-29 cells[63]. Moreover, lactobacilli in the small intestine of newborn piglets create an acid intestinal environment that is inhibitory to *Escherichia coli* and *Vibrio cholerae* enterotoxin production, contributing to a 'protective' effect.

***Stimulation of the immune system***

The intestine is the body's largest immune organ. Most of the antibody-producing cells reside in the intestine[64]. A recently recognized function of the intestinal microbiota is to provide stimulation of the immune system through immune cell proliferation, enhanced phagocytic activity, and increased production of secretory IgA. Malin *et al*[65] demonstrated that oral administration of *Lactobacillus* GG has the potential to increase the gut IgA immune response and to promote the intestinal immunological barrier in children with Crohn's disease.

In 1981, Yokokura[66] screened 26 strains of 14 species of lactic acid bacteria for *in vivo* antitumor activity against sarcoma 180, a transplantable mice tumor, and found that some had potent antitumor activity. Among them, especially *Lactobacillus casei* strain *Shirota* (LcS) showed a high potency. LcS has also been shown to prevent the recurrence of superficial bladder cancer in humans[67], and to have immunomodulatory effects in animal models[68]. Because this strain is not directly cytotoxic to tumor cells *in vitro*, it has been postulated that its antitumor action may be mediated by augmentation of the host's immune system. Oral feeding of LcS to 3-methylcholanthrene-treated mice rendered their natural killer (NK) cells tumoricidal in terms of both quality and quantity, resulting in suppression of tumor incidence[69]. To investigate the mechanism underlying the antitumor effect of LcS, Takeda *et al*[70] examined the effects of drinking fermented milk containing

LcS on the immune system of healthy individuals, especially the effects on the NK-cell activity of peripheral blood mononuclear cells. They demonstrated that NK activity significantly increased 3 weeks after the start of intake, and elevated NK cell activity remained for the next 3 weeks. This effect was particularly prominent in the low-NK-activity individuals, suggesting that daily intake of *Lactobacillus casei* strain *Shirota* can augment NK-cell activity.

Another study, aimed at elucidating whether consuming fermented milk containing lactic acid bacteria could induce changes in the intestinal flora and modulate the immune response in man, was undertaken by Link-Amster *et al*[71]. To this end, volunteers consumed fermented milk containing *L. acidophilus* La1 and bifidobacteria over a period of three weeks. During that period of time an attenuated *Salmonella typhi* Ty21a strain was administered to mimic an enteropathogenic infection. The specific serum IgA titre-rise to *S. typhi* Ty21a in the test group was more than 4-fold, and significantly higher than in the control group. An increase in total serum IgA was also observed. These results indicate that lactic acid bacteria, which can persist in the gastrointestinal tract, can act as adjuvant to the humoral immune response.

***Antiallergic effects***

The lower exposure of neonate and infants to intestinal microbial challenge in the last decades, as indicated by epidemiological data, has been associated with higher incidence of allergic disease[72,73]. Allergic infants have been observed to have an aberrant intestinal microbiota, *i.e*. they have higher levels of Clostridia and lower levels of Bifidobacteria[74]. Probiotics may provide a safe alternative to the microbial stimulation needed for the developing immune system in infants.

In newborns, the immune system is directed toward T-helper 2 (Th2) cells. The Th2 phenotype leads to the stimulated production of IgE by B-cells, and therefore increases the risk of allergic reactions through activation of mast cells. Microbial stimulation in early life will reverse the Th2 bias and stimulate the development of a Th1 phenotype[75,76], and increase the activity of Th3 cells[77]. Their combined action will lead to the production of IgA by B-cells. IgA contributes to allergen exclusion, and will thereby reduce exposure of the immune system to antigens.

Cytokines produced by the Th1 phenotype will also reduce inflammation, and stimulate tolerance towards common antigens[78]. The Bifidobacteria isolated from infants

with atopic dermatitis were found to induce a higher secretion of proinflammatory cytokines *in vitro*, whereas the Bifidobacteria from healthy infants induced the secretion of more anti-inflammatory cytokines[79]. Bifidobacteria of dairy origin stimulated more anti-inflammatory and less inflammatory cytokines than Bifidobacteria from allergic infants. Moreover, Bifidobacteria from allergic and healthy infants exhibited different *in vitro* adhesion to Caco-2 tissue culture cells[80].

Recent studies suggest that oral bacteriotherapy with probiotics might be useful in the treatment of atopic dermatitis (AD). Majamaa *et al*[81] evaluated the clinical and immunologic effects of replacing cow's milk by an extensively hydrolyzed whey formula, with or without the addition of a human intestinal floral *Lactobacillus* GG strain, in infants with atopic eczema and cow's milk allergy. The clinical score of atopic dermatitis improved significantly during the 1-month study period in infants treated with the extensively hydrolyzed whey formula fortified with *Lactobacillus* GG. Results suggested that probiotic bacteria promote local antigen-specific immune responses (particularly in the IgA class), prevent permeability defects, promote endogenous barrier mechanisms in patients with atopic dermatitis and food allergy. A study by Isolauri *et al*[82] demonstrated that infants administered with *Bifidobacterium lactis* Bb 12 and *Lactobacillus* strain GG not only presented diminished symptoms of atopic eczema, but also showed alleviation of allergic inflammation. Reduction of sCD4 and TGF-β1 levels in serum and of EPX in urine, respectively, associated with chronic inflammation[83], mucosal allergic inflammation[84], and childhood asthma[85], indicated that probiotics may counteract inflammatory responses beyond the intestinal milieu.

Contradictory results have recently been published by Brouwer *et al*[86], who supplemented infants with AD less than 5 months old with a hydrolyzed whey-based formula as placebo, or supplemented them with either *Lactobacillus rhamnosus* or *Lactobacillus* GG for 3 months. They found no clinical or immunological effects of the probiotic bacteria used in infants with AD, indicating that oral supplementation with these probiotic bacterial strains will not have a significant impact on the symptoms of infantile AD.

***Inflammatory bowel disease***

The gut mucosa has two major roles: it allows the passage of nutrients and protects against infectious agents. The gut lymphoid system differs from that of other tissues in

that it predominantly produces IgA antibodies. Substances introduced orally are usually ignored by the immune system, a phenomenon known as "oral-tolerance". A normal healthy gut microflora is necessary to induce oral tolerance and to protect the host against allergic sensitization[87]. In intestinal inflammation, the integrity of the mucosal barrier is disrupted and antigens are able to trespass it. Chronic intestinal inflammation, such as in Crohn's disease, is caused by an excessive immune response to mucosal antigens and elements of the normal bacterial microflora[88]. A possible aid is local delivery of specific bacteria engineered to produce anti-inflammatory cytokines and probiotic therapy. Alteration of the indigenous microflora by probiotic therapy has been shown to reverse some immunological disturbances typical of inflammatory bowel disease[89,90], colon cancer[91], ulcerative colitis[92], infectious diseases[93], and Crohn's disease. Probiotics that seem to give promising results in the maintenance treatment of Crohn's disease include *Saccharomyces boulardii*[94], *Lactobacillus* GG[95], and *E. coli* strain Nissle 1917[96].

Promising results in maintaining remission in ulcerative colitis, Crohn's diseases, and pouchitis have been obtained with VSL#3, a mixture of four lactobacilli strains (*Lactobacillus plantarum, L. casei, L. acidophilus*, *L. delbrueckii* ssp. *bulgaricus*), 3 Bifidobacteria strains (*Bifidobacterium infantis, B. breve, B. lomgum*), and one strain of *Streptococcus salivarius* ssp. *thermophilus*. Beneficial effects were a decreased expression of inflammatory markers *ex vivo*, increased immune response, improvement of the gut barrier function, maintenance of remission, and lower drug consumption[97-99].

***Treatment of diarrhea***

Probiotics have preventive as well as curative effects on several types of diarrhea of different etiologies. Treatment of diarrhea by administration of living or dried bacteria has a long tradition. Yoghurt was originally introduced into the market as an inexpensive, easy to prepare, and easily available remedy against diarrhea in children, and was sold in pharmacies. Fermented milk products are known to enhance lactose digestion and avoid intolerance symptoms in lactose malabsorbers. Fermented milk products with living bacteria contain microbial β-galactosidase that survives the passage through the stomach to be finally liberated in the small intestine and there to support lactose hydrolysis[100]. This is not a specific probiotic effect, because it does not depend on survival of the bacteria in the small intestine.

Probiotic strains are efficacious in preventing infectious diarrhea in healthy subjects. Sazawal *et al*[101] evaluated the efficacy of probiotics in prevention of acute diarrhea. Evidences suggest that probiotics significantly reduce antibiotic-associated diarrhea by 52%, the risk of travellers' diarrhea by 8%, and that of acute diarrhea by 34%. The protective effect does not vary significantly among the probiotic strains *Saccharomyces boulardii*, *Lactobacillus rhamnosus* GG, *L. acidophilus*, *L. bulgaricus*, and other strains used alone or in combinations of two or more strains. *Lactobacillus* GG has also found application in the treatment of diarrheal disorders such as treatment of recurrent infection with *Clostridium difficile*[102] and rotavirus infection in children[103,104].

***Genetically modified probiotics***

Extensive epithelial ruptures caused by a variety of infectious agents and/or by chemical contaminations, often lead to acute intestinal inflammation, also referred to as acute colitis.

The search for novel therapeutic approaches for acute and chronic colitis based on live recombinant lactic acid bacteria was extended by the construction and *in vivo* evaluation of *L. lactis* strains secreting bioactive murine trefoil factors (TFF). TFF are excellent candidates to restore a disrupted intestinal epithelial barrier, but they are mostly ineffective when administered orally. Vandenbroucke *et al.*[105] demonstrated that intragastric administration of TFF-secreting *L. lactis*, in contrast to purified TFF, led to effective prevention and healing of acute DSS-induced acute colitis. It was successful in reducing established chronic colitis in IL-10$^{-/-}$ mice.

Although recombinant strains would not be accepted today in functional food, their future use in therapeutic approaches can be foreseen provided that the benefit/risk balance is positive for consumers. Recently, a strain of *L. lactis* secreting human IL-10 has entered clinical testing for the treatment of severe, active Crohn's disease, and represents the first genetically modified lactic acid bacterium to be tested in humans.

**Prebiotics**

Today prebiotics are defined as "selectively fermented ingredients that allow specific changes, both in the composition and/or activity in the gastrointestinal microflora, that confer benefits upon host well-being and health". The main targets for prebiotics are

traditionally lactobacilli and bifidobacteria, due to their success in the probiotic area. The criteria established for classifying a food ingredient as a prebiotic are: resistance to gastric acidity, to hydrolysis by mammalian enzymes, and to gastrointestinal absorption; fermentation by intestinal microflora; selective stimulation of the growth and/or activity of those intestinal bacteria that contribute to health and well-being[106].

Currently the only food ingredients that have clearly demonstrated to fulfill the above listed criteria are galacto-oligosaccharides and fructo-oligosaccharides (inulin). Gluco-oligosaccharides, isomalto-oligosaccharides, polydextrose, lactosucrose, soybean oligosaccharides, and xylo-oligosaccharides are still being investigated for their prebiotic effects.

***Inulin and fructo-oligosaccharides***

The chemical structure of inulin is either an α-D-glucopyranosyl-[β-D-fructofuranosyl]$_{n-1}$-β-D-fructofuranoside ($G_{py}F_n$) or a β-D-fructopyranosyl-[β-D-fructo furanosyl]$_{n-1}$-β-D-fructofuranoside ($F_{py}F_n$). The term inulin describes β(2-->1) linear fructans with DP 2-60 and an average DP = 12.

Fructo-oligosaccharides (FOS) are mixtures of small inulin oligomers with $DP_{max}<10$[107]. FOS are produced by partial enzymatic hydrolysis of inulin using an endoinulinase or by enzymatic synthesis using the fungal enzyme β-fructosidase. In the first case a mixture of $G_{py}F_n$ and $F_{py}F_n$ with an average DP = 4 is obtained; in the second, all oligomers are of the $G_{py}F_n$ type and have a $DP_{av}$ = 3.6. The term inulin-type fructans covers native inulin, FOS, inulin HP (DP 10-60, $DP_{av}$ = 25), and Synergy 1, a specific combination of oligofructose and inulin HP[108].

Because of the β-configuration of the glycosidic linkage (anomeric C2) in the fructose monomers, inulin-type fructans resist hydrolysis by intestinal digestive enzymes. In the colon, they are rapidly fermented by bifidobacteria to produce short-chain fatty acids[109]. They also induce changes in colonic epithelium stimulating proliferation in the crypts, thereby increasing the concentration of polyamines, changing the profile of mucins, and modulating endocrine as well as immune functions. The prebiotic activity of FOS has been confirmed by laboratory and human tests[110-112]. Inulin and oligofructose were shown to exert beneficial effects on experimental colitis and the composition of intestinal microflora in rats[113]. A large number of animal data convincingly show that inulin-type

fructans reduce the risk of colon carcinogenesis, and nutrition intervention trials are now performed to test this hypothesis in human subjects known to be at risk for polyps and cancer development in the large bowel[114].

***Galacto-oligosaccharides***

Galacto-oligosaccharides (GOS) are the products of transgalactosylation reactions catalyzed by β-galactosidase, when using lactose or other structurally related galactosides as substrate. GOS generally consist of oligogalactosylated glucose dimers to pentamers, with β-D-Gal*p*-(1→2)-D-Glc*p*, β-D-Gal*p*-(1→3)-D-Glc*p*, β-D-Gal*p*-(1→4)-D-Glc*p*, and β-D-Gal*p*-(1→6)-D-Glc*p* linkages[115,116]. Recently, a novel form of transgalactosylating activity of β-galactosidase leading to the formation of α-D-Glc*p*-(1↔1)-β-D-Gal*p* has also been reported[117]. Resistance to digestion in the upper gastrointestinal tract is conferred by the β-glycosidically linked galactose, since humans lack enzymes able to hydrolyze β-glycosidic linkages other than lactose.

Some of the most important effects of prebiotics are outlined in the following paragraph.

**Effects of prebiotics**

***Intestinal colonization***

Intestinal colonization has a marked impact on the maturation of the infant's intestinal immune system[118]. Breast-fed babies develop a population richer in bifidobacteria, while formula-fed infants present a more diverse population composed of bifidobacteria, enterobacteria, lactobacilli, bacteroides, clostridia, and streptococci[119,120].

Breast-fed infants during the first year of life seem to have less gastrointestinal, respiratory and urinary infections than bottle-fed infants[121,122]. Enhancement of bifidobacteria in early stages may therefore have beneficial effects on infant's health. Human milk has a high content of oligosaccharides that stimulate bifidobacteria growth by fermenting lactose to produce lactic and acetic acid giving rise to an acidic medium, optimal for its growth and development[123]. These findings have motivated the dairy industry to add different ingredients to infant formulas, to induce a similar colonization pattern to that found in breast-fed infants. A study performed on 32 infants at the age of six months demonstrated that breast-fed infants and infants given partially hydrolyzed

formula supplemented with prebiotic oligosaccharides (a mixture of GOS and FOS 9:1) had identical levels of bifidobacteria in their feces, significantly exceeding those observed in formula-fed infants[124]. Mixtures of galacto-oligosaccharides and long-chain fructo-oligosaccharides in the ratio 9:1 have been demonstrated to stimulate the intestinal microflora of formula-fed infants similarly to breast-feeding, with respect to the count and distribution of Bifidobacteria, reduction of pathogens, amount of short chain fatty acids, and pH[125-127]. They also proved to reduce the incidence of atopic dermatitis during the first six months of age[128].

***Prevention of colon cancer***

Intestinal microbiota preferentially utilizes carbohydrates as energy source. In the absence of carbohydrates certain microbes, such as clostridia, revert to protein fermentation. Chronic putrefaction generates toxic fermentation products, *i.e.* ammonia, amines and nitrosoamines, phenols and cresols, indole and skatole, secondary bile acids, and aglycones[129-131], which can increase the risk of colon cancer. Prebiotics can be protective against carcinogenesis[132-133], by subverting the colon metabolism away from protein and lipid to saccharolysis, and by generating metabolites such as butyrate, which is known to stimulate apoptosis in colonic cancer cell lines[134-135]. To date, few prebiotics have been evaluated in human trials, but promising results have been obtained recently by using symbiotic preparation of prebiotics (oligofructose-enriched inulin) and probiotics (*Lactobacillus rhamnosus* GG and *Bifidobacterium lactis* Bb12) in polypectomized and colon cancer patients[136].

***Resistance to pathogens***

Probiotic microorganisms can reduce bacterial and viral infections by releasing natural antibiotics with a broad spectrum of activity[137], and by excreting short-chain fatty acids (mainly acetic and lactic acids) that lower the pH to levels below those pathogens are able to compete effectively[138]. Montreuil[139] postulated that the increased metabolic activity of a larger population in the lumen can decrease the intestinal pH, and that in turn can inhibit proliferation of pathogenic Gram-negative bacteria such as *Shigella flexneri* and *Escherichia coli*. By this last effect, prebiotics have been shown to inhibit certain strains of potentially pathogenic bacteria, especially *Clostridium*[140]and *E. coli*[141], and therefore prevent diarrhea.

Studies focused on clinically relevant pathogens such as *Staphylococcus aureus*, *Staphylococcus epidermidis*, *Staphylococcus haemolyticus*, *Pseudomonas aeruginosa*, *Enterobacter, Klebsiella*, *Proteus*, *Streptococcus* group B, *Clostridium difficile*, *Bacillus subtilis*, and *Acinetobacter* demonstrated that administration of prebiotic substances reduces the presence of pathogens in the faecal flora and might have the capacity to protect against enteral infections[142].

Asahara *et al*[143] examined the anti-infectious activity of Bifidobacteria in combination with galacto-oligosaccharides (GOS) against enteric pathogens under conditions in which indigenous flora had been eliminated by antibiotics. Antibiotic-induced intestinal overgrowth and extra-intestinal translocation of *Salmonella enterica serovar Typhimurium* in mice was shown to be inhibited by symbiotic administration of *B. breve* and GOS. Lowering of intestinal pH and organic acid production appeared to be important for this anti-infectious activity. These results indicate that certain bifidobacteria together with prebiotics may be used for the prophylaxis against opportunistic intestinal infections with antibiotic-resistant pathogens such as *Salmonella typhi.*

***Stimulation of the immune system***

In a recent study[144], it was demonstrated that mixtures of GOS and FOS enhance systemic Th1-dependent immune responses in a murine vaccination model. As Th1-responses are weak early in life of humans, this might suggest that application of these oligosaccharides in infant formulas will be beneficial for the development of the infant's immune system. A study performed by Bruzzese *et al*.[145] confirmed lower incidence of intestinal and respiratory infections in infants fed the GOS/FOS formula, while dietary supplementation of prebiotic mixtures of GOS and long-chain FOS showed to decrease parameters of allergenic asthma in mice[146]. These results support the hypothesis that specific mixtures of oligosaccharides modulate the Th1/Th2 balance by enhancing Th1-related and suppressing Th2-related parameters.

In a placebo-controlled trial, 1223 pregnant women carrying high-risk children were given probiotics for 2 to 4 weeks before delivery, and their infants received the same probiotic plus galacto-oligosaccharides for 6 months. The treatment showed no effect on the incidence of all allergic diseases by the age of 2 years, but significantly prevented eczema and especially atopic eczema[147].

***Hypocholesterol action***

Studies performed by Gilliland *et al.*[148] indicated that certain strains of *Lactobacillus acidophilus* may be beneficial in reducing serum cholesterol levels in human gastro-intestinal tract. Twelve strains of *L. acidophilus* of human origin have in fact been shown to assimilate cholesterol in *in-vitro* studies[149].

**Synbiotic formulations**

Nowadays it is accepted that formulations containing prebiotics and probiotics (synbiotics) may enhance the beneficial effect by synergistic activity. Bartosch *et al*[150] demonstrated that due to changes in gut physiology, immune system reactivity, and diet, elderly people are more susceptible to gastrointestinal infections than are younger adults. The gut microflora, which provides a natural defense against invading microorganisms, changes in elderly people with the development of potentially damaging bacterial populations, which may lead to alterations in bacterial metabolism and higher levels of infection. A randomized, double-blind, controlled feeding trial was done with 18 healthy elderly volunteers (age, >62 years) using a synbiotic comprising *Bifidobacterium bifidum* BB-02 and *Bifidobacterium lactis* BL-01 together with an inulin-based prebiotic (Synergy 1). Real-time PCR was employed to quantitate total bifidobacteria in fecal DNA before, during, and after synbiotic consumption. Counting all viable anaerobes, bifidobacteria and lactobacilli, and identification of bacterial isolates to species level was also done. Throughout feeding, both bifidobacteria species were detected in fecal samples obtained from all subjects receiving the synbiotic, with significant increases in the number of copies of the 16S rRNA genes of *B. bifidum*, *B. lactis*, and total bifidobacteria, compared with the pre-feeding period (1 week) and the placebo group. At least 1 of these species remained detectable in fecal samples 3 weeks after feeding in individuals that previously had no fecal *B. bifidum* and/or *B. lactis*, indicating that the probiotics persisted in the volunteers. Counting of viable organisms showed significantly higher total numbers of fecal bifidobacteria, total numbers of lactobacilli, and numbers of *B. bifidum* during synbiotic feeding, demonstrating that synbiotic consumption increased the size and diversity of protective fecal bifidobacterial populations.

**Aim of the thesis**

The primary aim of the thesis is to contribute to the isolation and characterization of prebiotics from non-human milk, in particular goat colostrum. High concentrations of lactose in milk form a great obstacle to isolate other milk oligosaccharides. A novel solution for this problem has to be developed. The study of the effects of such oligosaccharides on the adhesion of bacteria to intestinal epithelial cells should furnish insight in the potency of the oligosaccharides to act as prebiotics. The milk oligosaccharides require structural characterization, which should be done by means of NMR spectroscopy.

A further goal is to gain insight in the action of prebiotics in biological systems. It can be anticipated that these effects are mainly based on carbohydrate-protein interactions. To develop adequate tools for such studies, improvements in the application of NMR spectroscopy and surface plasmon resonance spectroscopy have to be explored.

**References**


[1] Dai D, Walker WA. Protective nutrients and bacterial colonization in the immature human gut. *Adv. Pediatr*. **1999**, *46*, 353-382.

[2] Isolauri E, Kaila M, Mykkänen H, Ling WH, Salminen S. Oral bacteriotherapy for viral gastroenteritis. *Dig. Dis. Sci.* **1994**, *39*, 2595-2600.

[3] Malin M, Verronen P, Mykkänen H, Salminen S, Isolauri E. Increased bacterial urease activity in faeces in juvenile chronic arthritis: evidence of altered intestinal microflora? *Br. J. Rheumatol.* **1996**, *35*, 689-694.

[4] Apostolou E, Pelto L, Kirjavainen PV, Isolauri E, Salminen SJ, Gibson GR. Differences in the gut bacterial flora of healthy and milk-hypersensitive adults, as measured by fluorescence in situ hybridization. *FEMS Immunol. Med. Microbiol.* **2001**, *30*, 217-221.

[5] Parracho HM, Bingham MO, Gibson GR, McCartney AL. Differences between the gut microflora of children with autistic spectrum disorders and that of healthy children. *J. Med. Microbiol.* **2005**, *54*, 987-991.

[6] Lilly DM, Stillwell RH. Probiotics: growth-promoting factors produced by microorganisms. *Science* **1965**, *147*, 747-748.

[7] Fuller R. Probiotics in man and animals *J. Appl. Bacteriol.* **1989**, *66*, 365-378.

[8] Salminen S, Bouley C, Boutron-Ruault MC, Cummings JH, Franck A, Gibson GR, Isolauri E, Moreau MC, Roberfroid M, Rowland I. Functional food science and gastrointestinal physiology and function. *Br. J. Nutr.* **1998**, *80*, S147-171.

[9] Gibson GR, Roberfroid MB. Dietary modulation of the human colonic microbiota: introducing the concept of prebiotics. *J. Nutr.* **1995**, *125*, 1401-1412.

[10] Gordon JI, Hooper LV, McNevin MS, Wong M, Bry L. Epithelial cell growth and differentiation. III. Promoting diversity in the intestine: conversations between the microflora, epithelium, and diffuse GALT. *Am. J. Physiol.* **1997**, *273*, G565-G570.

[11] Gionchetti P, Rizzello F, Venturi A, Brigidi P, Matteuzzi D, Bazzocchi G, Poggioli G, Miglioli M, Campieri M. Oral bacteriotherapy as maintenance treatment in patients with chronic pouchitis: a double-blind, placebo-controlled trial. *Gastroenterology* **2000**, *119*, 305-309.

[12] Xu J, Gordon JI. Inaugural Article: Honor thy symbionts. *Proc. Natl. Acad. Sci. USA* **2003**, *100*, 10452-10459.

[13] Drasar BS, Hill MJ, Human Intestinal Flora, 1974, Academic Press, London.

[14] Tannock GW Studies of the intestinal microbiota: a prerequisite for the development of probiotics. *Int. Diary J.* **1998**, *8*, 527-533.

[15] Mackie RI, Sghir A, Gaskins HR. Developmental microbial ecology of the neonatal gastrointestinal tract. *Am. J. Clin. Nutr.* **1999**, *69*, 1035S-1045S.

[16] Berg RD. The indigenous gastrointestinal microflora. *Trends Microbiol*. **1996**, *4*, 430-435.

[17] Zoetendal EG, Akkermans AD, de Vos WM. Temperature gradient gel electrophoresis analysis of 16S rRNA from human fecal samples reveals stable and host-specific communities of active bacteria. *Appl. Environ. Microbiol*. **1998**, *64*, 3854-3859.

[18] Savage DC. Microbial ecology of the gastrointestinal tract. *Ann. Rev. Microbiol.* **1977**, *31*, 107-133.

[19] Adlerberth I, Cerquetti M, Poilane I, Wold A, Collignon A. Mechanisms of colonisation and colonisation resistance of the digestive tract. *Microb. Ecol. Health Dis.* **2000**, *11*, 223-229.

[20] Gordon HA, Petsi L. The gnotobiotic animal as a tool in the study of host microbial relationships. *Bacteriol. Rev.* **1971**, *35*, 390-429.

[21] Gibson GR, Roberfroid MB. *Eds* Colonic Microbiota, Nutrition and Health. Dordrecht, Kluwer Academic, **1999**.

[22] Shanahan F. Inflammatory bowel disease: immunodiagnostics, immunotherapeutics, and ecotherapeutics. *Gastroenterology* **2001**, *120*, 622-635.

[23] Saavedra JM, Bauman NA, Oung I, Perman JA, Yolken RH. Feeding of *Bifidobacterium bifidum* and *Streptococcus thermophilus* to infants in hospital for prevention of diarrhoea and shedding of rotavirus. *Lancet* **1994**, *344*, 1046-1049.

[24] Zoetendal EG, Cheng B, Koike S, Mackie RI. Molecular microbial ecology of the gastrointestinal tract: from phylogeny to function. *Curr. Issues Intest. Microbiol*. **2004**, *5*, 31-47.

[25] Amann RI, Ludwig W, Schleifer KH. Phylogenetic identification and in situ detection of individual microbial cells without cultivation. *Microbiol. Rev.* **1995**, *59*, 143-169.

[26] Simpson JM, McCracken VJ, White BA, Gaskins HR, Mackie RI. Application of denaturant gradient gel electrophoresis for the analysis of the porcine gastrointestinal microbiota. *J. Microbiol. Methods.* **1999**, *36*, 167-179.

[27] van der Wielen PW, Keuzenkamp DA, Lipman LJ, van Knapen F, Biesterveld S. Spatial and temporal variation of the intestinal bacterial community in commercially raised broiler chickens during growth. *Microb. Ecol.* **2002**, *44*, 286-293.

[28] Zoetendal EG, von Wright A, Vilpponen-Salmela T, Ben-Amor K, Akkermans AD, de Vos WM. Mucosa-associated bacteria in the human gastrointestinal tract are uniformly distributed along the colon and differ from the community recovered from feces. *Appl. Environ. Microbiol.* **2002**, *68*, 3401-3407.

[29] Nielsen DS, Möller PL, Rosenfeldt PL, Pærregaard A, Michaelsen KF, Jakobsen M. Case study of the distribution of mucosa-associated *Bifidobacterium* species, *Lactobacillus* species, and other lactic acid bacteria in the human colon. *Appl. Environ. Microbiol*. **2003**, *69*, 7545-7548.

[30] Collins MD, Gibson GR. Probiotics, prebiotics, and synbiotics: approaches for modulating the microbial ecology of the gut. *Am. J. Clin. Nutr.* **1999**, *69*, 1052S-1057S.

[31] Vaahtovuo J, Toivanen P, Eerola E. Bacterial composition of murine fecal microflora is indigenous and genetically guided. *FEMS Microbiol. Ecol.* **2003**, *44*, 131-136.

[32] Hooper LV, Gordon JI Commensal host-bacterial relationships in the gut. *Science* **2001**, *292*, 1115-1118.

[33] Zoetendal EG, Akkermans ADL, Akkermans-van Vliet WM, de Visser JAGM, de Vos WM. The host genotype affects the bacterial community in the human gastrointestinal tract. *Microbial. Ecol. Health Dis.* **2001**, *13*, 129-134.

[34] Konstantinov SR, Zhu W-Y, Williams BA, Tamminga S, de Vos WM, Akkermans ADL. Effect of fermentable carbohydrates on faecal bacterial communities as revealed by DGGE analysis of 16rDNA. *FEMS Microbiol. Ecol.* **2003**, *43*, 225-235.

[35] Seksik P, Rigottier-Gois L, Gramet G, Sutren M, Pochart P, Marteau P, Jian R, Doré J. Alterations of the dominant faecal bacterial groups in patients with Crohn's disease of the colon. *Gut* **2003**, *52*, 237-242.

[36] Mitsuoka T. Intestinal flora and aging. *Nutr. Rev.* **1992**, *50*, 438-446.

[37] Favier CF, Vaughan EE, de Vos WM, Akkermans AD. Molecular monitoring of succession of bacterial communities in human neonates. *Appl. Environ. Microbiol.* **2002**, *68*, 219-226.

[38] Schwiertz A, Gruhl B, Löbnitz M, Michel P, Radke M, Blaut M. Development of the intestinal bacterial composition in hospitalized preterm infants in comparison with breast-fed, full-term infants. *Pediatr. Res.* **2003**, *54*, 393-399.

[39] Kruse HP, Kleessen B, Blaut M. Effects of inulin on faecal bifidobacteria in human subjects. *Brit. J. Nutr.* **1999**, *82*, 375-382.

[40] Harmsen HJ, Raangs GC, He T, Degener JE, Welling GW. Extensive set of 16S rRNA-based probes for detection of bacteria in human feces. *Appl. Environ. Microbiol.* **2002**, *68*, 2982-2990.

[41] Apajalahti JH, Kettunen A, Bedford MR, Holben WE. Percent G+C profiling accurately reveals diet-related differences in the gastrointestinal microbial community of broiler chickens. *Appl. Environ. Microbiol*. **2001**, *67*, 5656-5667.

[42] Apajalahti JH, Kettunen H, Kettunen A, Holben WE, Nurminen PH, Rautonen N, Mutanen M. Culture-independent microbial community analysis reveals that inulin in the diet primarily affects previously unknown bacteria in the mouse cecum. *Appl. Environ. Microbiol.* **2002**, 68, 4986-4995.

[43] McCracken VJ, Simpson JM, Mackie RI, Gaskins HR. Molecular ecological analysis of dietary and antibiotic-induced alterations of the mouse intestinal microbiota. *J. Nutr*. **2001**, *131*, 1862-1870.

[44] Tajima K, Aminov RI, Nagamine T, Matsui H, Nakamura M, Benno Y. Diet-dependent shifts in the bacterial population of the rumen revealed with real-time PCR. *Appl. Environ. Microbiol.* **2001**, *67*, 2766-2774.

[45] Tannock GW, Munro K, Bibiloni R, Simon MA, Hargreaves P, Gopal P, Harmsen H, Welling G, Impact of consumption of oligosaccharide-containing biscuits on the fecal microbiota of humans. *Appl. Environ. Microbiol*. **2004**, *70*, 2129-2136.

[46] Metchinkoff E. The Prolongation of Life. Optimistic Studies. New York, Putnam, **1908**.

[47] Gionchetti P, Rizzello F, Campieri M. Inflammatory bowel disease and probiotics. In: Gut Ecology, Martin Dunitz Ed. **2002**, 147-155.

[48] Lee Y-K, Salminen S. The coming of age of probiotics. *Trends in Food Sci. Technol.* **1995**, *6*, 241-245.

[49] Alander M, Satokari R, Korpela R, Saxelin M, Vilpponen-Salmela T, Mattila-Sandholm T, von Wright A. Persistence of colonization of human colonic mucosa by a probiotic strain, *Lactobacillus rhamnosus* GG, after oral consumption. *Appl. Environ. Microbiol*. **1999**, *65*, 351-354.

[50] Gardiner GE, Casey PG, Casey G, Lynch PB, Lawlor PG, Hill C, Fitzgerald GF, Stanton C, Ross RP. Relative ability of orally administered *Lactobacillus murinus* to

predominate and persist in the porcine gastrointestinal tract. *Appl. Environ. Microbiol.* **2004**, *70*, 1895-1906.

[51] Klingberg TD, Budde BB. The survival and persistence in the human gastrointestinal tract of five potential probiotic lactobacilli consumed as freeze-dried cultures or as probiotic sausage. *Int. J. Food Microbiol.* **2006**, *109*, 157-159.

[52] Goldin BR, Gorbach SL, Saxelin M, Barakat S, Gualtieri L, Salminen S. Survival of *Lactobacillus* species (strain GG) in human gastrointestinal tract. *Dig. Dis. Sci.* **1992**, *37*, 121-128.

[53] Rastall RA. Bacteria in the gut: friends and foes and how to alter the balance. *J. Nutr*. **2004**, 134, 2022S-2026S.

[54] Schultz M, Göttl C, Young RJ, Iwen P, Vanderhoof JA. Administration of oral probiotic bacteria to pregnant women causes temporary infantile colonization. *J. Pediatr. Gastroenterol. Nutr.* **2004**, *38*, 293-297.

[55] Ashenafi M Growth of *Listeria monocytogenes* in fermenting tempeh made of various beans and its inhibition by *Lactobacillus plantarum*. *Food Microbial.* **1991**, *8*, 303-310.

[56] Drago L, Gismondo MR, Lombardi A, de Haën C, Gozzini L. Inhibition of in vitro growth of enteropathogens by new *Lactobacillus* isolates of human intestinal origin. *FEMS Microbiol. Lett.* **1997**, *153*, 455-463.

[57] Hudault S, Liévin V, Bernet-Camard MF, Servin AL. Antagonistic activity exerted in vitro and *in vivo* by *Lactobacillus casei* (strain GG) against *Salmonella typhimurium* C5 infection. *Appl. Environ. Microbiol.* **1997**, *63*, 513-518.

[58] Nisbet D. Defined competitive exclusion cultures in the prevention of enteropathogen colonisation in poultry and swine. Antonie Van Leeuwenhoek. **2002**, *81*, 481-486.

[59] Axelsson LT, Chung TC, Dobrogosz WG, Lindgren SE. Production of a broad spectrum antimicrobial substance by *Lactobacillus reuteri*. *Microb. Ecol. Health Dis.* **1989**, *2*, 131-136.

[60] Juven BJ, Schved F, Linder P. Antagonistic compounds produced by a chicken intestinal strain of *Lactobacillus acidophilus*. *J. Food Prot.* **1992**, *55*, 157-161.

[61] Silva M, Jacobus NV, Deneke C, Gorbach SL. Antimicrobial substance from a human *Lactobacillus* strain. *Antimicrob. Agents Chemother.* **1987**, *31*, 1231-1233.

[62] Kirjavainen PV, Ouwehand AC, Isolauri E, Salminen SJ. The ability of probiotic bacteria to bind to human intestinal mucus. *FEMS Microbiol. Lett.* **1998**, *167*, 185-189.

[63] Mack DR, Michail S, Wei S, McDougall L, Hollingsworth MA. Probiotics inhibit enteropathogenic *E. coli* adherence in vitro by inducing intestinal mucin gene expression. *Am. J. Physiol.* **1999**, *276*, G941-G950.

[64] Brandtzaeg PE. Current understanding of gastrointestinal immunoregulation and its relation to food allergy. *Ann. N. Y. Acad. Sci.* **2002**, *964*, 13-45.

[65] Malin M, Suomalainen H, Saxelin M, Isolauri E. Promotion of IgA immune response in patients with Crohn's disease by oral bacteriotherapy with *Lactobacillus* GG. *Ann. Nutr. Metab.* **1996**, 40, 137-145.

[66] Kato I, Kobayashi S, Yokokura T, Mutai M. Antitumor activity of *Lactobacillus casei* in mice. *Gann* **1981**, *72*, 517-523.

[67] Aso Y, Akaza H, Kotake T, Tsukamoto T, Imai K, Naito S. Preventive effect of a *Lactobacillus casei* preparation on the recurrence of superficial bladder cancer in a double-blind trial. *The BLP Study Group Eur Urol*. **1995**, *27*, 104-109.

[68] Kato I, Endo K, Yokokura T. Effects of oral administration of *Lactobacillus casei* on antitumor responses induced by tumor resection in mice. *Int. J. Immunopharmacol.* **1994**, *16*, 29-36.

[69] Takagi A, Matsuzaki T, Sato M, Nomoto K, Morotomi M, Yokokura T. Enhancement of natural killer cytotoxicity delayed murine carcinogenesis by a probiotic microorganism. *Carcinogenesis* **2001**, *22*, 599-605.

[70] Takeda K, Okumura K. Effects of a fermented milk drink containing *Lactobacillus casei* strain Shirota on the human NK-cell activity. *J. Nutr.* **2007**, *137*, 791S-793S.

[71] Link-Amster H, Rochat F, Saudan KY, Mignot O, Aeschlimann JM Modulation of a specific humoral immune response and changes in intestinal flora mediated through fermented milk intake. *FEMS Immunol. Med. Microbiol.* **1994**, *10*, 55-63.

[72] Anderson WJ, Watson L. Asthma and the hygiene hypothesis. *N. Engl. J. Med.* **2001**, *344*, 1643-1644.

[73] Matricardi PM, Bonini S. High microbial turnover rate preventing atopy: a solution to inconsistencies impinging on the Hygiene hypothesis? *Clin. Exp. Allergy* **2000**, *30*, 1506-1510.

[74] Kalliomäki M, Kirjavainen P, Eerola E, Kero P, Salminen S, Isolauri E. Distinct patterns of neonatal gut microflora in infants in whom atopy was and was not developing. *J. Allergy Clin. Immunol.* **2001**, *107*, 129-134.

[75] Sudo N, Aiba Y, Oyama N, Yu XN, Matsunaga M, Koga Y, Kubo C. Dietary nucleic acid and intestinal microbiota synergistically promote a shift in the Th1/Th2 balance toward Th1-skewed immunity. *Int. Arch. Allergy Immunol.* **2004**, *135*, 132-135.

[76] Sudo N, Yu XN, Aiba Y, Oyama N, Sonoda J, Koga Y, Kubo C. An oral introduction of intestinal bacteria prevents the development of a long-term Th2-skewed immunological memory induced by neonatal antibiotic treatment in mice. *Clin. Exp. Allergy* **2002**, *32*, 1112-1116.

[77] Von der Weid T, Bulliard C, Schiffrin EJ. Induction by a lactic acid bacterium of a population of CD4(+) T cells with low proliferative capacity that produce transforming growth factor beta and interleukin-10. *Clin. Diagn. Lab. Immunol.* **2001**, *8*, 695-701.

[78] Kirjavainen PV, Gibson GR. Healthy gut microflora and allergy: factors influencing development of the microbiota. *Ann. Med.* **1999**, *31*, 288-292.

[79] He F, Morita H, Hashimoto H, Hosoda M, Kurisaki J, Ouwehand AC, Isolauri E, Benno Y, Salminen S. Intestinal *Bifidobacterium* species induce varying cytokine production. *J. Allergy Clin. Immunol.* **2002**, *109*, 1035-1036.

[80] Morita H, He F, Fuse T, Ouwehand AC, Hashimoto H, Hosoda M, Mizumachi K, Kurisaki J. Adhesion of lactic acid bacteria to caco-2 cells and their effect on cytokine secretion. *Microbiol. Immunol*. **2002**, *46*, 293-297.

[81] Majamaa H, Isolauri E. Probiotics: a novel approach in the management of food allergy. *J. Allergy. Clin. Immunol*. **1997**, *99*, 179-185.

[82] Isolauri E, Arvola T, Sütas Y, Moilanen E, Salminen S. Probiotics in the management of atopic eczema. *Clin. Exp. Allergy*. **2000**, *30*, 1604-1610.

[83] Goto H, Gidlund M. Soluble CD4: a link between specific immune mechanisms and non-specific inflammatory responses? *Scand. J. Immunol*. **1996**, *43*, 690-692.

[84] Hansen G, McIntire JJ, Yeung VP, Berry G, Thorbecke GJ, Chen L, DeKruyff RH, Umetsu DT CD4(+) T helper cells engineered to produce latent TGF-beta1 reverse allergen-induced airway hyperreactivity and inflammation. *J. Clin. Invest*. **2000**, 105, 61-70.

[85] Koller DY, Halmerbauer G, Frischer T, Roithner B. Assessment of eosinophil granule proteins in various body fluids: is there a relation to clinical variables in childhood asthma? *Clin. Exp. Allergy* **1999**, *29*, 786-793.

[86] Brouwer ML, Wolt-Plompen SA, Dubois AE, van der Heide S, Jansen DF, Hoijer MA, Kauffman HF, Duiverman EJ No effects of probiotics on atopic dermatitis in infancy: a randomized placebo-controlled trial. *Clin. Exp. Allergy* **2006**, *36*, 899-906.

[87] Moreau MC, Corthier G. Effect of the gastrointestinal microflora on induction and maintenance of oral tolerance to ovalbumin in C3H/HeJ mice. *Infect. Immun.* **1988**, *56*, 2766-2768.

[88] Duchmann R, Kaiser I, Hermann E, Mayet W, Ewe K, Meyer zum Büschenfelde KH. Tolerance exists towards resident intestinal flora but is broken in active inflammatory bowel disease (IBD). *Clin. Exp. Immunol*. **1995**, *102*, 448-455.

[89] Madsen KL, Doyle JS, Jewell LD, Tavernini MM, Fedorak RN Lactobacillus species prevents colitis in interleukin 10 gene-deficient mice. *Gastroenterology* **1999**, *116*, 1107-1114.

[90] Sartor RB. Therapeutic manipulation of the enteric microflora in inflammatory bowel diseases: antibiotics, probiotics, and prebiotics. *Gastroenterology* **2004**, *126*, 1620-1633.

[91] Dugas B, Mercenier A, Lenoir-Wijnkoop, Arnaud C, Dugas N, Postaire E. Immunity and probiotics. *Immunol. Today* **1999**, *20*, 387-390.

[92] Kruis K, Schütz E, Fric P, Fixa B, Judmeier G, Stolte M. Double-blind comparison of an oral *Escherichia coli* preparation and mesalazine in maintaining remission of ulcerative colitis. *Aliment. Pharmacol. Ther.* **1997**, *11*, 853-858.

[93] Vanderhoof JA, Whitney DB, Antonson DL, Hanner TL, Lupo JV, Young RJ. *Lactobacillus* GG in the prevention of antibiotic-associated diarrhea in children. *J. Pediatr.* **1999**, *135*, 564-568.

[94] Guslandi M, Mezzi G, Sorghi M, Testoni PA. *Saccharomyces boulardii* in maintenance treatment of Crohn's disease. *Dig. Dis. Sci.* **2000**, 45, 1462-1464.

[95] Gupta P, Andrew H, Kirschner BS, Guandalini S. Is *lactobacillus* GG helpful in children with Crohn's disease? Results of a preliminary, open-label study. *J. Pediatr. Gastroenterol. Nutr.* **2000**, *31*, 453-457.

[96] Malchow HA. Crohn's disease and *Escherichia coli*. A new approach in therapy to maintain remission of colonic Crohn's disease? *J. Clin. Gastroenterol.* **1997**, *25*, 653-658.

[97] Gionchetti P, Rizzello F, Morselli C, Poggioli G, Tambasco R, Calabrese C, Brigidi P, Vitali B, Straforini G, Campieri M. High-dose probiotics for the treatment of active pouchitis. *Dis. Colon Rectum* **2007**, *50*, 2075-2082.

[98] Venturi A, Gionchetti P, Rizzello F, Johansson R, Zucconi E, Brigidi P, Matteuzzi D, Campieri M. Impact on the composition of the faecal flora by a new probiotic preparation: preliminary data on maintenance treatment of patients with ulcerative colitis. *Aliment Pharmacol. Ther*. **1999**, *13*, 1103-1108.

[99] Campieri M, Rizzello F, Venturi A, Poggioli G, Ugolini F, Helwig U, Amasini C, Romboli E, Gionchetti P. Combination of antibiotic and probiotic treatment is efficacious in prophylaxis of post-operative recurrence of Crohn's disease: a randomized controlled study v. mesalazine. *Gastroenterology* **2000**, *118*, A4179.

[100] de Vrese M, Stegelmann A, Richter B, Fenselau S, Laue C, Schrezenmeir J. Probiotics--compensation for lactase insufficiency. *Am. J. Clin. Nutr.* **2001**, *73*, 421S-429S.

[101] Sazawal S, Hiremath G, Dhingra U, Malik P, Deb S, Black RE. Efficacy of probiotics in prevention of acute diarrhoea: a meta-analysis of masked, randomised, placebo-controlled trials. *Lancet Infect. Dis.* **2006**, *6*, 374-382.

[102] Biller JA, Katz AJ, Flores AF, Buie TM, Gorbach SL. Treatment of recurrent *Clostridium difficile* colitis with *Lactobacillus* GG. *J. Pediatr. Gastroenterol. Nutr.* **1995**, *21*, 224-226.

[103] Isolauri E, Juntunen M, Rautanen T, Sillanaukee P, Koivula T. A human *Lactobacillus* strain (*Lactobacillus casei* sp strain GG) promotes recovery from acute diarrhea in children. *Pediatrics* **1991**, *88*, 90-97.

[104] Kaila M, Isolauri E, Soppi E, Virtanen E, Laine S, Arvilommi H. Enhancement of the circulating antibody secreting cell response in human diarrhea by a human *Lactobacillus* strain. *Pediatr. Res.* **1992**, *32*, 141-144.

[105] Vandenbroucke K, Hans W, Van Huysse J, Neirynck S, Demetter P, Remaut E, Rottiers P, Steidler L. Active delivery of trefoil factors by genetically modified *Lactococcus lactis* prevents and heals acute colitis in mice. *Gastroenterology* **2004**, *127*, 502-513.

[106] Roberfroid M. Prebiotics: the concept revisited. *J. Nutr.* **2007**, *137*, 830S-837S.

[107] Roberfroid MB. Functional foods: concepts and application to inulin and oligofructose. *Br. J. Nutr.* **2002**, *87*, S139-143.

[108] Roberfroid MB. Inulin-type fructans: functional food ingredients. *J. Nutr.* **2007**, *137*, 2493S-2502S.

[109] Imamura L, Hisamitsu K, Kobashi K. Purification and characterization of beta-fructofuranosidase from *Bifidobacterium infantis*. *Biol. Pharmacol. Bull.* **1994**, *17*, 596-602.

[110] Gibson GR, Beatty ER, Wang X, Cummings JH. Selective stimulation of bifidobacteria in the human colon by oligofructose and inulin. *Gastroenterology* **1995**, *108*, 975-982.

[111] Kleessen B, Sykura B, Zunft H-J, Blaut M. Effects of inulin and lactose on fecal microflora, microbial activity, and bowel habit in elderly constipated persons. *Am. J. Clin. Nutr.* **1997**, *65*, 1397-1402.

[112] Rhee S-R, Song K-B, Kim C-H, Park B-S, Jang E-K, Jang K-H, Levan. Biopolymers. Steinbüchel A, Baets SD, Vandamme EH, Wiley VCH, Weinheim, **2002**, 351-378.

[113] Videla S, Vilaseca J, Antolín M, García-Lafuente A, Guarner F, Crespo E, Casalots J, Salas A, Malagelada JR. Dietary inulin improves distal colitis induced by dextran sodium sulfate in the rat. *Am. J. Gastroenterol*. **2001**, *96*, 1486-1493.

[114] Roberfroid MB. Introducing inulin-type fructans. *Br. J. Nutr.* **2005**, *93*, S13-25.

[115] Crittenden RG, Playne MG. Production, properties and applications of food-grade oligosaccharides. *Trend Food Sci. Technol.* 1997, *7*, 353-361.

[116] Prenosil JE, Stuker E, Bourne JR, Formation of oligosaccharides during enzymatic lactose: Part I: State of art. *Biotechnol. Bioeng.* **1987**, *30*, 1019-1025.

[117] Fransen CTM, Van Laere KMJ, van Wijk AAC, Brüll LP, Dignum M, Thomas-Oates JE, Haverkamp J, Schols HA, Voragen AGJ, Kamerling JP, Vliegenthart JFG. α-D-Glc*p*-(1↔1)-β-D-Gal*p*-containing oligosaccharides, novel products from lactose by the action of β-galactosidase. *Carbohydr. Res*. **1998**, *314*, 101-114.

[118] Cebra JJ. Influences of microbiota on intestinal immune system development. *Am. J. Clin. Nutr*. **1999**, *69*, 1046S-1051S.

[119] Fanaro S, Chierici R, Guerrini P, Vigi V. Intestinal microflora in early infancy: composition and development. *Acta Paediatr. Suppl.* **2003**, *91*, 48-55.

[120] Harmsen HJ, Wildeboer-Veloo AC, Raangs GC, Wagendorp AA, Klijn N, Bindels JG, Welling GW. Analysis of intestinal flora development in breast-fed and formula-fed infants by using molecular identification and detection methods. *J. Pediatr. Gastroenterol. Nutr.* **2000**, *30*, 61-67.

[121] Pisacane A, Graziano L, Mazzarella G, Scarpellino B, Zona G. Breast-feeding and urinary tract infection. *J. Pediatr.* **1992**, *120*, 87-89.

[122] Gueimonde M, Tölkkö S, Korpimäki T, Salminen S. New real-time quantitative PCR procedure for quantification of bifidobacteria in human fecal samples. *Appl. Environ. Microbiol*. **2004**, *70*, 4165-4169.

[123] Newburg DS. Oligosaccharides in human milk and bacterial colonization. *J. Pediatr. Gastroenterol. Nutr.* **2000**, *30*, S8-17.

[124] Rinne MM, Gueimonde M, Kalliomäki M, Hoppu U, Salminen SJ, Isolauri E. Similar bifidogenic effects of prebiotic-supplemented partially hydrolysed infant formula and breastfeeding on infant gut microbiota. *FEMS Immunol. Med. Microbiol.* **2005**, *43*, 59-65.

[125] Knol J, Scholtens P, Kafka C, Steenbakkers J, Gro S, Helm K, Klarczyk M, Schöpfer H, Böckler HM, Wells J. Colon microflora in infants fed formula with galacto- and fructo-oligosaccharides: more like breast-fed infants. *J. Pediatr. Gastroenterol. Nutr.* **2005**, *40*, 36-42.

[126] Boehm G, Lidestri M, Casetta P, Jelinek J, Negretti F, Stahl B, Marini A. Supplementation of a bovine milk formula with an oligosaccharide mixture increases counts of faecal bifidobacteria in preterm infants. *Arch. Dis. Child Fetal Neonatal.* **2002**, *86*, F178-181.

[127] Boehm G, Stahl B, Jelinek J, Knol J, Miniello V, Moro GE. Prebiotic carbohydrates in human milk and formulas. *Acta Paediatr. Suppl.* **2005**, *94*, 18-21.

[128] Moro G, Arslanoglu S, Stahl B, Jelinek J, Wahn U, Boehm G. A mixture of prebiotic oligosaccharides reduces the incidence of atopic dermatitis during the first six months of age. *Arch. Dis. Child* **2006**, *91*, 814-819.

[129] Tomotatsu H. Health effect of oligosaccharides. *Food Technol.* **1994**, *48*, 61-65.

[130] Smith EA, Macfarlane GT. Formation of phenolic and indolic compounds by anaerobic bacteria in the human large intestine. *Microb. Ecol.* **1997**, *33*, 180-188.

[131] Cummings JH, Macfarlane GT. The control and consequences of bacterial fermentation in the human colon. *J. Appl. Bacteriol.* **1991**, *70*, 443-459.

[132] Pool-Zobel BL. Inulin-type fructans and reduction in colon cancer risk: review of experimental and human data. *Br. J. Nutr.* **2005**, *93*, S73-9.

[133] Hylla S, Gostner A, Dusel G, Anger H, Bartram HP, Christl SU, Kasper H, Scheppach W. Effects of resistant starch on the colon in healthy volunteers: possible implications for cancer prevention. *Am. J. Clin. Nutr.* **1998**, *67*, 136-42.

[134] Prasad KN. Butyric acid: a small fatty acid with diverse biological functions. *Life Sci.* **1980**, *27*, 1351-1358.

[135] Tsao D, Shi ZR, Wong A, Kim YS. Effect of sodium butyrate on carcinoembryonic antigen production by human colonic adenocarcinoma cells in culture. *Cancer Res.* **1983**, *43*, 1217-1222.

[136] Rafter J, Bennett M, Caderni G, Clune Y, Hughes R, Karlsson PC, Klinder A, O'Riordan M, O'Sullivan GC, Pool-Zobel B, Rechkemmer G, Roller M, Rowland I, Salvadori M, Thijs H, Van Loo J, Watzl B, Collins JK. Dietary synbiotics reduce cancer risk factors in polypectomized and colon cancer patients. *Am. J. Clin. Nutr.* **2007**, *85*, 488-496.

[137] Gibson GR, Wang X. Regulatory effects of bifidobacteria on the growth of other colonic bacteria. *J. Appl. Bacteriol.* **1994**, *77*, 412-420.

[138] Mackey BM, Gibson GR. *Escherichia coli* O157: From farm to fork and beyond. *Soc. Gen. Microbiol. Q.* **1997**, *24*, 55-57.

[139] Monteuil J. The saga of human milk oligosaccharides. In: New Perspectives in Infant Nutrition. **1994**, Ed Renner B, Sawatzki G, Thieme, Stuttgart.

[140] Cummings JH, Macfarlane GT. Gastrointestinal effects of prebiotics. *Br. J. Nutr.* **2002**, *87*, S145-151.

[141] Costalos C. Kapiki A. Apostolou M. Papathoma E. The effect of a prebiotic supplemented formula on growth and stool microbiology of term infants. *Early Hum. Dev.* **2008**, *84*, 45-49.

[142] Knol J, Boehm G, Lidestri M, Negretti F, Jelinek J, Agosti M, Stahl B, Marini A, Mosca F. Increase of faecal bifidobacteria due to dietary oligosaccharides induces a reduction of clinically relevant pathogen germs in the faeces of formula-fed preterm infants. *Acta Paediatr. Suppl.* **2005**, *94*, 31-33.

[143] Asahara T, Nomoto K, Shimizu K, Watanuki M, Tanaka R. Increased resistance of mice to *Salmonella enterica* serovar *Typhimurium* infection by synbiotic administration of Bifidobacteria and transgalactosylated oligosaccharides. *J. Appl. Microbiol.* **2001**, *91*, 985-996.

[144] Vos AP, Haarman M, van Ginkel JW, Knol J, Garssen J, Stahl B, Boehm G, M'Rabet L. Dietary supplementation of neutral and acidic oligosaccharides enhances Th1-dependent vaccination responses in mice. *Pediatr. Allergy Immunol.* **2007**, *18*, 304-312.

[145] Bruzzese E, Volpicelli M, Salvini F, Bisceglia M, Lionetti P, Cinquetti M, Iacono G, Guarino A. Early administration of GOS/FOS prevents intestinal and respiratory infections in infants. *J. Pediatr. Gastroenterol. Nutr.* **2006**, *42*, E95.

[146] Vos AP, van Esch BC, Stahl B, M'Rabet L, Folkerts G, Nijkamp FP, Garssen J. Dietary supplementation with specific oligosaccharide mixtures decreases parameters of allergic asthma in mice. *Int. Immunopharmacol.* **2007**, *7*, 1582-1587.

[147] Kukkonen K, Savilahti E, Haahtela T, Juntunen-Backman K, Korpela R, Poussa T, Tuure T, Kuitunen M. Probiotics and prebiotic galacto-oligosaccharides in the prevention of allergic diseases: a randomized, double-blind, placebo-controlled trial. *J. Allergy Clin. Immunol*. **2007**, *119*, 192-198.

[148] Gilliland SE, Nelson CR, Maxwell C. Assimilation of cholesterol by *Lactobacillus acidophilus*. *Appl. Environ. Microbiol.* **1985**, *49*, 377-381.

[149] Gilliland SE, Walker DK. Factors to consider when selecting a culture of *Lactobacillus acidophilus* as a dietary adjunct to produce a hypocholesterolemic effect in humans. *J. Dairy Sci.* **1990**, *73*, 905-911.

[150] Bartosch S, Woodmansey EJ, Paterson JC, McMurdo ME, Macfarlane GT Microbiological effects of consuming a synbiotic containing *Bifidobacterium bifidum*, *Bifidobacterium lactis*, and oligofructose in elderly persons, determined by real-time polymerase chain reaction and counting of viable bacteria. *Clin. Infect. Dis.* **2005**, *40*, 28-37.

# 2

# An improved protocol to isolate lactose-free oligosaccharide fractions from non-human milks - characterization of major components and their effect on bacterial adhesion

Daniela Beccati[1], Luisa Sturiale[2], Marco Guerrini[2], Annamaria Naggi[2], Giangiacomo Torri[2], Lucia Zampini[3], Giovanni V. Coppa[3], Johannes F.G. Vliegenthart[1], Johannis P. Kamerling[1]

[1]*Bijvoet Center, Department of Bio-Organic Chemistry, Utrecht University, Padualaan 8, 3584 CH Utrecht, The Netherlands*

[2]*G. Ronzoni Institute for Chemical and Biochemical Research, Via G. Colombo 81, 20133 Milan, Italy*

[3]*Institute of Paediatrics, University of Ancona, Via Corridoni 11, 60123 Ancona, Italy*

**Abstract**

The relatively high content of lactose in non-human milk/colostrum/whey complicates the isolation of commercially interesting amounts of additional oligosaccharides present. A fast and scalable approach for goat, sheep, and cow milk/colostrum/whey has been developed, by making use of β-galactosidase from *Escherichia coli* to degrade lactose. In this procedure the original oligosaccharide compositional profile is preserved, thereby improving the efficiency of the neutral oligosaccharide fractionation by gel-permeation chromatography. Investigation of the goat neutral oligosaccharide pool showed the major components to be α3'-galactosyllactose, β3'-galactosyllactose, and β6'-galactosyllactose, products being completely absent in human milk. In contrast to human milk, fucosylated oligosaccharides are nearly absent. The goat acidic oligosaccharide pool contains both *N*-acetyl- and *N*-glycolyl-neuraminyl oligosaccharides, among others sialyl-*N*-acetyllactosamine, a product being absent in human milk. Although most of these components have been identified earlier in goat colostrum or milk, the improved protocol makes their isolation much more straightforward. Bacterial adhesion studies with isolated acidic oligosaccharide fractions showed a significant inhibition of the adherence to faecal *Salmonella fyris* B8132 to cultured intestinal epithelial cells. However, for faecal *Escherichia coli* 0119 no detectable inhibitory effect was found.

*Keywords*

Goat milk; milk oligosaccharides; β-galactosidase; *Escherichia coli*; *Salmonella fyris*

## Introduction

Human milk contains a large variety of free oligosaccharides, of which lactose is the predominant component[1]. Since the pioneering studies performed in the late fifties by Kuhn[2] and Montreuil[3], more than 80 oligosaccharides have been isolated from human milk, and fully structurally characterized[4,5]. One of the reasons for the still growing interest in these compounds is the discovery that breast-fed babies seem to have fewer or less severe gastrointestinal, respiratory, and urinary infections than formula-fed infants[6,7], suggesting that human milk oligosaccharides may protect infants from pathogenic agents[8,9]. It has been proved that, being soluble structural analogs of receptor glycan chains, oligosaccharides are able to prevent adhesion of bacteria, viruses, and fungi to epithelial cells[10-14]. For example, sialyllactose has been shown to inhibit adhesion of cholera toxin, enterotoxin, and possibly influenza virus[15-17], and at the same time to promote the growth of *Bifidobacterium bifidum* in the lower gastrointestinal tract, thereby inhibiting the proliferation of pathogenic organisms[18,19].

Non-human milk also contains a high variation of free oligosaccharides, but their complete pattern, as well as their biological function, has not been elucidated yet. It has been proposed that some oligosaccharides found in rat milk[20] or in bovine and equine colostrum, may be of nutritional significance. But it might as well be speculated that, in analogy to human-milk oligosaccharides, their function may be primarily protective, by inhibiting the adhesion of pathogenic organisms to the intestinal mucosa of newborn calves and lambs[21]. Further studies are required to prove these hypotheses, since up to now oligosaccharides from non-human milk have not been investigated to such an extent as human ones. Moreover, a direct comparison with human oligosaccharides is not straightforward, as it has been shown that significant structural differences[22] exist, like the almost complete absence of fucosylated structures in sheep, cow, and goat milk[23]. Characterization and biological testing of non-human milk oligosaccharides are currently hampered by their low availability, due to the lack of efficient isolation procedures. Complete removal of lactose, whose relative percentage is significantly higher in non-human than in human milk, is the major bottleneck for the isolation of additional oligosaccharides in large amounts. Lactose alone seems to be inactive in bacterial adhesion tests. However, its high abundance complicates the detection of biological effects of the other oligosaccharides. Traditionally, hundreds of milligrams of material are

needed for *in vitro* testing of bacterial adhesion, while multigram quantities are usually employed for comprehensive animal studies.

In this communication we present a fast and simple procedure for the preparative isolation of oligosaccharides from non-human milk. To circumvent tedious desalting procedures after the separation of the total pool of oligosaccharides into pools of neutral and charged oligosaccharides, the traditional approach of anion-exchange chromatography[24-26] has been replaced by size-exclusion chromatography. Then, the neutral oligosaccharide pool is treated with β-galactosidase to digest lactose, followed by elimination of the released monosaccharides and residual lactose by size-exclusion chromatography. In this way, amounts of 1.5 g of acidic oligosaccharides and 1.5-2.5 g of lactose-free neutral oligosaccharides could easily be obtained from 1 L of goat colostrum, milk or whey. Structural analysis studies were carried out by high-pH anion-exchange chromatography, MALDI-TOF mass spectrometry, and NMR spectroscopy. Additionally, isolated acidic oligosaccharide fractions were tested in bacterial adhesion studies, and it will be shown that goat acidic oligosaccharide fractions inhibited significantly the adhesion of *Salmonella fyris*, but not of *Escherichia coli*, to cultured intestinal epithelial cells.

## Materials and Methods

### *Materials*

Goat and sheep milk, colostrum, and whey, obtained from a local diary (Potenza, Italy), were collected within 1 h of milking and kept frozen at –15°C until use; cow milk was purchased from Centrale del Latte (Milano, Italy). β-Galactosidase (EC 3.2.1.23; *E. coli*, grade VI) was obtained from Sigma-Aldrich (St. Louis, MO, USA). Oligosaccharide standards for HPAEC-PAD calibration were purchased from Sigma-Aldrich, BioCarb (Lund, Sweden), and/or Dextra Laboratories (Reading, UK): lactose, lacto-*N*-difucohexaose (LNDFH II), trifucosyllacto-*N*-hexaose (TFLNH), difucosyllacto-*N*-hexaose b (DFLNH b), difucosyllacto-*N*-hexaose (DFLNH), difucosyllacto-*N*-hexaose I (DFLNH I), 3'-fucosyllactose (3'FL), lacto-*N*-fucopentaose II (LNFP II), 2'-fucosyllactose (2'FL), lacto-*N*-fucopentaose I (LNFP I), monofucosyllacto-*N*-hexaose II (MFLNH II), lacto-*N*-neotetraose (LNnT), lacto-*N*-neohexaose (LNnH), lacto-*N*-tetraose

(LNT), lacto-*N*-hexaose (LNH), monofucosylmonosialyllacto-*N*-neohexaose (FSLNnH), sialyllacto-*N*-tetraose c (LST c), 6'-sialyllactose (6'SL), 3'-sialyllactose (3'SL), 6'-sialyllactosamine (6'SLN), sialyllacto-*N*-tetraose a (LST a), and disialyllacto-*N*-tetraose (DSLNT). In all cases, sialic acid correlates with *N*-acetylneuraminic acid.

*Isolation of the oligosaccharide fraction from pooled colostrum (or milk)*

Oligosaccharide fractions were isolated from pooled colostrum (or milk) as previously described[27] with the following modifications. Goat colostrum (1 L) was thawed and centrifugated at 3000 r.p.m. for 45 min, then cooled to 4°C for 2 h, and manually skimmed. The liquid phase was mixed with 68% aqueous ethanol and allowed to settle overnight at 4°C. Precipitated proteins and lactose (partly) were removed by centrifugation (3000 r.p.m., 4°C, 15 min), and the aqueous phase collected and concentrated under reduced pressure to remove ethanol. After lyophilization, the resulting powder was dissolved in distilled water (50 mL), and the pH adjusted to 6.8-7.0 with 4% NaOH. Then, the solution was heated at 85-90°C for 10 min, cooled down at room temperature, filtered over Whatman 1 Chr paper, and ultrafiltered on an Amicon Miniplate (molecular mass cut-off, 10 kDa; Millipore, Billerica, MA, USA). The complete recovery of the oligosaccharide fraction was checked with the phenol-$H_2SO_4$ assay[28]. Concentration of the oligosaccharide fraction under reduced pressure, and subsequent lyophylization yielded almost 50 g of a mixture of lactose and neutral / acidic oligosaccharides.

*Isolation of neutral and acidic oligosaccharide pools by size-exclusion chromatography*

Portions (750 mg) of the oligosaccharide pool of goat colostrum were applied separately to a column (2.5 x 170 cm) of Sephadex G25 (Sigma-Aldrich), eluted with 20% aqueous ethanol at a flow rate of 2 mL/min. Fractions of 4.4 mL were collected, and their absorbance at 210 nm was monitored using a variable-wavelength UV-monitor (Uvikon, Bruker, Bremen, Germany). Additionally, aliquots of each fraction were analyzed for their hexose content using the phenol-$H_2SO_4$ assay. Carbohydrate-positive fractions were pooled into two subfractions, one containing acidic oligosaccharides (fraction **B**) and one containing neutral oligosaccharides with lactose as major component (fraction **C**). Both fractions were concentrated and lyophilized.

*β-Galactosidase treatment of the neutral oligosaccharide pool*

Sephadex G25 fraction **C** (1.5 g) was dissolved in distilled water (1 mL), then incubated with 250 U β-galactosidase (*E. coli*) for 16 h at 37°C with gentle stirring. The digestion was monitored by ascending paper chromatography on Whatman 1 Chr paper using *n*-butanol-pyridine-water (5:3:2, v/v) as eluent. Sugars were located with an alkaline $AgNO_3$ reagent. The process was interrupted before complete lactose digestion. After heating for 2 min at 100°C, the solution was filtered over Whatman GF/A paper, then lyophilized.

*Isolation of the lactose-free pool of neutral oligosaccharides*

The β-galactosidase-treated Sephadex G25 Fraction **C** was separated into two parts of 750 mg, each dissolved in 0.5 mL distilled water, and applied to a Toyopearl TSK HW40S column (2.6 x 60 cm; Supelco, Bellefonte, PA, USA), eluted with 20% aqueous ethanol at a flow rate of 0.7 mL/min. Fractions were collected every 5 min, and their absorbance at 210 nm was monitored. Aliquots of each fraction were analyzed for their hexose content by the phenol-$H_2SO_4$ assay. The effective separation between neutral oligosaccharides, lactose, and monosaccharides was verified by ascending paper chromatography on Whatman 1 Chr paper using *n*-butanol-pyridine-water (5:3:2, v/v) as eluent. Sugars were located with an alkaline $AgNO_3$ reagent.

*Monosaccharide analysis*

Oligosaccharides were subjected to methanolysis (methanolic 1 M HCl, 18 h, 85°C), and the resulting mixtures of (methyl ester) methyl glycosides were trimethylsilylated using hexamethyldisilazane-trimethylchlorosilane-pyridine (1:1:5, v/v), and quantitatively analyzed by GLC.

*Methylation analysis*

Permethylation was carried out essentially as described[29]. Permethylated oligosaccharides were hydrolyzed with 2 M trifluoroacetic acid (2 h, 120°C). The resulting partially methylated monosaccharides were reduced with $NaBD_4$ (2 h, room temperature), and the alditols acetylated[30,31]. GLC-EI/MS analysis of the mixtures of partially methylated alditol acetates was carried out on a MD800/8060 system (Fisons

Instruments, Manchester, UK), equipped with a WCOT CP-SIL 5CB fused-silica capillary column (25 m x 0.25 mm; Chrompack, Middelburg, The Netherlands), using a temperature program of 140-240°C at 4°C/min.

*High-pH anion-exchange chromatography with pulsed amperometric detection (HPAEC-PAD) analysis*

Qualitative and preparative HPAEC of the lactose-free neutral and acidic oligosaccharide pools were performed on a Dionex (Sunnyvale, CA, USA) HPLC A1 450 instrument, equipped with a CarboPac precolumn (3 x 25 mm; Dionex) and a CarboPac PA-1 (4 x 250 mm; Dionex) column, mainly as reported earlier[32,33]. Briefly, a solution of an oligosaccharide pool (0.5 mg) in water (50 μL) was injected on a CarboPac PA-1 column, running at 0.7 mL eluent/min at room temperature. The eluents used for the analysis of neutral and acidic oligosaccharides were 100 mM NaOH (eluent 1) and 100 mM NaOH in 1 M NaOAc (eluent 2). The two eluents were mixed according to the following gradient: isocratically with 100% eluent 1 for 10 min; linear gradient to 95% eluent 1 and 5% eluent 2 in 8 min; linear gradient to 90% eluent 1 and 10% eluent 2 in 12 min; isocratically at 90% eluent 1 and 10% eluent 2 in 7 min; linear gradient to 50% eluent 1 and 50% eluent 2 in 10 min; isocratically at 50% eluent 1 and 50% eluent 2 in 5 min. HPAEC profiles were obtained by pulsed amperometric detection. The major fractions were collected, immediately neutralized by on-line addition of 0.1 M HCl, then applied to carbon columns (Carbograph Extract-clean columns, Alltech, Deerfield, IL, USA) for desalting, and recovered by elution with 25% aqueous acetonitrile.

*Matrix-assisted laser desorption/ionization time-of-flight mass spectrometry (MALDI-TOF-MS)*

MALDI-TOF-MS analyses were performed on a Biflex™ III time-of-flight mass spectrometer (Bruker Saxonia Analytik, GmbH, Leipzig, Germany), equipped with a pulsed nitrogen laser emitting at 337 nm. Neutral and acidic oligosaccharides were analyzed in the linear and the reflector positive-ion mode, with an accelerating voltage of 19 kV. Samples were dissolved in water (0.2-1 μg/μL) and mixed 1:1 with the matrix 2,5-dihydroxybenzoic acid (DHB) in water-ethanol (80:20, v/v) (10 μg/μL). 1 μL of this mixture was then allowed to dry on a mass spectrometer target plate, and the obtained spot

was re-crystallized *in situ* from 0.5 μL methanol[34]. The acidic fractions were also run in the negative-ion mode using the matrix 6-aza-2-thiothymine (ATT) in ethanol-20 mM dibasic ammonium citrate (1:1, v/v) (10 μg/μL)[35].

*NMR spectroscopy*

Samples for NMR analysis were dissolved in $D_2O$ (99.96 atom% D, Isotec, USA), and spectra were recorded on a Bruker AMX-500 instrument at a probe temperature of 300 K. Acetone ($\delta = 2.225$) was used as internal standard. 1D $^1H$ NMR spectra were recorded by applying a WEFT pulse as described[36]. 2D TOCSY spectra were recorded with mixing times of 10, 50, and 100 ms; 2D ROESY spectra with mixing times of 200-250 ms. $^1H/^{13}C$ HSQC spectra were recorded using z-gradients for coherence selection; they were phase sensitive using echo/antiecho gradient selection. Spectra were acquired with the proton offset at about 4.6 ppm and a sweep width of about 6 ppm. In the $^{13}C$ dimension the offset was placed around 80 ppm and a sweep width of 60 ppm was used. 2D HSQC-TOCSY spectra[37] were recorded with mixing times of 60 ms. Usually, 300-350 free induction decays of 1024 data points were acquired using 64-256 scans per decay. NMR data sets were processed using ProspectND software (Bijvoet Center, Utrecht University). Briefly, the final matrix size was zero-filled to 2Kx1K or 4Kx2K and multiplied with a phase-shifted (squared-)sine-bell function prior to Fourier transformation. All chemical shifts of adequately resolved signals were determined from $^1H$ 1D spectra, and are represented with three decimals. Values obtained from 2D spectra are instead given with two decimals (protons) or one decimal (carbon), respectively.

*Adhesion test*

Cell lines of intestinal epithelial adenocarcinoma of human colon (Caco-2 long term cultures, ATCC HBT37) were used to test the effects of acidic oligosaccharides on the adhesion of *Escherichia coli* (serotype 0119; enteropathogenic, clinical strain isolated from faeces) and *Salmonella fyris* (strain B8132; clinical strain isolated from faeces). The Caco-2 cells were grown in 25 $cm^2$ plastic tissue culture flasks (Corning, NY, USA) at 37°C in a humidified atmosphere of 5% $CO_2$ in air. The culture medium (Dulbecco's modified Eagle essential medium, DMEM) contained 25 mM glucose, 4 mM L-glutamine, 3.7 mg/mL $NaHCO_3$, and 1% (w/v) non-essential amino acids, and was supplemented

with 10% (v/v) fetal calf serum (Gibco®, Invitrogen, Paisley, Scotland), 100 U penicillin/mL, and 100 μg streptomycin/mL. Confluent cell monolayers were trypsinized and adjusted to a concentration of 2.5 x $10^5$ cells/mL in culture medium; 1 mL cell suspension was dispensed into each 22 mm well of a 12-well tissue culture plate (Corning), and incubated to obtain, after 4 days, semiconfluent monolayers and, after 15 days, fully differentiated monolayers. The adhesiveness of *E. coli* and *S. fyris* to Caco-2 cells was tested on 15-day old cultures, after the confluence of monolayers and the formation of tight junctions and microvilli. *E. coli* was grown on MacConkey agar (Merck, Darmstadt, Germany) at 37°C for 18 h, then suspended in DMEM at a concentration of 2 x $10^8$ CFU/mL (CFU = colony-forming units). *S. fyris* was grown at 37°C for 18-24 h in trypticase soy broth (TSB), Lauria-Bertani broth, or nutrient broth. To bring forth bacterial infection, 0.5 mL bacterial inoculum ($10^8$ CFU/mL) was added to Caco-2 cells. After 2 h of incubation at 37°C in 5% $CO_2$, the cells were washed three times with PBS to remove non-adherent bacteria, then lysed in Triton X-100 (0.1% in cold sterile water) to kill the cells and release adherent bacteria. CFUs of viable bacteria were counted by plating suitable dilutions of the lysates on BHI agar, incubated for 2 days at 37°C. Results were expressed as percentages of the initial inoculum. In inhibition experiments, before bacterial infection, Caco-2 cells at a concentration of 2.4 x $10^6$ cells/mL were incubated for 1 h at 37°C in 5% $CO_2$ with oligosaccharide fractions dissolved in DMEM at a concentration of 1, 5 and 10 mg/mL. Lactose was used as a blank, since it is known not to bring forth any inhibitory activity toward bacteria. Experiments were carried out in triplicate and repeated three times.

Bacterial adhesion to Caco-2 monolayers was evaluated by Gram staining. Stained monolayers grown on slides (SlideFlask; Nunc, Roskilde, Denmark) were examined microscopically[38]. The percentage of Caco-2 cells with associated bacteria was determined by counting all Caco-2 cells in ten random microscopic areas. A positive result was scored when there was at least one bacterial cell per Caco-2 cell. The number of cell-associated bacteria was determined by examining 100 cells.

## Results

*Generation of goat lactose-free neutral and acidic colostrum oligosaccharide pools*

Following the protocol, described in Materials and Methods, an oligosaccharide fraction was prepared from pooled goat colostrum. Although more than 80% of lactose could be removed from thawed and manually skimmed goat colostrum, applying a precipitation step with 68% aqueous ethanol, the HPAEC profile of the retentate showed still extremely high amounts of lactose (Figure 1).

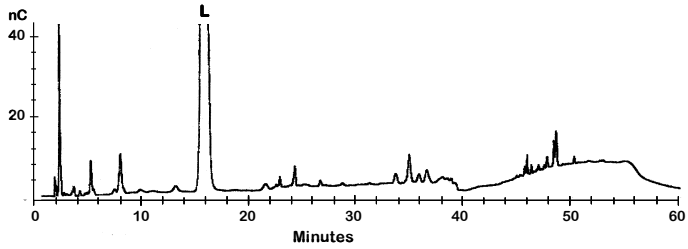


**Figure 1**: HPAEC profile of the oligosaccharide pool (about 80% of the lactose originally present has been removed by crystallization to permit oligosaccharide detection) isolated from goat colostrum. The strong peak **L** at 16 min is due to remaining non-precipitated lactose from the ethanol treatment.

Fractionation of this oligosaccharide pool on Sephadex G25 (Figure 2) yielded three fractions. Fraction **A** contained residual peptides and proteins, and was therefore discarded. Fraction **B** was composed of acidic oligosaccharides, as revealed by HPAEC-PAD analysis (see below) and paper chromatography. The yield of acidic oligosaccharides was about 1.5 g/L of goat colostrum. Fraction **C** contained neutral oligosaccharides including lactose.

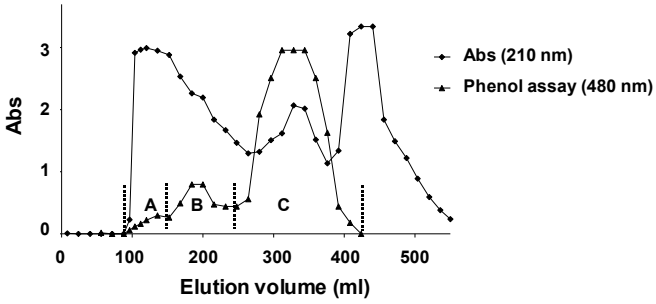


**Figure 2**: Fractionation of the goat colostrum oligosaccharide pool on Sephadex G25. Fraction **A**, residual peptides and proteins; Fraction **B**, acidic oligosaccharides; Fraction **C**, lactose and neutral oligosaccharides.

Since the high content of lactose disturbs the isolation of larger neutral oligosaccharides by size-exclusion chromatography, fraction **C** was subjected to β-galactosidase digestion (16 h, 37°C), thereby converting lactose into galactose and glucose. To avoid β-galactosidase to act also on higher saccharides, the digestion was interrupted by heat denaturation of the enzyme before complete lactose-degradation. After filtration, the digested neutral fraction was loaded on Fractogel Toyopearl TSK HW40S to separate the released monosaccharides and residual lactose from the larger neutral oligosaccharides. A typical example of a preparative separation of 750 mg of a digested neutral oligosaccharide pool **C** is shown in Figure 3.

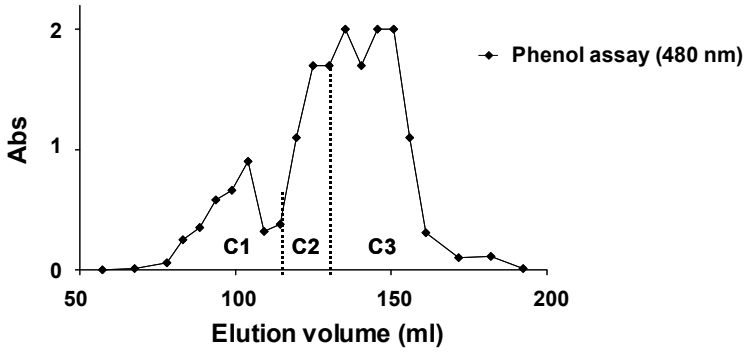


**Figure 3**: Fractionation of the β-galactosidase-treated goat colostrum neutral oligosaccharide pool **C** on Toyopearl TSK HW40S. Fraction **C1**, higher oligosaccharides; Fraction **C2**, traces of lactose and tri- and tetrasaccharides; Fraction **C3**, residual lactose, small oligosaccharides, and monosaccharides.

Three major fractions, **C1**, **C2**, and **C3**, were collected and screened by HPAEC-PAD (see below) and paper chromatography. Fraction **C1** contained oligosaccharides with DP >4. Fraction **C2** contained mainly neutral tri- and tetrasaccharides, and was almost free of lactose. Fraction **C3** turned out to contain residual lactose and traces of neutral compounds; therefore this fraction was digested again with β-galactosidase followed by gel-filtration on Fractogel Toyopearl TSK HW40S. The obtained mixture of lactose-free small neutral oligosaccharides was pooled with fraction **C2**. Following this protocol, in total about 2.0 g of lactose-free neutral oligosaccharides could be isolated from 1 L of goat colostrum.

A similar protocol applied to goat milk or whey yielded similar amounts of acidic (1.5 g/L) and neutral (2.0 g/L) oligosaccharides.

*Evaluation of the trans-glycosylation activity of β-galactosidase*

To evaluate the β-galactosidase trans-glycosylation activity under the applied conditions, lactose was used as a model substrate. The saccharide pattern before and after enzymatic digestion was investigated by methylation analysis. As is clear from Figure 4, the peak of 4-substituted glucose has disappeared after β-galactosidase treatment, while a peak due to free glucose appeared. No other macroscopic changes could be detected; only a trace peak eluting after 13.186 min revealed the presence of 6-substituted galactose, as indicated by GLC-EI/MS and comparison with reference compounds.

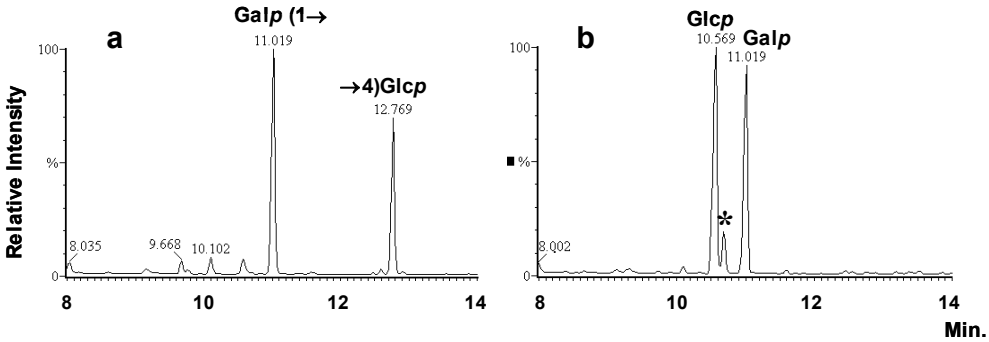


**Figure 4**: Methylation analysis of lactose (**a**) before and (**b**) after enzymatic digestion with β-galactosidase. The peak indicated with * is due to non-saccharide structures (GLC-EI/MS analysis).

*HPAEC profiling of goat colostrum oligosaccharides*

HPAEC-PAD on CarboPac PA-1 was used to analyse major oligosaccharide fractions obtained at each stage of the isolation procedure. Under the applied conditions, both acidic and neutral compounds could be well resolved in the same run. Column calibrations were performed using the following commercially available human milk oligosaccharides, listed according to increasing retention times: LNDFH II (6.80 min), TFLNH (7.95 min), DFLNH b (9.05 min), DFLNH (10.05 min), DFLNH I (11.30 min), 3'FL (12.05 min), LNFP II (13.35 min), lactose (16.50 min), 2'FL (18.20 min), LNFP I (22.70 min), MFLNH II (24.00 min), LNnT (24.50 min), LNnH (25.50 min), LNT (26.60 min), LNH (27.90 min), FSLNnH (29.70 min), 6'SLN (34.00 min), LST c (35.00 min), 6'SL (35.40 min), 3'SL (36.00 min), LST a (37.80 min), and DSLNT (47.40 min). With the applied gradient protocol (see Materials and Methods), lactose has a retention time of 16.5 min, fucosylated neutral oligosaccharides elute between 7 and 24 min, non-fucosylated neutral

oligosaccharides between 16 and 28 min, monosialylated oligosaccharides between 29 and 38 min, and disialylated structures > 45 min. However, for reasons of convenience, the isolation of products was carried out by HPAEC starting from acidic oligosaccharide pool **B** (see Figure 2) and neutral oligosaccharide pool **C2** (see Figure 3).

In Figure 5a and 5b typical HPAEC profiles of the goat colostrum acidic (fraction **B**) and neutral (fraction **C2**) oligosaccharides, respectively, are depicted. As is evident from Figure 5, the applied work-up methodology allows a good separation between acidic and neutral compounds, whereas lactose can be efficiently removed from the neutral fraction by β-galactosidase digestion. The HPAEC profiles show highly heterogeneous patterns: more than 10 peaks can be visualized in the chromatogram of the neutral fraction and more than 9 in the profile of the acidic fraction, suggesting a more complex pattern than previously reported[23].

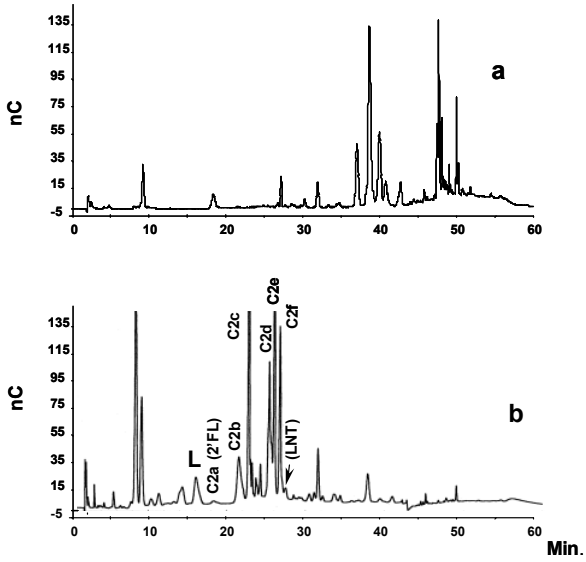


**Figure 5**: HPAEC profiles of (**a**) goat colostrum acidic oligosaccharide fraction **B** and (**b**) goat colostrum neutral oligosaccharide fraction **C2**. **L** indicates the peak of residual lactose, and **C2a-f** the structures isolated by HPAEC and characterized by NMR spectroscopy.

*Characterization of major acidic goat colostrum oligosaccharides*

Major components of the acidic fraction **B** were identified by HPAEC, comparing their retention time with those of the commercial standards. Additionally, standards were added to the acidic fraction to correct for eventual changes in the HPAEC profiles. As a

typical example, in Figure 6 the effect of the addition of 3'SL is shown. From these analyses, it could be concluded that the major monosialyloligosaccharides (sialyl = *N*-acetylneuraminyl) obtained from goat colostrum are the α2-3 and α2-6 isomers of sialyllactose (3'SL and 6'SL), and the α2-6 isomer of sialyl-*N*-acetyllactosamine (6'SLN).

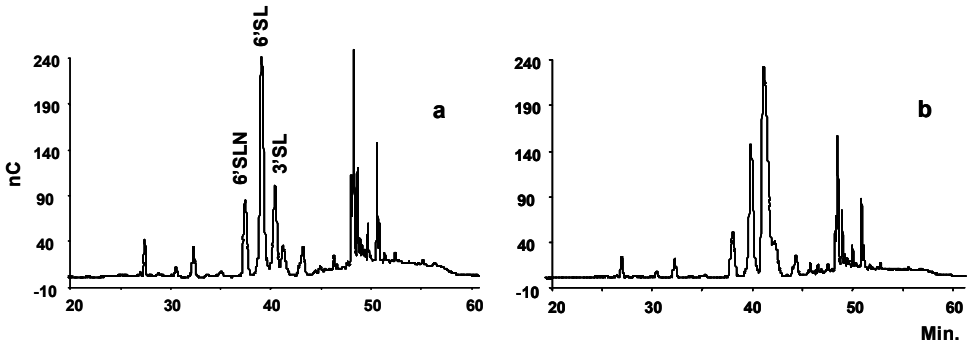


**Figure 6**: HPAEC profiles of the goat colostrum acidic oligosaccharide fraction **B** (**a**) without and (**b**) with added 3'SL. Major components identified by comparison with standards are indicated.

Major as well as minor components in fraction **B** were identified by MALDI-TOF-MS analysis. In the positive-ion mode, the acidic oligosaccharides were detected as multiple sodium-adduct ions. In the negative-ion mode, monosialyloligosaccharides were detected as $[M-H]^-$ ions, while compounds containing two sialic acid residues were detected as $[M+Na-2H]^-$ adduct ions. MS profiling in the negative-ion mode revealed a molecular mass distribution ranging from about *m/z* 600 to 1700 (Figure 7). The three peaks at *m/z* 633, 649, and 674 reflect the presence of *N*-acetylneuraminyllactose (SL), *N*-glycolylneuraminyllactose (Neu5Gc-L), and *N*-acetylneuraminyllactosamine (SLN), respectively. In addition, *N*-glycolylneuraminyl-*N*-acetyllactosamine (Neu5Gc-LN; *m/z* 690), sialylgalactosyllactose (S-Gal-L; *m/z* 795), and disialyllactose (DSL *m/z* 946) were identified. Peaks sometimes detected at *m/z* 811 and *m/z* 836 indicate the presence of a tetrasaccharide containing *N*-glycolylneuraminic acid (Neu5Gc-Gal-L) and S-HexNAc-L, respectively (data not shown). Minor components were detected up to *m/z* 1677.

For an overview of the MALDI-TOF-MS data, see Table 1. Most of the proposed structures have been reported earlier for goat colostrum or milk[39,40].

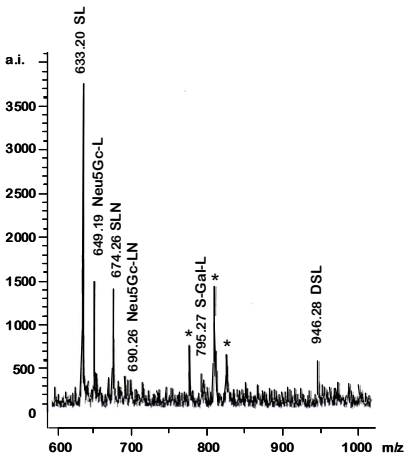


**Figure 7**: Negative-ion mode MALDI-TOF mass spectrum of acidic oligosaccharides from goat colostrum. Monosialyl oligosaccharides were detected as deprotonated molecules, while structures containing two sialic acid residues were detected as monosodium adduct. Only the region from *m/z* 600 to 1000 is shown. Peaks indicated with * are not due to oligosaccharides.

**Table 1**: Acidic oligosaccharides detected by negative-ion mode MALDI-TOF-MS in goat milk and colostrum. Structures of less abundant components are proposed according to literature data.

| Oligosaccharides | | Mass |
|---|---|---|
| SL | Neu5Ac(α2-3)Gal(β1-4)Glc[c] | 633[a] |
| | Neu5Ac(α2-6)Gal(β1-4)Glc[c] | |
| Neu5Gc-L | Neu5Gc(α2-6)Gal(β1-4)Glc[c] | 649[a] |
| SLN | Neu5Ac(α2-6)Gal(β1-4)GlcNAc[c] | 674[a] |
| Neu5Gc-LN | Neu5Gc(α2-6)Gal(β1-4)GlcNAc[d] | 690[a] |
| S-Gal-L | Gal(β1-6)[Neu5Ac(α2-3)]Gal(β1-4)Glc[c] | 795[a] |
| | Gal(β1-3)[Neu5Ac(α2-6)]Gal(β1-4)Glc[c] | |
| Neu5Gc-Gal-L | Neu5Gc-Gal-Gal(β1-4)Glc | 811[a] |
| S-HexNAc-L | Neu5Ac-HexNAc-Gal(β1-4)Glc | 836[a] |
| DSL | Neu5Ac(α2-8)Neu5Ac(α2-3)Gal(β1-4)Glc[d] | 946[b] |
| S-Neu5Gc-L | Neu5Ac-Neu5Gc-Gal(β1-4)Glc | 962[b] |
| S-$HexNAc_2$-L | Neu5Ac-$HexNAc_2$-Gal(β1-4)Glc | 1061[b] |
| DS-LNH | $Neu5Ac_2$-(Gal-GlcNAc)$_2$-Gal(β1-4)Glc | 1677[b] |

Abbreviations: Gal, galactose; Glc, glucose; Neu5Ac, *N*-acetylneuraminic acid; Neu5Gc, *N*-glycolylneuraminic acid; S, sialic acid; L, lactose; LN, *N*-acetyl lactosamine; HexNAc, *N*-acetylhexosamine; DS, (sialic acid)$_2$; LNH, lacto-*N*-hexaose.

[a]deprotonated form
[b]deprotonated monosodium adduct ion
[c]reported in goat colostrum or milk[39,40]
[d]reported in cow colostrum or milk[41,42]

*Characterization of major neutral goat colostrum oligosaccharides*

In the HPAEC profile of the neutral oligosaccharide fraction **C2**, only 2'FL and LNT could be assigned by comparison with retention times of the human milk standards. Therefore, the major components were isolated by preparative HPAEC (Figure 5b), and further characterized by NMR spectroscopy.

MALDI-TOF-MS analysis of fraction **C2b** showed the presence of a trisaccharide {*m/z* 527, $(Hex)_3$, $[M + Na]^+$}; monosaccharide analysis together with methylation analysis indicated the occurrence of terminal Gal*p*, 6-substituted Gal*p*, and 4-substituted Glc*p*. 1D $^1H$ NMR analysis (Figure 8a) showed four anomeric doublets at δ 5.221, 4.667, 4.484/4.481, and 4.460/4.455, assigned to α-D-Glc*p* (reducing), β-D-Glc*p* (reducing), β-D-Gal*p* (terminal) and β-D-Gal*p* (internal), respectively.

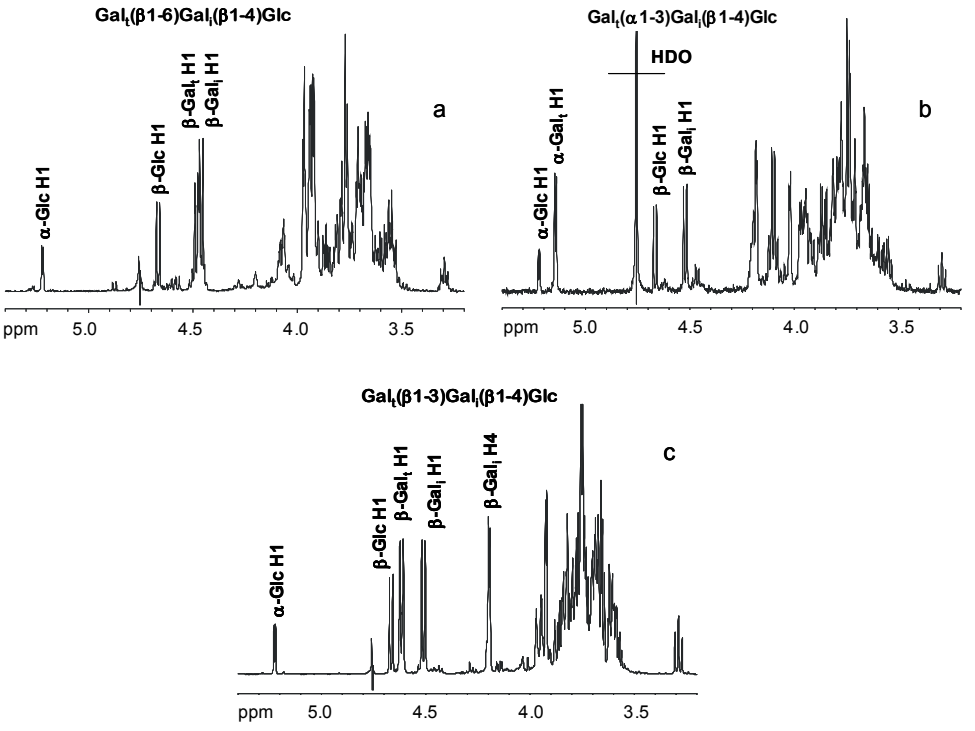


**Figure 8**: 500 MHz $^1H$-NMR spectra in $D_2O$ of (**a**) fraction **C2b**, (**b**) fraction **C2d**, and (**c**) fraction **C2f**, recorded at 300K.

Detailed NMR assignments were achieved by 2D COSY, TOCSY, ROESY, and HSQC (Figure 9) measurements (Table 2).

**Table 2**: $^{1}$H and $^{13}$C Chemical shifts of β-D-Gal*p*-(1→6)-β-D-Gal*p*-(1→4)-D-Glc*p*

| | β-D-Galp-(1- ($Gal_t$) | -6)-β-D-Galp-(1- ($Gal_i$) | -4)-α-D-Glcp (αGlc) | -4)-β-D-Glcp (βGlc) |
|---|---|---|---|---|
| H-1 | 4.484/4.481[a] | 4.460/4.455[a] | 5.221 | 4.667 |
| H-2 | 3.54 | 3.57 | 3.59 | 3.292 |
| H-3 | 3.67 | 3.68 | 3.85 | 3.66 |
| H-4 | 3.92 | 3.97 | 3.65 | 3.66 |
| H-5 | 3.71 | 3.95 | 3.95 | 3.61 |
| H-6 | 3.76 | 3.92 | 3.87 | 3.80 |
| H-6' | 3.79 | 4.07 | 3.87 | 3.95 |
| C-1 | 106.2 | 106.0 | 94.7 | 98.6 |
| C-2 | 73.7 | 73.7 | 74.0 | 76.6 |
| C-3 | 75.5 | 75.3 | 74.5 | 77.5 |
| C-4 | 71.5 | 71.3 | 82.3 | 82.0 |
| C-5 | 78.0 | 76.9 | 72.8 | 77.6 |
| C-6 | 63.8 | 72.0 | 62.8 | 63.0 |

[a] Doubling, due to the reducing Glc unit in α- and β-form

To assign overlapping proton signals, a HSQC-TOCSY experiment was carried out; Figure 10 shows part of the anomeric region, including correlations between H1/C1 of β-D-Glc*p* and β-D-Gal*p* and their corresponding C2, C3, and C4 atoms. The various data indicate the compound to be β-D-Gal*p*-(1→6)-β-D-Gal*p*-(1→4)-D-Glc*p*[43].

MALDI-TOF-MS analysis of fraction **C2f** showed the occurrence of one main trisaccharide {*m/z* 527, $(Hex)_3$, $[M + Na]^+$}. Monosaccharide analysis revealed the presence of D-Gal and D-Glc in the molar ratio of 2:1, and methylation analysis the occurrence of terminal Gal*p*, 3-substituted Gal*p*, and 4-substituted Glc*p*. Its 1D $^{1}$H NMR spectrum (Figure 8c) presented four anomeric signals at δ 5.224, 4.668, 4.616, and 4.513, identified as belonging to α-D-Glc*p* (reducing), β-D-Glc*p* (reducing), β-D-Gal*p* (terminal), and β-D-Gal*p* (internal), respectively. Detailed NMR assignments were obtained by 2D TOCSY (Figure 11) and HSQC (Figure 12) measurements (Table 3).

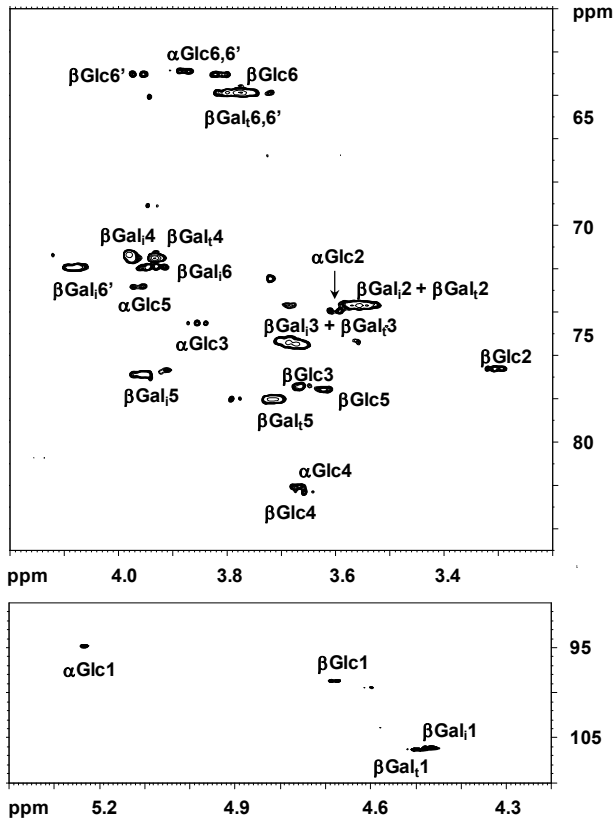


**Figure 9**: HSQC spectrum of β-D-Gal*p*-(1→6)-β-D-Gal*p*-(1→4)-D-Glc*p* (fraction **C2b**) in $D_2O$ at 300K. Assignments are indicated next to the relevant contours. The signals for the β-D-Gal*p* units are differentiated by subscripts "i" (internal) and "t" (terminal).

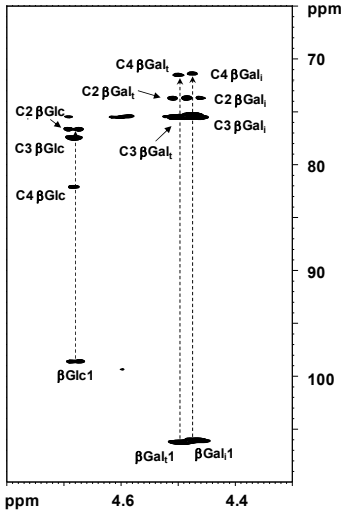


**Figure 10**: Part of the anomeric region of the HSQC-TOCSY spectrum of fraction **C2b** in $D_2O$ at 300K. Dashed arrows indicate correlations between anomeric signals and corresponding C2, C3, and C4 atoms. The signals for the β-D-Gal*p* units are differentiated by subscripts "i" (internal) and "t" (terminal).

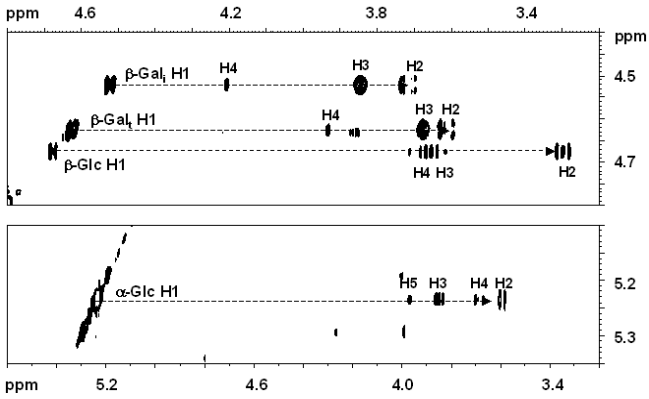


**Figure 11**: 500 MHz 2D TOCSY spectrum (anomeric region) in $D_2O$ of fraction **C2f**. The signals for the β-D-Gal*p* units are differentiated by subscripts "i" (internal) and "t" (terminal).

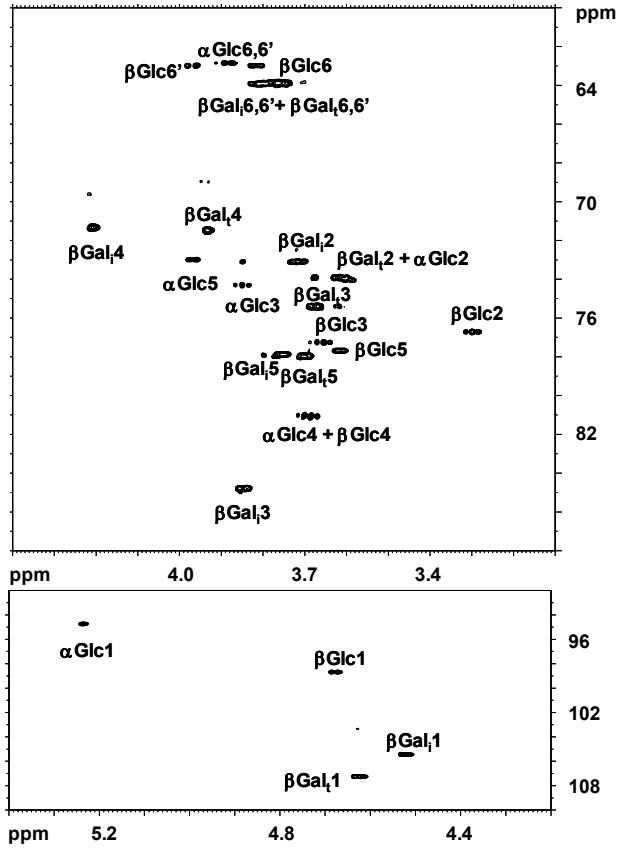


**Figure 12**: HSQC spectrum of β-D-Gal*p*-(1→3)-β-D-Gal*p*-(1→4)-D-Glc*p* (fraction **C2f**) in $D_2O$ at 300K. Assignments are indicated next to the relevant contours.

Sequence analysis, using 2D ROESY (data not shown), demonstrated cross-peaks between β-D-Gal H-1 (terminal) and β-D-Gal H-3 (internal), and between β-D-Gal H-1 (internal) and D-Glc H-4 (reducing). The various data establish the main trisaccharide in fraction **C2f** to be β-D-Gal*p*-(1→3)-β-D-Gal*p*-(1→4)-D-Glc*p*.

**Table 3**: $^{1}$H and $^{13}$C Chemical shifts of β-D-Gal*p*-(1→3)-β-D-Gal*p*-(1→4)-D-Glc*p*

| | β-D-Galp-(1- ($Gal_t$) | -3)-β-D-Galp-(1- ($Gal_i$) | -4)-α-D-Glcp (αGlc) | -4)-β-D-Glcp (βGlc) |
|---|---|---|---|---|
| H-1 | 4.616 | 4.513 | 5.224 | 4.668 |
| H-2 | 3.60 | 3.71 | 3.58 | 3.287 |
| H-3 | 3.67 | 3.84 | 3.84 | 3.64 |
| H-4 | 3.92 | 4.20 | 3.67 | 3.67 |
| H-5 | 3.69 | 3.75 | 3.96 | 3.60 |
| H-6 | 3.8-3.7 | 3.8-3.7 | 3.87 | 3.80 |
| H-6’ | 3.8-3.7 | 3.8-3.7 | 3.87 | 3.96 |
| C-1 | 107.2 | 105.4 | 94.7 | 98.7 |
| C-2 | 73.9 | 73.1 | 74.0 | 76.7 |
| C-3 | 75.4 | 84.8 | 74.3 | 77.2 |
| C-4 | 71.5 | 71.3 | 81.0 | 81.1 |
| C-5 | 78.0 | 77.9 | 73.0 | 77.7 |
| C-6 | 63.9 | 63.9 | 62.8 | 63.0 |

Fraction **C2d** was analyzed following the same protocol. The combined data of the MALDI-TOF-MS analysis {*m/z* 527, $(Hex)_3$, $[M + Na]^+$}, the monosaccharide analysis (Gal:Glc = 2:1), the methylation analysis (terminal Gal*p*, 3-substituted Gal*p*, 4-substituted Glc*p*), and the 1D $^{1}$H NMR analysis (Figure 8b; H-1’s at δ 5.222, 5.143, 4.665, and 4.524, belonging to α-D-Glc*p* (reducing), α-D-Gal*p*, β-D-Glc*p* (reducing), and β-D-Gal*p*, respectively), support the trisaccharide in fraction **C2d** to be α-D-Gal*p*-(1→3)-β-D-Gal*p*-(1→4)-D-Glc*p*[43].

MALDI-TOF-MS analysis of fraction **C2a** indicated the presence of a trisaccharide {*m/z* 511, $dHex(Hex)_2$, $[M + Na]^+$}. Monosaccharide analysis showed Fuc, Gal, and Glc in the molar ratio of 1:1:1, and methylation analysis revealed the occurrence of terminal Fuc*p*, 2-substituted Gal*p*, and 4-substituted Glc*p*. 1D $^{1}$H NMR analysis presented a characteristic $CH_3$ signal at δ 1.226 of L-Fuc*p*, and a series of anomeric doublets at δ 5.315 (α-L-Fuc*p*), δ 5.227 (α-D-Glc*p*, reducing unit), δ 4.634 (β-D-Glc*p*, reducing unit),

and δ 4.526 (β-D-Gal*p*). Combination of the various results identifies the structure as α-L-Fuc*p*-(1→2)-β-D-Gal*p*-(1→4)-D-Glc*p*[43].

The oligosaccharides in fractions **C2c** and **C2e** are mainly tri- and tetrasaccharides, as indicated by MALDI-TOF-MS. Both miss the β-D-Gal*p*-(1→4)-D-Glc*p* moiety, suggesting that they have been formed by a trans-galactosylation reaction during lactose hydrolysis with *E. coli* β-galactosidase. Methylation analysis as well as HSQC experiments showed the presence of 6-linked Gal and Glc residues. A detailed analysis of these products is presented elsewhere (Beccati *et al.*, 2008).

*Profiling of the neutral goat colostrum oligosaccharide fraction by MALDI-TOF-MS*

MALDI-TOF-MS analysis in the positive-ion mode (DHB as matrix) of the intact neutral goat oligosaccharide fraction gave rise to a series of $[M + Na]^+$ adduct ions, with low-intensity signals for $[M + K]^+$ adduct ions (Figure 13).

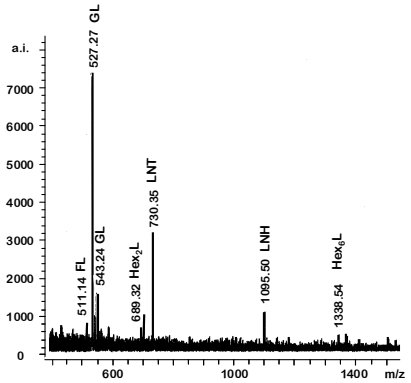


**Figure 13**: Positive-ion mode MALDI-TOF mass spectrum of neutral oligosaccharides from goat colostrum.

The most prominent peak detected at *m/z* 527 ($[M + Na]^+$), with a satellite at *m/z* 543 ($[M + K]^+$), has to be due to a mixture of galactosyllactose trisaccharides (GL), namely 3'-α-galactosyllactose, 3'-β-galactosyllactose, and 6'-β-galactosyllactose, as already demonstrated above by NMR analysis (Figure 8). The peak at *m/z* 689 can be attributed to digalactosyllactose tetrasaccharides ($Hex_2L$), and the peaks at *m/z* 511 and 730 are due to 2'-fucosyllactose (FL) (for NMR analysis, see above) and lacto-*N*-tetraose (LNT), respectively. A peak at *m/z* 1095 has been attributed to LNH.

A survey of the MALDI-TOF-MS data is presented in Table 4. Besides the major components, for several trace components monomer compositions could be formulated, and a possible structure has been proposed guided by literature data. Interestingly, high-

molecular-mass oligosaccharides such as LNO-F and LND could be identified. Most of the proposed structures have been reported earlier for goat colostrum or milk[43-45].

**Table 4**: Neutral oligosaccharides detected by positive-ion mode MALDI TOF-MS in goat milk and colostrum.

| Oligosaccharides | | Mass[a] |
|---|---|---|
| Major components | | |
| FL | Fuc(α1-2)Gal(β1-4)Glc[b] | 511 |
| GL | Gal(α1-3)Gal(β1-4)Glc[b] | 527 |
| | Gal(β1-3)Gal(β1-4)Glc[b] | |
| | Gal(β1-6)Gal(β1-4)Glc[b] | |
| GalNAc-L | GalNAc(α1-6)Gal(β1-4)Glc[b] | 568 |
| $Hex_2L$ | Gal(β1-3)Gal(β1-3)Gal(β1-4)Glc[c] | 689 |
| Trace components | | |
| LNT | Gal(β1-4)GlcNAc(β1-3)Gal(β1-4)Glc[d] | 730 |
| | Gal(β1-4)GlcNAc(β1-6)Gal(β1-4)Glc[b,d] | |
| LNFP | Gal(β1-4)[Fuc(α1-3)]GlcNAc(β1-6)Gal(β1-4)Glc[b] | 876 |
| | Gal(β1-3)GlcNAc(β1-6)Gal(β1-4)[Fuc(α1-3)]Glc[b] | |
| $Hex_2$GlcNAc-L | Gal(β1-4)[Gal(β1-3)]GlcNAc(β1-3)Gal(β1-4)Glc[b] | 892 |
| $Hex_3L$ | Gal(β1-3)Gal(β1-3)Gal(β1-3)Gal(β1-4)Glc[c] | 851 |
| $Hex_4L$ | Gal(β1-3)Gal(β1-3)Gal(β1-3)Gal(β1-3)Gal(β1-4)Glc[c] | 1013 |
| LNH | Gal(β1-4)GlcNAc(β1-6) \ Gal(β1-4)Glc[d] / Gal(β1-4)GlcNAc(β1-3) | 1095 |
| $Hex_6L$ | $Hex_6$-Gal(β1-4)Glc | 1338 |
| $Hex_8L$ | $Hex_8$-Gal(β1-4)Glc | 1662 |
| $Hex_{10}L$ | $Hex_{10}$-Gal(β1-4)Glc | 1986 |
| LNO-F | $(Gal\text{-}GlcNAc)_3Fuc$-Gal(β1-4)Glc | 1606 |
| LNO-$F_2$ | $(Gal\text{-}GlcNAc)_3Fuc_2$-Gal(β1-4)Glc | 1753 |
| LNH-$F_5$ | $(Gal\text{-}GlcNAc)_2Fuc_5$-Gal(β1-4)Glc | 1826 |
| LND | $(Gal\text{-}GlcNAc)_4$-Gal(β1-4)Glc | 1826 |
| LND-F | $(Gal\text{-}GlcNAc)_4Fuc$-Gal(β1-4)Glc | 1972 |
| LN12-$F_4$ | $(Gal\text{-}GlcNAc)_5Fuc_4$-Gal(β1-4)Glc | 2776 |

Abbreviations: Glc, glucose; Gal, galactose; Fuc, fucose; GlcNAc, *N*-acetylglucosamine; GalNAc, *N*-acetylgalactosamine; Hex, hexose (Glc or Gal); L, lactose; FL, fucosyllactose; GL, galactosyllactose; LNT, lacto-*N*-tetraose; LNFP, lacto-*N*-fucopentaose; LNH, lacto-*N*-hexaose; LNO, lacto-*N*-octaose; LND, lacto-*N*-decaose; LN12, lacto-*N*-dodecaose.

[a]monosodium adduct ion

[b]reported in goat colostrum or milk[44,45]

[c]reported in tammar wallaby milk[46]

[d]reported in horse colostrum[47]

*Oligosaccharide isolation from sheep and cow milk*

The protocol developed for the isolation of oligosaccharides from goat colostrum and milk was also successfully applied to milks from other sources, notably sheep and cow. The neutral fractions from sheep, goat, and cow milk also appeared to be mainly composed of α3'-galactosyllactose, β3'-galactosyllactose, and β6'-galactosyllactose, and contain minor amounts of tetrasaccharides with the molecular formulae $Hex_2L$, HexNAc-L, LNT. Moreover, traces of octa- and nonasaccharides were found. In Figure 14 a comparison of the HPAEC profiles of the neutral fractions obtained from sheep, goat and cow milk is shown. Preliminary results indicate that the oligosaccharide recovery from sheep and cow milk is in the same range as of goat colostrum/milk (e.g. 1.5-2 g of lactose-free neutral oligosaccharides from 1 L of milk).

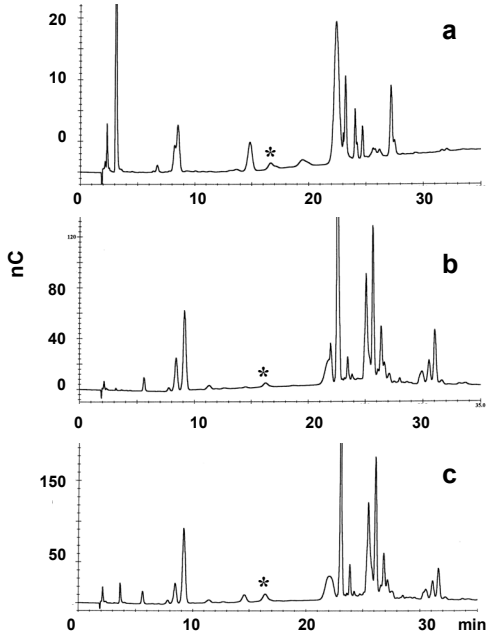


**Figure 14:** HPAEC profiles of neutral oligosaccharide pools from (**a**) sheep, (**b**) goat, and (**c**) cow milk. Traces of residual lactose are indicated with *.

*Biological assay on the isolated acidic fraction*

Cell lines of intestinal epithelial adenocarcinoma of human colon (Caco-2) were used to test the effects of acidic milk oligosaccharides on the adhesion of *E. coli* and *S. fyris*. Counts of colony-forming units (CFU) indicated that bacteria associated with the monolayers ranged from 2 to 3% of initial inoculum. In Gram-stained preparations, approximately 80% of the Caco-2 cells with associated bacteria (30-40 bacteria per cell) were observed (Figure 15).

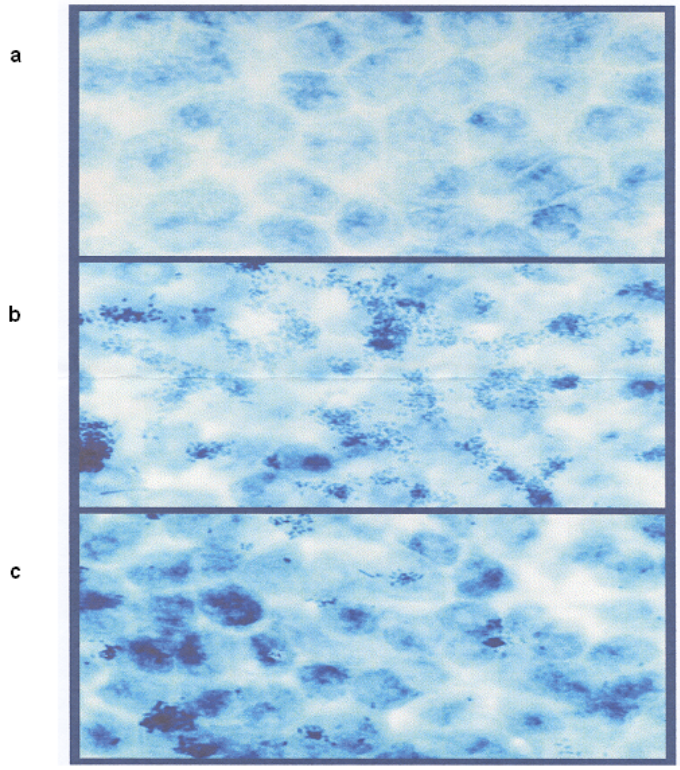


**Figure 15**: (**a**) Caco-2 long term culture, (**b**) Caco-2 long term culture after adhesion of enteropathogenic *E. coli* strain 0119, (**c**) Caco-2 long term culture after incubation for 60 min at 37ºC with 10 mg/mL 3'-SL followed by adhesion of *E. coli*.

To perform inhibition experiments, before bacterial infection Caco-2 cells were incubated with oligosaccharide fractions at the concentration of 10 mg/mL. Results of the inhibition test performed on 3'-sialyllactose (3'-SL), a mixture of 3'-SL plus 6'-SL, and acidic oligosaccharides isolated from goat colostrum are summarized in Table 5. 3'-SL

was effective in inhibiting adhesiveness of *E.coli* to cell cultures, but was completely inactive towards *S. fyris*. On the other hand, 6'-SL displayed a stronger activity towards *S. fyris*. Experiments performed on acidic fractions isolated from goat milk showed that pretreatment of Caco-2 cells with acidic oligosaccharides competitively inhibited the adhesion of *S. fyris*, with an inhibition percentage of 24%. On the contrary, acidic oligosaccharides did not bring forth any significant inhibition activity towards *E. coli*.

**Table 5**: Results of experiments on bacterial adhesiveness inhibition

| Oligosaccharide fraction (10 mg/mL) | % inhibition of Salmonella fyris | % inhibition of Escherichia coli |
|---|---|---|
| Lactose | 0 | 0 |
| 3'SL | 0 | 26 |
| 3'SL+6'SL | 16 | 13 |
| Acidic fraction from goat colostrum | 24 | 0 |

**Discussion**

Traditionally, lactose removal remains by far the main obstacle to the isolation of large amounts of oligosaccharides from non-human milk. Recent studies prove that no enzymatic degradation of human milk oligosaccharides occurs during lactose hydrolysis by β-galactosidase[48]. In addition, being lactose by far the most abundant component of non-human milk, it is believed that interrupting digestion before complete lactose removal could prevent degradation of higher oligosaccharides. Since β-galactosidase possesses also trans-glycosylation activity, it is likely to produce variable amounts of oligosaccharides during lactose hydrolysis. Factors like enzyme source, substrate concentration, salt concentration, temperature, and pH strongly influence this side reaction. However, it has been shown that under controlled conditions, β-galactosidase from *E. coli* operating on skimmed milk gives the lowest conversion rates[49]; oligosaccharides produced by trans-glycosylation account for less than 0.5 % of the total sugar content.

In this paper we present a new fast and scalable approach for the quantitative recovery of, compared with lactose, minor neutral and acidic oligosaccharides from mammalian

milk/colostrum/whey (goat, sheep, and cow). In this approach use has been made of β-galactosidase to degrade lactose, while preserving the original oligosaccharide compositional profile. Reducing the amounts of lactose strongly improves the efficiency of the neutral oligosaccharide fractionation by gel-permeation chromatography. For all three mammals as much as 1.5 g of acidic oligosaccharides and 2.0 g of neutral oligosaccharides could be obtained from 1 L starting material. Using this protocol it is possible to obtain complex oligosaccharides from animal milk in the gram range, which allows undertaking detailed *in vitro* and *in vivo* studies. Recognition of the anti-adhesive role of naturally occurring oligosaccharides and the possibility to isolate them in large scale might lead to their practical utilization as a vehicle of protection against enteric infection for infants who cannot be breast-fed[50].

The development of the new protocol was checked and supported by detailed structural studies of isolated goat colostrum/milk oligosaccharides. Earlier reported differences between this source and human milk could be confirmed. First, in goat milk oligosaccharides two kinds of sialic acid, *N*-acetylneuraminic acid (Neu5Ac) and *N*-glycolylneuraminic acid (Neu5Gc), were found, whereas those from human milk contain Neu5Ac only. Earlier it has been demonstrated that Neu5Gc is present in all mammals apart from humans. This is due to a mutation in CMP-sialic acid hydroxylase that occurred in the hominid lineage subsequent to its divergence from the lineage of the great apes[51,52]. Secondly, goat colostrum contains sialyl-*N*-acetyllactosamine in addition to sialyllactose, while human milk contains only sialyllactose. Thirdly, a striking difference is the near absence of fucosylated oligosaccharides in goat colostrum/milk, being the main components of human milk oligosaccharides. Finally, the main components of the goat colostrum/milk neutral fraction are the trisaccharides α3'-galactosyllactose, β3'-galactosyllactose and β6'-galactosyllactose, which are completely absent in human milk. The question whether the structural differences between human and goat oligosaccharides may lead to different biological functions has still to be answered.

Finally, attention was paid to the bacterial adhesion properties of acidic oligosaccharides from goat colostrum. Human milk oligosaccharides are known to be efficient anti-infective agents by preventing adhesion of microbial pathogens to host cells[53]. To assess whether non-human oligosaccharides could play a similar role, we assayed the ability of acidic fractions to inhibit the adherence of *E. coli* and *S. fyris* to

epithelial cells. While no inhibition towards *E. coli* was detected, acidic oligosaccharides from goat colostrum inhibited adhesion of *S. fyris* to Caco-2 cells to an extent of 24%. This value is higher than the 16% inhibition displayed by a commercial mixture of 3'-SL and 6'-SL (Neu5Ac(α2-3)lactose and Neu5Ac(α2-6)lactose, respectively). Such a difference can be due to the presence in goat colostrum of Neu5Gc(α2-3)lactose and Neu5Gc(α2-6)lactose, which are absent in commercial preparations.

**Acknowledgements**

We gratefully thank Prof. B. Casu for helpful scientific discussions and valuable advice. We acknowledge Dr. S. Rubino (University of Potenza, Italy) for providing the milk samples. This study was supported by a grant from the European Community (NOFA, Contract Fair CT 97-3142).

**References**


[1] Jenness R, Regehr EA, Sloan RE. Comparative biochemical studies of milk. II. Dialyzable carbohydrates. *Comp. Biochem. Physiol.* **1964**, *13*, 339-352.

[2] Kuhn R. Biological importance of amino sugars. *Proc. Intern. Congr. Biochem*. **1959**, *1*, 67-79.

[3] Montreuil J. Glucides of human milk. *Bull. Soc. Chim. Biol*. **1957**, *39*, 395-411.

[4] Newburg DS, Neubauer SH. *Handbook of milk composition* **1995**. Academic Press, New York.

[5] Chai W, Piskarev VE, Zhang Y, Lawson AM, Kogelberg H. Structural determination of novel lacto-*N*-decaose and its monofucosylated analogue from human milk by electrospray tandem mass spectrometry and $^{1}$H NMR spectroscopy. *Arch. Biochem. Biophys*. **2005**, *434*, 116-127.

[6] Kovar MG, Serdula MK, Marks JS, Fraser DW. Review of the epidemiologic evidence for an association between infant feeding and infant health. *Pediatrics* **1984**, *74*, 615-638.

[7] Marild S, Jodal U, Hanson LA. Breastfeeding and urinary-tract infection. *Lancet* **1990**, *336*, 942.

[8] Kunz C, Rudloff S. Biological functions of oligosaccharides in human milk. *Acta Paediatr.* **1993**, *82*, 903-912.

[9] Zopf D, Roth S. Oligosaccharide anti-infective agents. *Lancet* **1996**, *347*, 1017-1021.

[10] Coppa GV, Bruni S, Zampini L, Galeazzi T, Facinelli, Capretti R, Carlucci A, Gabrielli O. Oligosaccharides of human milk inhibit the adhesion of *Listeria monocytogenes* to Caco-2 cells. *Ital. J. Pediatr*. **2003**, *29*, 61-68.

[11] Newburg DS. Oligosaccharides and glycoconjugates in human milk: their role in host defense. *J. Mamm. Gland Biol. Neoplasia* **1996**, *1*, 271-283.

[12] Andersson B, Porras O, Hanson LA, Lagergard T, Svanborg-Eden C**.** Inhibition of attachment of *Streptococcus pneumoniae* and *Haemophilus influenzae* by human milk and receptor oligosaccharides. *J. Infect. Dis.* **1986**, *153*, 232-237.

[13] Coppa GV, Gabrielli O, Giorgi P, Catassi C, Montanari MP, Varaldo PE, Nichols BL. Preliminary study of breastfeeding and bacterial adhesion to uroepithelial cells. *Lancet* **1990**, *335*, 569-571.

[14] Newburg DS, Ruiz-Palacios GM, Morrow AL. Human milk glycans protect infants against enteric pathogens. *Annu. Rev. Nutr.* **2005**, *25*, 37-58.

[15] Idota T, Matsuoka Y. Changes in the content of *N*-acetylneuraminic acid in human milk during lactation. *J. Jpn. Soc. Nutr. Food Sci.* **1994**, *47*, 363-367.

[16] Idota T, Kawakami H, Murakami Y, Sugawara M. Inhibition of cholera toxin by human milk fractions and sialyllactose. *Biosci. Biotechnol. Biochem.* **1995**, *59*, 417-419.

[17] Holmgren J, Svennerholm AM, Ahren C. Nonimmunoglobulin fraction of human milk inhibits bacterial adhesion (hemagglutination) and enterotoxin binding of *Escherichia coli* and *Vibrio cholerae*. *Infect. Immun.* **1981**, *33*, 136-141.

[18] Bezkorovainy A, Miller-Catchpole R. *Biochemistry and Physiology of Bifidobacteria.* CRC Press, Boca Raton, FL **1989**, 30-72.

[19] Yoshioka H, Iseki K, Fujita K. Development and differences of intestinal flora in the neonatal period in breast-fed and bottle-fed infants. *Paediatrics* **1983**, *72*, 317-321.

[20] Sturman JA, Lin YY, Higuchi T, Fellman JH. *N*-acetylneuraminyllactose sulfate: a newly identified nutrient in milk. *Pediatr. Res.* **1985**, *19*, 216-219.

[21] Kyogashima M, Ginsburg V, Krivan HC. *Escherichia coli* K99 binds to *N*-glycolylsialoparagloboside and *N*-glycolyl-GM3 found in piglet small intestine. *Arch. Biochem. Biophys.* **1989**, *270*, 391-397.

[22] Milupa studies for NOFA project, unpublished work.

[23] Urashima T, Saito T, Nakamura T, Messer M. Oligosaccharides of milk and colostrum in non-human mammals. *Glycoconjugate J.* **2001**, *18*, 357-371.

[24] Thurl S, Offermanns J, Muller-Werner B, Sawatzki G. Determination of neutral oligosaccharide fractions from human milk by gel permeation chromatography. *J. Chromatogr.* **1991**, *568*, 291-300.

[25] Thibault J-F. Separation of α-D-galacturonic acid oligomers by chromatography on polyacrylamide gel. *J. Chromatogr.* **1980**, *194*, 315-322.

[26] Kunz C, Rudloff S, Hintelmann A, Pohlentz G, Egge H. High-pH anion-exchange chromatography with pulsed amperometric detection and molar response factors of human milk oligosaccharides. *J. Chromatogr*. **1996**, *685*, 211-221.

[27] Kobata A. Isolation of oligosaccharides from human milk. *Methods Enzymol.* **1972**, *28*, 262-271.

[28] Dubois M, Gilles KA, Hamilton JK, Rebers PA, Smith F. Colorimetric methods for determination of sugars and related substances. *Anal. Chem.* **1956**, *28*, 350-356.

[29] Hakomori S. A rapid permethylation of glycolipids and polysaccharide catalyzed by methylsulfinyl carbanion in dimethyl sulfoxide. *J. Biochem. (Tokyo)* **1964**, *55*, 205-208.

[30] Harris PJ, Henry RJ, Blakeney AB, Stone BA. An improved procedure for the methylation analysis of oligosaccharides and polysaccharides. *Carbohydr. Res* **1984**, *127*, 59-73.

[31] Ciucanu I, Kerek F. A simple and rapid method for the permethylation of carbohydrates. *Carbohydr. Res.* **1984**, *131*, 209-217.

[32] Townsend RR, Hardy MR, Lee YC. Separation of oligosaccharides using high-performance anion-exchange chromatography with pulsed amperometric detection. *Methods Enzymol.* **1989**, *179*, 65-76.

[33] Coppa GV, Pierani P, Zampini L, Carloni I, Bruschi B, Carlucci A, Gabrielli O. Caratterizzazione degli oligosaccaridi del latte umano mediante cromatografia a scambio anionico ad alta risoluzione. *Riv. Ital. Pediatr. (IJP)* **1999**, *25*, 209-212.

[34] Harvey DJ. Matrix-assisted laser desorption/ionisation mass spectrometry of oligosaccharides and glycoconjugates. *J. Chromatogr.* **1996**, *720*, 429-446.

[35] Stahl B, Thurl S, Zeng J, Karas M, Hillenkamp F, Steup M, Sawatzki G. Oligosaccharides from human milk as revealed by matrix-assisted laser desorption/ionization mass spectrometry. *Anal Biochem.* **1994**, *223*, 218-226.

[36] Hård K, van Zadelhoff G, Moonen P, Kamerling JP, Vliegenthart JFG. The Asn-linked carbohydrate chains of human Tamm-Horsfall glycoprotein of one male. Novel sulfated and novel *N*-acetylgalactosamine-containing N-linked carbohydrate chains, *Eur. J. Biochem.* **1992**, *209*, 895-915.

[37] Willker W, Leibfritz D, Kerssebaum R, Bermel W. Gradient selection in inverse heteronuclear correlation spectroscopy. *Magn. Reson. Chem.* **1993**, *31*, 287-292.

[38] Facinelli B, Giovanetti E, Casolari C, Varaldo PE, Interactions with lectins and agglutination profiles of clinical, food, and environmental isolates of *Listeria*. *J. Clin. Microbiol.* **1994**, *32*, 2929-2935.

[39] Urashima T, Murata S, Nakamura T. Structural determination of monosialyl trisaccharides obtained from caprine colostrum. *Comp. Biochem. Physiol. B Biochem. Mol. Biol.* **1997**, *116B*, 431-435.

[40] Viverge D, Grimmonprez L, Solere M, Chemical characterization of sialyl oligosaccharides isolated from goat (*Capra hircus*) milk. *Biochim. Biophys. Acta* **1997**, *1336*, 157-164.

[41] Veh RW, Michalski J-C, Corfield AP, Sander-Wewer M, Gies D, Schauer R. New chromatographic system for the rapid analysis and preparation of colostrum sialyloligosaccharides. *J. Chromatogr.* **1981**, *212*, 313-322.

[42] Parkkinen J, Finne J. Isolation of sialyl oligosaccharides and sialyl oligosaccharide phosphates from bovine colostrum and human urine. *Methods Enzymol.* **1987**, *138*, 289-300.

[43] Urashima T, Bubb WA, Messer M, Tsuji Y, Taneda Y. Studies of the neutral trisaccharides of goat (*Capra hircus*) colostrum and of one- and two-dimensional $^{1}$H and $^{13}$C NMR spectra of 6'-*N*-acetylglucosaminyllactose, *Carbohydr. Res*. **1994**, *262*, 173-184.

[44] Chaturvedi P, Sharma CB. Goat milk oligosaccharides: purification and characterization by HPLC and high-field $^{1}$H-NMR spectroscopy. *Biochim. Biophys. Acta* **1988**, *967*, 115-121.

[45] Chaturvedi P, Sharma CB. Purification, by high-performance liquid chromatography, and characterization, by high-field $^{1}$H-n.m.r. spectroscopy, of two fucose-containing pentasaccharides of goat's milk, *Carbohydr. Res*. **1990**, *203*, 91-101.

[46] Collins JG, Bradbury JH, Trifonoff E, Messer M. Structures of four oligosaccharides from marsupial milk, determined by $^{13}$C-n.m.r. spectroscopy. *Carbohydr. Res.* **1981**, *92*, 136-140.

[47] Urashima T, Saito T, Kimura T. Chemical structures of three neutral oligosaccharides obtained from horse (thoroughbred) colostrum, *Comp. Biochem. Physiol. B* **1991**, *100*, 177-183.

[48] Sarney DB, Hale C, Frankel G, Vulfson EN. A novel approach to the recovery of biologically active oligosaccharides from milk using a combination of enzymatic treatment and nanofiltration. *Biotechnol. Bioeng.* **2000**, *69*, 461-467.

[49] Zárate S, López-Leiva MH. Oligosaccharide formation during enzymatic lactose hydrolysis: a literature review. *J. Food Protection* **1990**, *53*, 262-268.

[50] Endo T, Koizumi S. Large-scale production of oligosaccharides using engineered bacteria. *Curr. Opin. Struct. Biol.* **2000**, *10*, 536-554.

[51] Brinkman-Van der Linden ECM, Sjoberg ER, Juneja LR, Crocker PR, Varki N, Varki A. Loss of *N*-glycolylneuraminic acid in human evolution. Implications for sialic acid recognition by siglecs. *J. Biol. Chem*. **2000**, *275*, 8633-8640.

[52] Bardor M, Nguyen DH, Diaz S, Varki A. Mechanism of uptake and incorporation of the non-human sialic acid *N*-glycolylneuraminic acid into human cells. *J. Biol. Chem.* **2005**, *280*, 4228-4237.

[53] Hanson LA, Ahlstedt S, Andersson B, Carlsson B, Fallstrom SP, Mellander L, Porras O, Soderstrom T, Eden CS. Protective factors in milk and the development of the immune system. *Pediatrics* **1985**, *75*, 172-176.

# 3

# Characterization of galacto-oligosaccharides isolated from a goat milk oligosaccharide pool after enzymatic lactose hydrolysis with *E. coli* β-galactosidase

Daniela Beccati, Johannes F.G. Vliegenthart, Johannis P. Kamerling

*Bijvoet Center, Department of Bio-Organic Chemistry, Utrecht University, Padualaan 8, 3584 CH Utrecht, The Netherlands*

**Abstract**

Galacto-oligosaccharides and oligosaccharides naturally occurring in milk are nowadays considered as important prebiotics. The relatively high content of lactose in non-human milk complicates the isolation of commercially interesting amounts of oligosaccharides. A new easily scalable approach to the recovery of biologically active oligosaccharides relies on enzymatic treatment of defatted milk using β-galactosidase. β-Galactosidase catalyses not only the cleavage of the lactose glycosidic linkage to give galactose and glucose while preserving the original oligosaccharide compositional profile, but also, via a trans-galactosylation reaction, generates galacto-oligosaccharides. In the present paper the isolation of di- and trisaccharides formed by this trans-galactosylation process, namely, β-D-Gal*p*-(1→6)-D-Gal, β-D-Gal*p*-(1→2)-D-Glc, β-D-Gal*p*-(1→3)-β-D-Gal*p*-(1→6)-D-Glc, and β-D-Gal*p*-(1→6)-β-D-Gal*p*-(1→6)-D-Glc, and their structural analysis by methylation analysis, mass spectrometry, and NMR spectroscopy, is described.

*Keywords*

Goat milk; galacto-oligosaccharides; trans-galactosylation; β-galactosidase; *Escherichia coli*

## Introduction

Oligosaccharides present naturally in human milk have proved to be beneficial for human health by promoting the growth of bifidobacteria and lactobacilli in the large intestine[1-3] and by preventing adhesion of pathogenic agents to intestinal epithelial cells[4-7]. Additionally, several studies have suggested that volatile fatty acids produced by the intestinal microflora from the fermentation of galacto-oligosaccharides improve the absorption ability of the intestinal epithelium[8-11]. Therefore, attempts have been made by the food industry to bring the composition of infant formula closer to that of human milk by enriching the oligosaccharide content in terms of human-milk-specific compounds and of compounds such as galacto-oligosaccharides, considered as prebiotics[12,13]. Using lactose as substrate, β-galactosidase catalyses not only the cleavage of its glycosidic linkage to give galactose and glucose, but also, via a trans-galactosylation reaction, to yield galacto-oligosaccharides[14-20]. Various parameters such as enzyme source, substrate concentration, pH, and temperature can influence the trans-galactosylation in the sense of structure and final yields of the different compounds formed[21]. Analysis of the generated oligosaccharides and control of the process are important in the development of applications of enzymatic lactose hydrolysis on a technical scale. So far, the characterized structures of oligosaccharides obtained via trans-galactosylation are in the range of di- to pentasaccharides[19,20,22-26].

As we have recently demonstrated, naturally occurring galacto-oligosaccharides can be isolated in large amounts from a skimmed goat milk oligosaccharide pool, when incorporating a β-galactosidase (*E. coli*) digestion in the isolation protocol[27]. This extra step allows a fast removal of lactose, traditionally a cumbersome task for the isolation of such oligosaccharides. However, while under the applied conditions the β-galactosidase treatment largely preserved the original oligosaccharide pattern, also novel oligosaccharides were generated via trans-galactosylation. In the present paper the isolation of di- and trisaccharides formed by this trans-galactosylation process is described, as well as their structural analysis by methylation analysis, mass spectrometry, and NMR spectroscopy.

## Materials and Methods

*Materials*

Goat milk was obtained from a local diary (Potenza, Italy), collected within 1 h of milking and kept frozen at –15°C until use. Oligosaccharide standards for HPAEC-PAD calibration were purchased from Sigma-Aldrich (St. Louis, MO, USA), BioCarb (Lund, Sweden), and/or Dextra Laboratories (Reading, UK): lactose, lacto-*N*-difucohexaose (LNDFH II), trifucosyllacto-*N*-hexaose (TFLNH), difucosyllacto-*N*-hexaose b (DFLNH b), difucosyllacto-*N*-hexaose (DFLNH), difucosyllacto-*N*-hexaose I (DFLNH I), 3'-fucosyllactose (3'FL), lacto-*N*-fucopentaose II (LNFP II), 2'-fucosyllactose (2'FL), lacto-*N*-fucopentaose I (LNFP I), monofucosyllacto-*N*-hexaose II (MFLNH II), lacto-*N*-neotetraose (LNnT), lacto-*N*-neohexaose (LNnH), lacto-*N*-tetraose (LNT), and lacto-*N*-hexaose (LNH). Fractogel Toyopearl TSK HW40S was obtained from Supelco (Bellefonte, PA, USA), Sephadex G25 from Sigma-Aldrich, and Carbograph Extract-clean columns from Alltech (Deerfield, IL, USA). β-Galactosidase (EC 3.2.1.23; *E. coli*, grade VI) was obtained from Sigma-Aldrich. Chemicals not listed were of analytical grade from standard commercial sources.

*Isolation of the neutral oligosaccharide pool*

Total oligosaccharide fractions were isolated from pooled goat milk as previously described[28], and recently modified by us[27]. Starting from 100 mL milk, almost 5 g of a mixture of lactose, neutral and acidic oligosaccharides was obtained. The lactose/neutral oligosaccharide pool was separated from the acidic one by Sephadex G25 size-exclusion chromatography, as described recently[27].

Part of the neutral saccharide pool (1.5 g) was dissolved in distilled water (1 mL) and incubated with 250 U β-galactosidase from *E. coli* for 16 h at 37°C with gentle stirring[27]. The digestion was monitored by ascending paper chromatography on Whatman 1 Chr paper using *n*-butanol-pyridine-water (5:3:2, v/v) as eluent. Sugars were located with an alkaline $AgNO_3$ reagent. The process was interrupted before complete lactose digestion by heating at 100°C for 2 min, and the solution was filtered over Whatman GF/A paper, then lyophilized. The freeze-dried material was dissolved in 0.5 mL distilled water, and applied to a Toyopearl TSK HW40S column (2.6 x 60 cm), eluted with 20% aqueous EtOH at a

flow rate of 0.7 mL/min. Fractions were collected every 5 min, and analyzed for hexose content by the phenol-$H_2SO_4$ assay[29]. Saccharide fractions **I**, **II**, and **III** were pooled as indicated in Figure 1, and lyophilized.

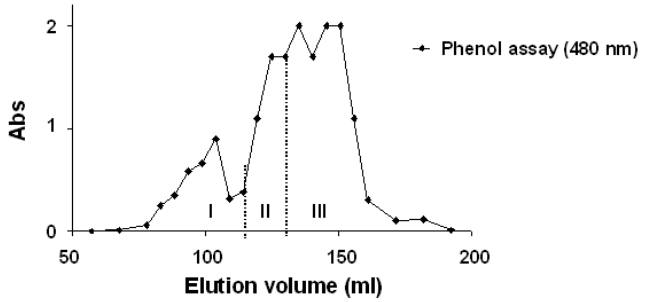


**Figure 1**: Fractionation pattern on Toyopearl TSK HW40S of the goat milk neutral saccharide pool, digested with β-galactosidase from *E. coli*. Fraction **I**, high-molecular-mass oligosaccharides; Fraction **II**, di-, tri-, and tetrasaccharides; Fraction **III**, residual lactose and generated monosaccharides.

*Purification of individual milk oligosaccharides*

Preparative HPAEC was performed on a Dionex HPLC A1 450 (Sunnyvale, CA, USA) instrument, equipped with a CarboPac precolumn (3 x 25 mm; Dionex) and a CarboPac PA-1 (4 x 250 mm; Dionex) column, as previously described[27]. Briefly, a solution of oligosaccharide pool **II** (0.5 mg) in water (50 μL) was injected on a CarboPac PA-1 column, running at 0.7 mL eluent/min at room temperature. The eluents used were 100 mM NaOH (eluent 1) and 100 mM NaOH in 1 M NaOAc (eluent 2). The two eluents were mixed according to the following gradient: isocratically with 100% eluent 1 for 10 min; linear gradient to 95% eluent 1 and 5% eluent 2 in 8 min; linear gradient to 90% eluent 1 and 10% eluent 2 in 12 min; isocratically at 90% eluent 1 and 10% eluent 2 in 7 min; linear gradient to 50% eluent 1 and 50% eluent 2 in 10 min; isocratically at 50% eluent 1 and 50% eluent 2 in 5 min. HPAEC profiles were obtained by pulsed amperometric detection. The major fractions were collected, and immediately neutralized by on-line addition of 0.1 M HCl. Ten runs were performed to collect enough material for further analysis. Relevant fractions were applied to Carbograph Extract-clean carbon columns (300 mg/8 mL) for desalting, and recovered by elution with 25% aqueous acetonitrile.

*Monosaccharide analysis*

Oligosaccharides were subjected to methanolysis (methanolic 1 M HCl, 18 h, 85°C), and the resulting mixtures of methyl glycosides were trimethylsilylated using hexamethyldisilazane-trimethylchlorosilane-pyridine (1:1:5, v/v), and quantitatively analyzed by GLC[30].

*Methylation analysis*

Permethylation was carried out essentially as described[31]. Briefly, freshly ground NaOH pellets (10 mg) were added to a sample in $Me_2SO$ (200 μL), then 200 μL MeI were added, and the solution was sonicated for 20 min. After addition of two more portions of MeI followed by sonication, the reaction was stopped by adding 1 mL aqueous 4 mM $Na_2S_2O_3$ and 0.5 mL $CHCl_3$. The chloroform layer was extracted with water (3 x 0.5 mL), then concentrated. The permethylated sample was hydrolyzed with 2 M $CF_3COOH$ (0.5 mL; 2 h, 120°C), and the resulting partially methylated monosaccharides were reduced with an excess of $NaBD_4$ (10 mg/mL) in 0.5 M $NH_4OH$. After 2 h, the solution was neutralized with 4 M HOAc, then concentrated. Boric acid was removed by repetitive co-evaporation with MeOH until dryness. After acetylation with freshly prepared $Ac_2O$-pyridine (1:1, v/v; 120°C, 30 min) and evaporation to dryness[32,33], the generated mixture of partially methylated alditol acetates was analyzed by GLC and GLC-EI/MS.

*Gas-liquid chromatography-electron impact mass spectrometry*

GLC-EI/MS analyses were carried out on a MD800/8060 system (Fisons Instruments, Manchester, UK), equipped with a WCOT CP-SIL 5CB fused-silica capillary column (25 m x 0.25 mm, Chrompack, Middelburg, The Netherlands), using a temperature program of 140-240°C at 4°C/min.

*MALDI-TOF mass spectrometry*

Positive-ion mode MALDI-TOF-MS analyses were performed on a Voyager-DE Pro (Applied Biosystems, Foster City, CA, USA) instrument, equipped with a pulsed nitrogen laser emitting at 337 nm. Oligosaccharides were analyzed in the reflector mode, with an accelerating voltage of 22 kV. Samples were dissolved in water (0.2-1 μg/μL) and mixed 1:1 with the matrix 2,5-dihydroxybenzoic acid (DHB) in water (20 μg/μL). 1 μL of this

mixture was then allowed to dry on a mass spectrometer target plate, and the obtained spot was re-crystallized *in situ* from 0.5 μL methanol[34].

*NMR spectroscopy*

Prior to NMR analysis, samples were exchanged twice in $D_2O$ (99.9 atom% D, Cambridge Isotope Laboratories, MA, USA) and then dissolved in $D_2O$ (99.96 atom% D, Isotec, USA). NMR spectra were recorded on a Bruker AMX-500 Instrument at a probe temperature of 300 K. Chemical shifts are expressed in ppm relative to internal acetone ($^1$H δ 2.225; $^{13}$C δ 32.91). 1D $^1$H NMR spectra were recorded by applying a WEFT pulse to suppress the residual water signal[35].

2D TOCSY spectra were acquired using MLEV 17 mixing sequences of 10, 50, and 100 ms with the spin-lock field strength adjusted for a 90° pulse-length of 29-30 μs, preceded by a trim pulse of 2.5 ms. TOCSY spectra were measured in the phase-sensitive mode using the time-proportional phase increment TPPI. Typically, 400-512 experiments of 2048 data points were acquired with 32-64 scans per increment. 2D ROESY experiments employed the STATES-TPPI method[36]. The HOD signal was suppressed using presaturation during a relaxation delay for 1 s, whereas the spin-lock field strength was in accordance with a 90° pulse of 100-120 μs. 2D ROESY spectra were obtained with mixing times of 200-250 ms. The frequency offset was initially placed on the HOD resonance and switched to about 5.7 ppm just before application of the spin-lock pulse thereby reducing the Hartmann-Hahn transfer during the ROE mixing time[37]. Typically, spectra were acquired with 32-64 scans for each of the 512 free induction decays. The $^1$H/$^{13}$C chemical shift correlation (HSQC) spectra were recorded using z-gradients for coherence selection. They were phase sensitive using echo/antiecho gradient selection. Spectra were acquired with the proton offset at about 4.6 ppm and a sweepwidth of about 6 ppm. In the $^{13}$C dimension the offset was placed around 80 ppm and a sweep width of 60 ppm was used. Usually, 300-350 free induction decays of 1024 data points were acquired using 64-256 scans per decay. 2D HMBC spectra were recorded using gradient pulses for selection, using the STATES-TPPI method[36]. The fixed delay for the evolution of long-range $^{13}$C-$^1$H couplings was 40-50 ms.

NMR data sets were processed using ProspectND software (Bijvoet Center, Utrecht University). Briefly, the final matrix size was zero-filled to 2Kx1K or 4Kx2K and

multiplied with a phase-shifted (squared-)sine-bell function prior to Fourier transformation. All chemical shifts of adequately resolved signals were determined from $^{1}$H 1D spectra, and are represented with three decimals. Values obtained from 2D spectra are instead given with two (protons) or one (carbon) decimals, respectively.

**Results**

As described recently[27], the oligosaccharide fraction isolated from skimmed goat milk can easily be separated on Sephadex G25 into an acidic and a neutral oligosaccharide pool. Acidic oligosaccharides elute in the first carbohydrate fraction, and were discarded. Neutral oligosaccharides, co-eluting with lactose in the second fraction, were submitted to a β-galactosidase treatment to hydrolyze the relatively larger amounts of lactose. Gel-permeation chromatography of the digested material on Toyopearl TSK HW40S (Figure 1) separated the mixture of high-molecular-mass oligosaccharides (fraction **I**) from di-, tri- and tetrasaccharides (fraction **II**) and generated monosaccharides/residual lactose (fraction **III**). Fraction **II** was subfractionated by high-pH anion-exchange chromatography (HPAEC) on CarboPac PA-1, yielding a profile as depicted in Figure 2. The subfractions denoted **F1**-**F11** were collected, desalted, and analyzed.

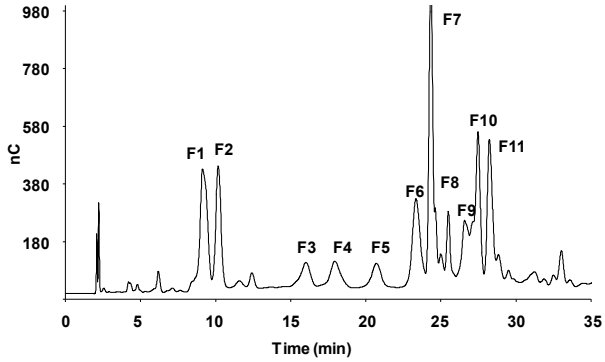


**Figure 2**: HPAEC profile on CarboPac PA-1 of the neutral oligosaccharide fraction **II** (see Figure 1). Fraction **F1**, D-Glc; **F2**, D-Gal; **F3**, β-D-Gal*p*-(1→6)-D-Gal; **F4**, β-D-Gal*p*-(1→4)-D-Glc*p*; **F5**, β-D-Gal*p*-(1→2)-D-Glc + α-L-Fuc*p*-(1→2)-β-D-Gal*p*-(1→4)-D-Glc*p*; **F6**, β-D-Gal*p*-(1→6)-β-D-Gal*p*-(1→4)-D-Glc*p*; **F7**, β-D-Gal*p*-(1→6)-β-D-Gal*p*-(1→6)-D-Glc; **F8**, α-D-Gal*p*-(1→3)-β-D-Gal*p*-(1→4)-D-Glc*p*; **F9**, not characterized; **F10**, β-D-Gal*p*-(1→3)-β-D-Gal*p*-(1→6)-D-Glc; **F11**, β-D-Gal*p*-(1→3)-β-D-Gal*p*-(1→4)-D-Glc*p*. For details of the structural analysis of fractions **F1**-**F11**, see text.

Using HPAEC retention times and $^{1}$H NMR spectroscopy[27], oligosaccharides in subfractions **F5**, **F6**, **F8**, and **F11** were identified as the following earlier reported[27,38] goat milk oligosaccharides:

α-L-Fuc*p*-(1→2)-β-D-Gal*p*-(1→4)-D-Glc*p* (**F5.1**; C2a in Ref. 27)

β-D-Gal*p*-(1→6)-β-D-Gal*p*-(1→4)-D-Glc*p* (**F6**; C2b in Ref. 27)

α-D-Gal*p*-(1→3)-β-D-Gal*p*-(1→4)-D-Glc*p* (**F8**; C2d in Ref. 27)

β-D-Gal*p*-(1→3)-β-D-Gal*p*-(1→4)-D-Glc*p* (**F11**; C2f in Ref. 27)

As the subfractions **F3**, **F5**, **F7**, and **F10** contained oligosaccharides produced by the trans-galactosylation activity of β-galactosidase, their characterization is described in more detail in the following paragraphs.

The remaining fractions **F1**, **F2**, and **F4** corresponded with glucose, galactose, and lactose, respectively, probably due to overloading of the TSK column. Fraction **F9** was not further analyzed, because of its complexity.

*Characterization of subfraction **F3***

The main component of subfraction **F3** is built up from galactose only (monosaccharide analysis). Methylation analysis indicated the occurrence of a terminal Gal*p* and a 6-substituted Gal*p* residue, whereas 1D $^{1}$H NMR analysis showed H-1 signals at δ 5.266 ($^{3}J_{1,2}$ 3.8 Hz; reducing α-Gal*p*), 4.593 ($^{3}J_{1,2}$ 7.9 Hz; reducing β-Gal*p*), and 4.453 ($^{3}J_{1,2}$ 7.8 Hz; terminal β-Gal*p*). When combined with 2D TOCSY and ROESY NMR analysis (data not shown), the structure turned out to be[39]:

β-D-Gal*p*-(1→6)-D-Gal (**F3**)

*Characterization of subfraction **F5***

Besides the trisaccharide α-L-Fuc*p*-(1→2)-β-D-Gal*p*-(1→4)-D-Glc*p*, mentioned above to occur in subfraction **F5** (**F5.1**), this subfraction also contained a second saccharide. MALDI-TOF-MS analysis revealed this product to have a molecular mass of 365 ([M + Na]$^{+}$), corresponding with the brutoformula $Hex_2$. Besides the presence of residues due to α-L-Fuc*p*-(1→2)-β-D-Gal*p*-(1→4)-D-Glc*p*, methylation analysis indicated the occurrence

of terminal Gal*p* and 2-substituted Glc*p*. Additional 1D (H-1 signals at δ 5.285 ($^3J_{1,2}$ 3.1 Hz; reducing α-Glc*p*), 4.634 ($^3J_{1,2}$ 7.3 Hz; reducing β-Glc*p*), and 4.607 ($^3J_{1,2}$ 7.3 Hz; terminal β-Gal*p*) and 2D NMR experiments indicated the structure to be:

β-D-Gal*p*-(1→2)-D-Glc (**F5.2**)

In the ROESY spectrum (data not shown) a strong cross-peak can be observed between H-1 of β-D-Gal*p* and H-2 of D-Glc*p*. This disaccharide has previously been reported as one of the saccharides formed by a trans-galactosylation reaction during lactose hydrolysis with *Bacillus circulans* β-galactosidase[24,40].

*Characterization of subfraction **F7***

MALDI-TOF-MS analysis of subfraction **F7** showed the occurrence of a major peak at *m/z* 527 (**F7.1**) and a minor peak at *m/z* 689 (**F7.2**), corresponding to sodium-cationized pseudo-molecular ions $[M + Na]^+$ for $Hex_3$ and $Hex_4$, respectively. MALDI-TOF-MS analysis of the permethylated sample revealed $[M + Na]^+$ peaks at *m/z* 681 and 885, consistent with the presence of a permethylated tri- and tetrasaccharide, respectively. Monosaccharide analysis demonstrated the presence of D-Glc and D-Gal in the molar ratio of 1:2.5, while methylation analysis indicated the occurrence of terminal Gal*p* and 6-substituted Hex*p* residues.

The 1D $^1$H NMR spectrum (Figure 3) showed five anomeric signals at δ 5.226, 4.656, and 4.48-4.44 (three overlapping doublets), integrating for 0.4:0.6:2.5, respectively.

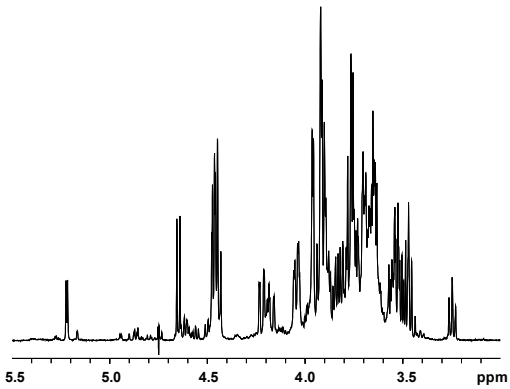


**Figure 3**: 500 MHz 1D $^1$H-NMR spectrum of fraction **F7**, recorded in $D_2O$ at 300 K.

In Table 1 a survey is presented of the $^{1}H$ and $^{13}C$ chemical shifts, as deduced from a series of 2D COSY, TOCSY, ROESY, HSQC, and HMBC experiments.

**Table 1**: $^{1}H$ and $^{13}C$ chemical shifts of oligosaccharide **F7.1**.[a]

| | β-D-Galp-(1- | -6)-β-D-Galp-(1- | -6)-D-Glcp |
|---|---|---|---|
| | III | $II^{\alpha}/II^{\beta}$ | Iα/Iβ |
| H-1 | 4.477 | 4.446/4.466 | 5.226/4.656 |
| H-2 | 3.52 | 3.55/3.56 | 3.54/3.251 |
| H-3 | 3.66 | 3.66 | 3.71/3.48 |
| H-4 | 3.92 | 3.97 | 3.50/3.48 |
| H-5 | 3.70 | 3.89/3.91 | 3.99/3.63 |
| H-6a | 3.8-3.7 | 3.92 | 3.87/3.83 |
| H-6b | 3.8-3.7 | 4.05 | 4.18/4.23 |
| C-1 | 104.0 | 104.0 | 92.8/96.7 |
| C-2 | 71.5 | 71.5 | 72.1/74.7 |
| C-3 | 73.4 | 73.4 | 73.5/70.2 |
| C-4 | 69.4 | 69.4/69.5 | 70.3/76.4 |
| C-5 | 75.9 | 74.6 | 71.2/75.6 |
| C-6 | 61.7 | 69.6 | 69.5 |

[a] α and β in $\mathbf{II^{\alpha}}$ and $\mathbf{II^{\beta}}$, respectively, stand for the anomeric configuration of **I** (**Iα** or **Iβ**).

Inspection of the TOCSY spectra (mixing times 10, 50, 100 ms) revealed cross-peaks for the doublet at δ 5.226 ($^{3}J_{1,2}$ 3.6 Hz) with H-2,3,4,5,6a,6b (Figure 4); the assignment of H-4 is supported by its cross-peak on the H-6b track. A similar correlation pattern is presented by the anomeric signal at δ 4.656 ($^{3}J_{1,2}$ 7.9 Hz).

Both complete H-1 – H-6 patterns support the *gluco*-configuration, and not the *galacto*-configuration for these residues, and combined with the ratio of both H-1 signals (see above), a reducing Glc unit (δ 5.226, α-Glc*p*-**Iα**; δ 4.656, β-Glc*p*-**Iβ**) is indicated. The three overlapping H-1 signals in the range δ 4.48-4.44 could be resolved by 2D NMR experiments, and were assigned to three β-anomeric protons, resonating at δ 4.477 ($^{3}J_{1,2}$ 7.7 Hz), 4.466 ($^{3}J_{1,2}$ 8.0 Hz), and 4.446 ($^{3}J_{1,2}$ 8.6 Hz), respectively. In the TOCSY spectra each of these H-1 signals showed cross-peaks with H-2,3,4 only. This feature, combined with the typical peak pattern of the H-4 signals ($^{3}J_{3,4}$ 3 Hz, $^{3}J_{4,5}$ ~ 0.5 Hz), supports the *galacto*-configuration for these three pyranose units. Taking together the TOCSY and

ROESY (Figure 5) experiments, the H-1 signals at δ 4.446 and 4.466 could be assigned to internal β-Gal*p*-**II**, i.e. β-Gal*p*-**II**$^{\alpha}$ and β-Gal*p*-**II**$^{\beta}$, respectively (anomerization effect induced by Glc-**I**).

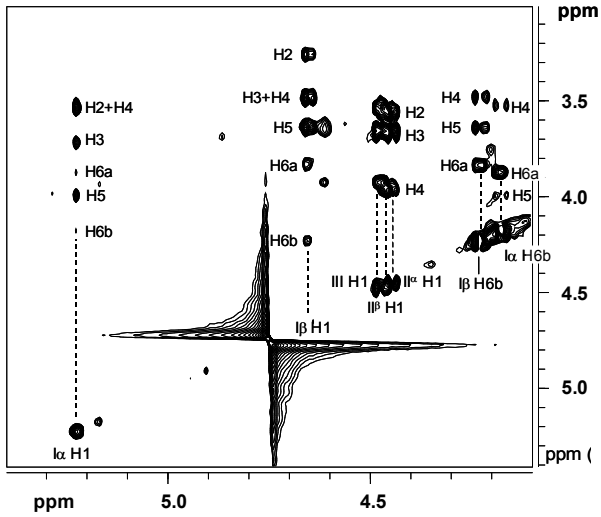


**Figure 4**: Partial 500 MHz 2D $^{1}$H-$^{1}$H TOCSY spectrum of fraction **F7**, recorded in $D_2O$ at 300 K, with a mixing time of 100 ms.

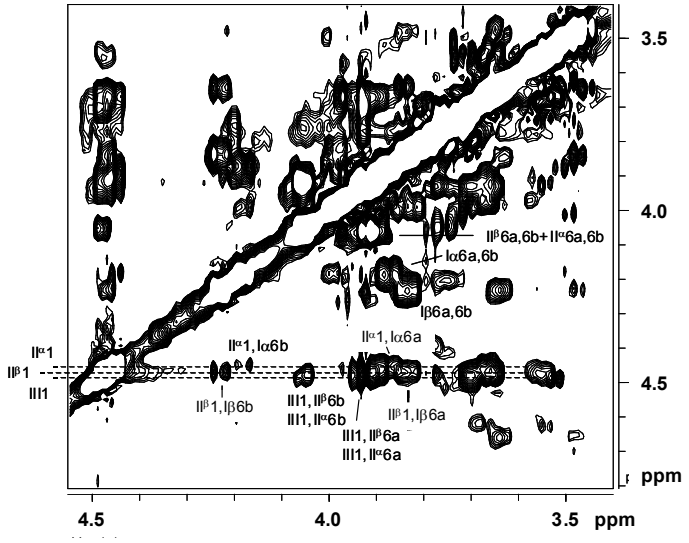


**Figure 5**: Partial 500 MHz 2D $^{1}$H-$^{1}$H ROESY spectrum of fraction **F7**, recorded in $D_2O$ at 300 K. In the coding system, **II** H1,**I** H6 means a cross-peak between Gal-**II** H-1 and Glc-**I** H-6, etc.

Analysis of the HSQC spectrum (Figure 6) yielded the $^{13}C$ data for all C-atoms. The downfield shifts of βGal*p*-**II** C-6 (δ 69.6) and Glc*p*-**I** C-6 (δ 69.5) indicated that both residues are substituted at C-6 (β-D-Gal*p*1Me, $\delta_{C\text{-}6}$ 62.0; β-D-Glc*p*1Me, $\delta_{C\text{-}6}$ 61.6[41]). Sequence analysis using the interresidual ROESY cross-peaks (Figure 5) revealed correlations between β-Gal*p*-**II**$^{\beta}$ H-1 (δ 4.466) and β-Glc*p*-**Iβ** H-6a,6b (δ 3.83, 4.23), between β-Gal*p*-**II**$^{\alpha}$ H-1 (δ 4.446) and α-Glc*p*-**Iα** H-6a,6b (δ 3.87, 4.18), and between β-Gal*p*-**III** H-1 (δ 4.477) and β-Gal*p*-**II** H-6a,6b (δ 3.92, 4.05). The various assignments, as made so far, were further supported by HMBC experiments. The assignment of the anomeric configurations of the different residues are supported by $^{1}J_{C\text{-}1,H\text{-}1}$ values: α-Glc*p*-**Iα**, 166 Hz; β-Glc*p*-**Iβ**, 156 Hz; β-Gal*p*-**II**, 156 Hz; β-Gal*p*-**III**, 156 Hz). The ROESY-based sequence analysis is confirmed by long-range HMBC contacts between β-Gal*p*-**III** H-1 and β-Gal*p*-**II** C-6, and between β-Gal*p*-**II** H-1 and Glc*p*-**I** C-6 (data not shown).

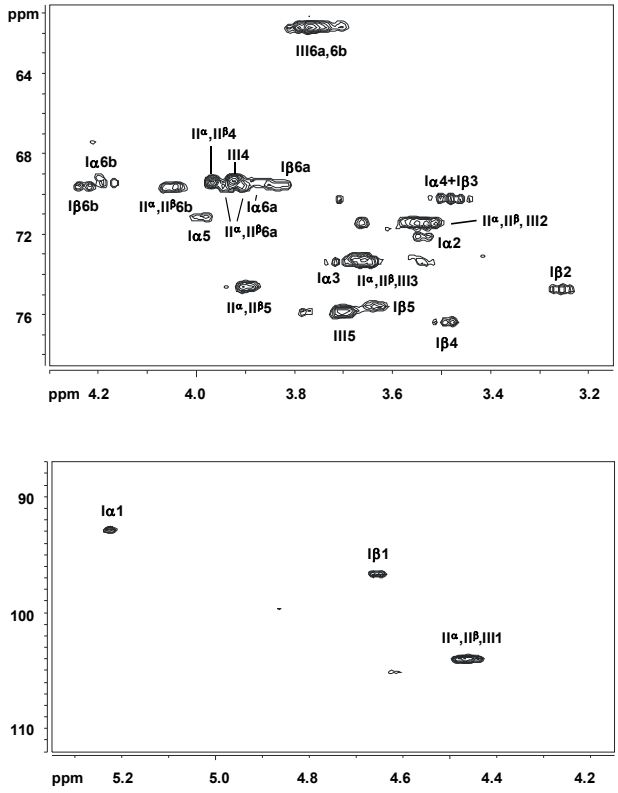


**Figure 6**: 2D $^{1}H$-$^{13}C$ HSQC spectrum of fraction **F7**, recorded in $D_2O$ at 300 K.

Combining the various results above, the following structure is deduced for **F7.1**:

β-D-Gal*p*-(1→6)-β-D-Gal*p*-(1→6)-D-Glc*p* (**F7.1**)

III II I

Taking into account the MALDI-TOF-MS and monosaccharide analyses, it is suggested that besides **F7.1**, also tetrasaccharides are present, but structural details could not be obtained.

*Characterization of subfraction **F10***

MALDI-TOF-MS analysis of subfraction F10 showed an ion at *m/z* 527, which can be attributed to a sodium-cationized pseudo-molecular ion $[M + Na]^+$ for $Hex_3$. MALDI-TOF-MS analysis of the permethylated sample gives rise to a $[M + Na]^+$ peak at *m/z* 681, thereby supporting the finding of a trisaccharide. Monosaccharide analysis revealed the trisaccharide to consist of D-Glc and D-Gal in the molar ratio of 1:2, whereas methylation analysis shows the presence of terminal Gal*p*, 3-substituted Hex*p* and 6-substituted Hex*p* residues.

The 1D $^1$H NMR spectrum (Figure 7) showed three major anomeric signals at δ 5.228, 4.656, and 4.617 and two overlapping doublets at δ 4.504 and 4.487, integrating for 0.4:0.6:1.0:0.6:0.4, respectively**.** In Table 2 a survey is presented of the $^1$H and $^{13}$C chemical shifts, as deduced from a series of 2D COSY, TOCSY, ROESY, HSQC, and HMBC experiments.

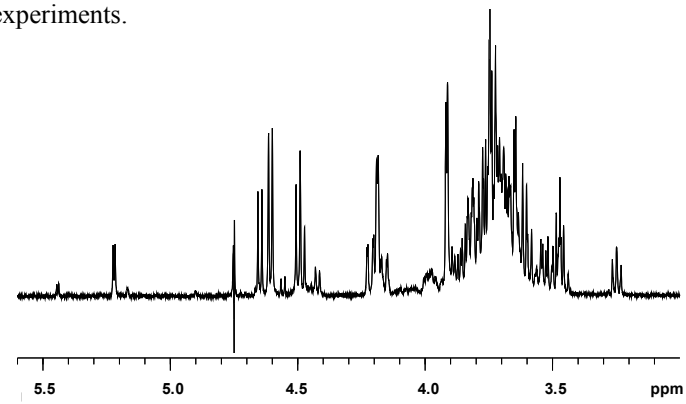


**Figure 7**: 500 MHz 1D $^1$H-NMR spectrum of fraction **F10**, recorded in $D_2O$ at 300 K.

**Table 2**: $^{1}$H and $^{13}$C chemical shifts of oligosaccharide **F10**.[a]

| | β-D-Galp-(1- | -3)-β-D-Galp-(1- | -6)-D-Glcp |
|---|---|---|---|
| | **III** | **II$^{\alpha}$/II$^{\beta}$** | **Iα/Iβ** |
| H-1 | 4.617 | 4.487/4.504 | 5.228/4.656 |
| H-2 | 3.60 | 3.72 | 3.54/3.252 |
| H-3 | 3.66 | 3.83 | 3.71/3.48 |
| H-4 | 3.920 | 4.193 | 3.51/3.49 |
| H-5 | 3.69 | 3.72 | 3.99/3.64 |
| H-6a | 3.76 | 3.69 | 3.88/3.84 |
| H-6b | 3.80 | 3.73 | 4.162/4.222 |
| C-1 | 104.4 | 103.1 | 92.2/96.1 |
| C-2 | 71.1 | 74.9 | 71.5/74.1 |
| C-3 | 72.6 | 82.2 | 72.7/69.6 |
| C-4 | 68.7 | 68.5 | 69.5/75.8 |
| C-5 | 75.2 | 70.1 | 70.5/75.0 |
| C-6 | 61.1 | 61.0 | 68.7 |

[a] α and β in **II$^{\alpha}$** and **II$^{\beta}$**, respectively, stand for the anomeric configuration of **I** (**Iα** or **Iβ**).

In the TOCSY spectrum (100 ms, Figure 8), the anomeric proton at δ 5.228 ($^{3}J_{1,2}$ 3.9 Hz) showed correlations with H-2,3,4,5,6a,6b, supporting a residue with the *gluco*-configuration, and not the *galacto*-configuration. The H-4 signal, overlapping with H-2, could be identified via a TOCSY cross-peak on the H-6b track. The chemical shift pattern is very similar to that of the reducing α-Glc*p*-**I** unit of **F7.1**, supporting a 6-linked reducing α-Glc*p*-**I** residue. Analogously, the H-1 signal at δ 4.656 ($^{3}J_{1,2}$ 7.9 Hz) is assigned to a 6-linked reducing β-Glc*p*-**I** residue. For the β-anomeric signals at δ 4.504 ($^{3}J_{1,2}$ 8.5 Hz; Gal-**II$^{\alpha}$**), 4.487 ($^{3}J_{1,2}$ 8.5 Hz; Gal-**II$^{\beta}$**), and 4.617 ($^{3}J_{1,2}$ 7.3 Hz; Gal-**III**), the TOCSY spectra revealed only cross-peaks with H-2,3,4, whereby the doublets at δ 4.504 and 4.487 present an identical correlation pattern. The typical small coupling constants for the H-4 signals ($^{3}J_{3,4}$ 3 Hz, $^{3}J_{4,5}$ < 1 Hz) are in accordance with *galacto*-configurations. Analysis of the HSQC spectrum yielded the $^{13}$C data for all C-atoms. The downfield shifts for Gal*p*-**II** C-3 (δ 82.2) and Glc*p*-**I** C-6 (δ 68.7) indicated a 3-substituted Gal*p* and a 6-substituted Glc*p* residue, respectively (β-D-Gal*p*1Me, $\delta_{C\text{-}3}$ 73.8; β-D-Glc*p*1Me, $\delta_{C\text{-}6}$

61.6[41]). Note also the downfield position of 3-substituted Gal-**II** H-3 (δ 3.83), when compared with terminal Gal-**III** H-3 (δ 3.66).

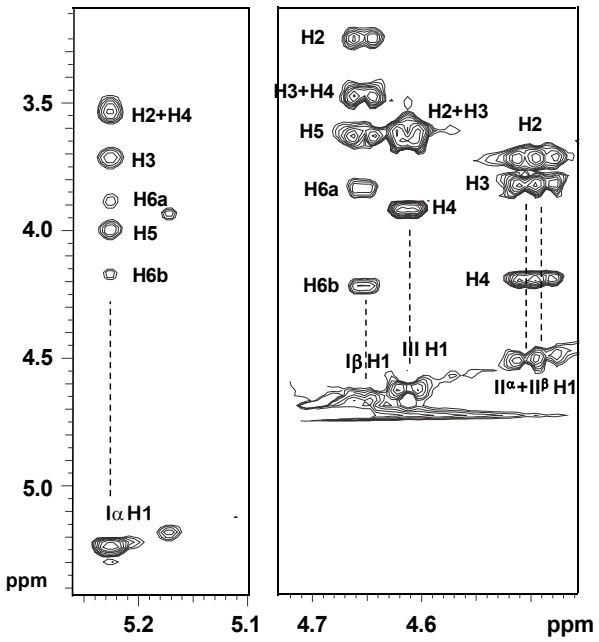


**Figure 8**: Partial 500 MHz 2D $^{1}$H-$^{1}$H TOCSY spectrum of fraction **F10**, recorded in $D_2O$ at 300 K, with a mixing time of 100 ms.

Sequence analysis using interresidual ROESY correlations showed cross-peaks between β-Gal*p*-**III** H-1 (δ 4.617) and β-Gal*p*-**II** H-3 (δ 3.83), between β-Gal*p*-**II** H-1 (δ 4.504) and β-Glc*p*-**I** H-6a,6b (δ 3.84, 4.22), and between α-Gal*p*-**II** H-1 (δ 4.487) and α-Glc*p*-**I** H-6a,6b (δ 3.88, 4.16). As is evident from Figure 9, long-range HMBC contacts (Gal*p*-**II** H-3, Gal*p*-**III** C-1 / Gal*p*-**III** H-1, Gal*p*-**II** C-3; Gal*p*-**II** H-1, Glc*p*-**I** C-6) confirmed the ROESY-based sequence analysis.

Combining the various results above, the following structure is determined for **F10**:

β-D-Gal*p*-(1→3)-β-D-Gal*p*-(1→6)-D-Glc*p* (**F10**)

III II I

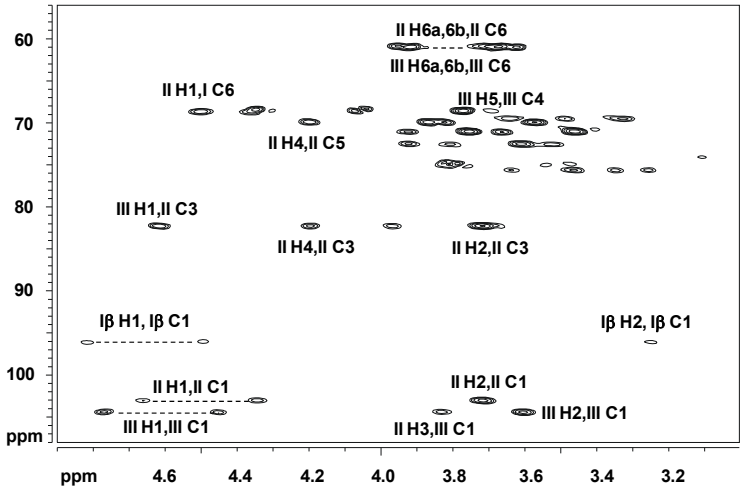


**Figure 9**: 2D $^{1}H$-$^{13}C$ HMBC spectrum of fraction **F10**, recorded in $D_2O$ at 300 K. In the coding system, **II** H1,**I** C1 means a cross-peak between Gal-**II** H-1 and Glc-**I** C-1, etc.

**Discussion**

β-Galactosidases acting on lactose catalyze both hydrolytical and transfer reactions, the type and the amount of oligosaccharides formed via trans-galactosylation being dependent on the source of the enzyme, the substrate concentration, salts, temperature, pH, and the degree of lactose conversion. It has been shown that the amounts of oligosaccharides produced via trans-galactosylation are lower when β-galactosidases act on milk or milk products [42,43] instead of on pure lactose dissolved in buffered saline solution. β-Galactosidases seem therefore to have a higher hydrolytic activity and a lower transferase activity in milk than in lactose solutions. By treating an isolated pool of oligosaccharides from goat milk at 37°C in water with β-galactosidase from *E.coli*, mainly di-, tri- and tetrasaccharides were formed.

Among the identified trisaccharides described in this paper, α-L-Fuc*p*-(1→2)-β-D-Gal*p*-(1→4)-D-Glc*p*, β-D-Gal*p*-(1→6)-β-D-Gal*p*-(1→4)-D-Glc*p*, α-D-Gal*p*-(1→3)-β-D-Gal*p*-(1→4)-D-Glc*p*, and β-D-Gal*p*-(1→3)-β-D-Gal*p*-(1→4)-D-Glc*p* are known to be originally present in goat milk[44]. While β-D-Gal*p*-(1→6)-β-D-Gal*p*-(1→4)-D-Glc*p* and β-D-Gal*p*-(1→3)-β-D-Gal*p*-(1→4)-D-Glc*p* might as well be generated by the trans-galactosylation activity of β-galactosidase on lactose[19,27], α-D-Gal*p*-(1→3)-β-D-Gal*p*-

(1→4)-D-Glc*p* must derive from the natural source. The identified saccharides β-D-Gal*p*-(1→6)-D-Gal, β-D-Gal*p*-(1→2)-D-Glc, β-D-Gal*p*-(1→3)-β-D-Gal*p*-(1→6)-D-Glc, and β-D-Gal*p*-(1→6)-β-D-Gal*p*-(1→6)-D-Glc are typical products of trans-galactosylation.

The galacto-oligosaccharides β-D-Gal*p*-(1→3)-β-D-Gal*p*-(1→6)-D-Glc and β-D-Gal*p*-(1→6)-β-D-Gal*p*-(1→6)-D-Glc are likely formed by the elongation of allolactose, β-D-Gal*p*-(1→6)-D-Glc. Previously, it has been demonstrated that allolactose can be produced from the direct enzymatic transfer of Gal from Glc O-4 to Glc O-6 in lactose without prior release of Glc from the enzyme[16]. Allolactose accumulates in the course of the hydrolytic reaction and it seems to be the natural inducer of the *E.coli lac* operon[45,46]. It can be assumed that the initial formation of galacto-oligosaccharides will use lactose as substrate, while after allolactose formation the latter will be used as acceptor. Interestingly, the newly formed oligosaccharides have no (1→4) linkages. Wallenfels[47] reported that the velocity of synthesis of galactosylglucoses and galactosylgalactoses by *E.coli β*-galactosidase is (1-6) > (1-3) and (1-4). On the other hand, the rate of oligosaccharide hydrolysis decreases in the order (1-6) > (1-4) > (1-3) > (1-2). It can therefore be assumed that the structure of oligosaccharides in the end product is strongly dependent on the degree of hydrolysis[48]. The use of β-galactosidase from *E. coli* does not lead to the production of penta- or higher oligosaccharides, in agreement with earlier reports[16].

**Acknowledgements**

This study was supported by a grant from the European Community (NOFA, Contract Fair CT 97-3142).

**References**


[1] Bezkorovainy A, Miller-Catchpole R. *Biochemistry and Physiology of Bifidobacteria*, **1989**, 30-72, CRC Press, Boca Raton, FL.

[2] Yoshioka H, Iseki K, Fujita K. Development and differences of intestinal flora in the neonatal period in breast-fed and bottle-fed infants. *Pediatrics* **1983**, *72*, 317-321.

[3] Zopf D, Roth S. Oligosaccharide anti-infective agents. *Lancet* **1996**, *347*, 1017-1021.

[4] Kunz C, Rudloff S. Biological functions of oligosaccharides in human milk. *Acta Paediatr.* **1993**, *82*, 903-912.

[5] Newburg DS. Oligosaccharides and glycoconjugates in human milk: their role in host defense. *J. Mamm. Gland Biol. Neoplasia* **1996**, *1*, 271-283.

[6] Andersson B, Porras O, Hanson LA, Lagergard T, Svanborg-Eden C**.** Inhibition of attachment of *Streptococcus pneumoniae* and *Haemophilus influenzae* by human milk and receptor oligosaccharides. *J. Infect. Dis.* **1986**, *153*, 232-237.

[7] Coppa GV, Gabrielli O, Giorgi P, Catassi C, Montanari MP, Varaldo PE, Nichols BL. Preliminary study of breastfeeding and bacterial adhesion to uroepithelial cells. *Lancet* **1990**, *335*, 569-571.

[8] Levrat MA, Rémésy C, Demigne C. High propionic acid fermentations and mineral accumulation in the cecum of rats adapted to different levels of inulin. *J. Nutr.* **1991**, *121*, 1730-1737.

[9] Varki A. Biological roles of oligosaccharides: all of the theories are correct. *Glycobiology* **1993**, *3*, 97-130.

[10] Yoshida T, Oowada T, Ozaki A, Mizutani T. Role of gastrointestinal microflora in the mineral absorption of young adult mice. *Biosci. Biotech. Biochem.* **1993**, *57*, 1775-1776.

[11] Yanahira S, Morita M, Aoe S, Suguri T, Takada Y, Miura S, Nakajima I. Effects of lactitol-oligosaccharides on calcium and magnesium absorption in rats. *J. Nutr. Sci. Vitaminol.* **1997**, *43*, 123-132.

[12] Perrin V, Fenet B, Praly J-P, Lecroix F, Ta CD. Identification and synthesis of a trisaccharide produced from lactose by transgalactosylation. *Carbohydr. Res.* **2000**, *325*, 202-210.

[13] Donald ASR, Feeney J. Separation of human milk oligosaccharides by recycling chromatography. First isolation of lacto-*N*-neo-difucohexaose II and 3'-galactosyllactose from this source. *Carbohydr. Res.* **1988**, *178*, 79-91.

[14] Pazur JH. The enzymatic conversion of lactose into galactosyl oligosaccharides. *Science* **1953**, *117*, 355-356.

[15] Roberts HR, Pettinati JD. Oligosaccharide production, concentration effects in the enzymatic conversion of lactose to oligosaccharides. *J. Agric. Food Chem.* **1957**, *5*, 130-134.

[16] Huber RE, Kurz G, Wallenfels K. A quantitation of the factors which affect the hydrolase and transgalactosylase activities of β-galactosidase (*E. coli*) on lactose. *Biochemistry* **1976**, *15*, 1994-2001.

[17] Toba T, Adachi S. Hydrolysis of lactose by microbial β-galactosidase. Formation of oligosaccharides with special reference to 2-O-β-D-galactopyranosyl-D-glucose. *J. Dairy Sci.* **1978**, *61*, 33-38.

[18] Burvall A, Asp NG, Dahlqvist A. Oligosaccharide formation during hydrolysis of lactose with *Saccharomyces lactis* lactase (Maxilact$^{R}$). Part 1 – Quantitative aspects. *Food Chem*. **1979**, *4*, 243-250.

[19] Toba T, Yokota A, Adachi S. Oligosaccharide structures formed during the hydrolysis of lactose by *Aspergillus oryzae* β-galactosidase. *Food Chem*. **1985**, *16*, 147-162.

[20] Fransen CTM, Van Laere KMJ, van Wijk AAC, Brüll LP, Dignum M, Thomas-Oates JE, Haverkamp J, Schols HA, Voragen AGJ, Kamerling JP, Vliegenthart JFG. α-D-Glc*p*-(1↔1)-β-D-Gal*p*-containing oligosaccharides, novel products from lactose by the action of β-galactosidase. *Carbohydr. Res.* **1998**, *314*, 101-114.

[21] Zárate S, López-Leiva MH. Oligosaccharide formation during enzymatic lactose hydrolysis: a literature review. *J. Food Protection* **1990**, *53*, 262-268.

[22] Onishi N, Yamashiro A, Yokozeki K. Production of galacto-oligosaccharide from lactose by *Sterigmatomyces elviae* CBS8119. *Appl. Environ. Microbiol.* **1995**, *61*, 4022-4025.

[23] Asp NG, Burvall A, Dahlqvist A, Hallgren P, Lundblad A. Oligosaccharide formation during hydrolysis of lactose with *Saccharomyces lactis* lactase (Maxilact$^{R}$). Part 2 – Oligosaccharide structures. *Food Chem.* **1980**, *5*, 147-153.

[24] Yanahira S, Kobayashi T, Suguri T, Nakakoshi M, Miura S, Ishikawa H, Nakajima I. Formation of oligosaccharides from lactose by *Bacillus circulans β*-galactosidase. *Biosci. Biotechnol. Biochem.* **1995**, *59*, 1021-1026.

[25] Usui T, Morimoto S, Hayakawa Y, Kawaguchi M, Murata T, Matahira Y, Nishida Y. Regioselectivity of β-D-galactosyl-disaccharide formation using the β-D-galactosidase from *Bacillus circulans*. *Carbohydr. Res*. **1996**, *285*, 29-39.

[26] Dumortier V, Montreuil J, Bouquelet S. Primary structure of ten galactosides formed by transgalactosylation during lactose hydrolysis by *Bifidobacterium bifidum*. *Carbohydr. Res.* **1990**, *201*, 115-123.

[27] Beccati D, Sturiale L, Guerrini G, Naggi A, Torri G, Zampini L, Coppa GV, Vliegenthart JFG, Kamerling JP. An improved protocol to isolate lactose-free oligosaccharide fractions from non-human milks - characterization and their effect on bacterial adhesion. Chapter 2.

[28] Kobata A. Isolation of oligosaccharides from human milk. *Methods Enzymol.* **1972**, *28*, 262-271.

[29] Dubois M, Gilles KA, Hamilton JK, Rebers PA, Smith F. Colorimetric method for the determination of sugars and related substances. *Anal. Chem.* **1956**, *28*, 350-356.

[30] Kamerling JP, Vliegenthart JFG. Carbohydrates. In: Clinical Biochemistry: Principles, Methods, Applications, Vol. 1 (Lawson AM, Ed), Walter de Gruyter, Berlin, **1989**, pp. 176-263.

[31] Hakomori S. A rapid permethylation of glycolipids and polysaccharide catalyzed by methylsulfinyl carbanion in dimethyl sulfoxide. *J. Biochem. (Tokyo)* **1964**, *55*, 205-208.

[32] Harris PJ, Henry RJ, Blakeney AB, Stone BA. An improved procedure for the methylation analysis of oligosaccharides and polysaccharides. *Carbohydr. Res.* **1984**, *127*, 59-73.

[33] Ciucanu I, Kerek F. A simple and rapid method for the permethylation of carbohydrates. *Carbohydr. Res.* **1984**, *131*, 209-217.

[34] Harvey DJ. Matrix-assisted laser desorption/ionisation mass spectrometry of oligosaccharides and glycoconjugates. *J. Chromatogr.* **1996**, *720*, 429-446.

[35] Hård K, van Zadelhoff G, Moonen P, Kamerling JP, Vliegenthart JFG. The Asn-linked carbohydrate chains of human Tamm-Horsfall glycoprotein of one male. Novel sulfated and novel *N*-acetylgalactosamine-containing N-linked carbohydrate chains. *Eur. J. Biochem*. **1992**, *209*, 895-915.

[36] Marion D, Ikura M, Tschudin R, Bax A. Rapid recording of 2D NMR spectra without phase cycling. Application to the study of hydrogen exchange in proteins. *J. Magn. Reson.* **1989**, *85*, 393-399.

[37] Leeflang BR, Kroon-Batenburg LMJ. CROSREL: Full relaxation matrix analysis for NOESY and ROESY NMR spectroscopy. *J. Biomol. NMR* **1992**, *2*, 495-518.

[38] Urashima T, Bubb WA, Messer M, Tsuji Y, Taneda Y. Studies of the neutral trisaccharides of goat (*Capra hircus*) colostrum and of one- and two-dimensional $^{1}H$ and $^{13}C$ NMR spectra of 6'-*N*-acetylglucosaminyllactose. *Carbohydr. Res*. **1994**, *262*, 173-184.

[39] Odonmazig P, Ebringerova A, Machova E, Alfoldi J. Structural and molecular properties of the arabinogalactan isolated from Mongolian larchwood (Larix dahurica L.). *Carbohydr. Res.* **1994**, *252*, 317-324.

[40] Pazur JH, Tipton CL, Budovich T, Marsh JM. Structural characterization of products of enzymatic disproportionation of lactose**.** *J. Am. Chem. Soc.* **1958**, *80*, 119-121.

[41] Bock K, Pedersen C. Carbon-13 nuclear magnetic resonance spectroscopy of monosaccharides. *Adv. Carbohydr. Chem. Biochem*. **1983**, *41*, 27–66.

[42] Mozaffar Z, Nakanishi K, Matsuno R. Production of trisaccharide from lactose using β-galactosidase from *Bacillus circulans* modified by glutaraldehyde. *J. Food Sci.* **1985**, *50*, 1602-1606.

[43] Greenberg NA, Mahoney RR, Formation of oligosaccharides by β-galactosidase from *Streptococcus thermophilus*. *Food Chem.* **1983**, *10*, 195-204.

[44] Urashima T, Saito T, Nakamura T, Messer M., Oligosaccharides of milk and colostrum in non-human mammals. *Glycoconjugate J.* **2001**, *18*, 357-371.

[45] Jobe A, Bourgeois S. lac Repressor-operator interaction. VI. The natural inducer of the lac operon. *J. Mol. Biol*. **1972**, *69*, 397-408.

[46] Müller-Hill B, Rickenberg HV, Wallenfels K. Specificity of the induction of the enzyme of the lac operon in *Escherichia coli*. *J. Mol. Biol.* **1964**, *10*, 303-318.

[47] Wallenfels K, Malhotra OP. Galactosidases. *Adv. Carbohydr. Chem.* **1961**, *16*, 239-298.

[48] Burvall A, Asp NG, Dahlqvist A, Hallgren P, Lundblad A. Oligosaccharide formation during hydrolysis of lactose with *Saccharomyces lactis* lactase (Maxilact®). Part 3 – Digestibility by human intestinal enzymes *in vitro*. *Food Chem.* **1980**, *5*, 189-194.

# 4

# Conformation analysis of the *C*-linkage Man1α-Trp in human RNase 2

Daniela Beccati[1], Florence Casset[1,3], Bas R. Leeflang[1], Jan Hofsteenge[2], and Johannes F.G. Vliegenthart[1,*]

[1]*Bijvoet Center, Department of Bio-Organic Chemistry, Utrecht University, Padualaan 8, 3584 CH Utrecht, The Netherlands*

[2]*Friedrich Miescher-Institut, P.O. Box 2543, CH-4002 Basel, Switzerland*

[3]*Serono International S.A., 15bis Chemin des Mines, CH-1211 Geneva*

Manuscript in preparation

**Abstract**

*C*-Mannosylation is a relatively novel form of glycosylation, involving the *C*-glycosidic attachment of a mannosyl residue to the indole moiety of Trp. This type of linkage was discovered in RNase 2 from human urine. It was previously demonstrated by NMR spectroscopy that the orientation around the *C*-linkage occupied by the mannose residue in the native protein is different from that in denatured form. Moreover, NMR data indicated that the mannopyranose ring is not rigid in the hexapeptide FTW$^{Man}$AQW derived from RNase 2[1,2].

In this study, NMR experiments and molecular modeling calculations for ($C^2$-α-D-Man-)Trp demonstrated that the *C*-linked mannopyranosyl residue exists in an ensemble of conformations, among which $^1C_4$ is the most represented.

For isolated glycopeptides, NMR showed no evidence for long-range connectivities and secondary structure, arguing against a stabilization of the analyzed glycopeptides due to the *C*-linked mannopyranosyl residue. For native RNase 2, molecular modeling studies revealed that the mannopyranosyl residue interacts with the loop residues Asp115-123 of RNase 2, the end of the β strands Met105-Arg114 and the beginning of the β strands Pro124-Ile134. These interactions stabilize not only to the mannose residue and Trp7 in a specific orientation, but also the N-terminal loop of the protein. NMR data confirmed these results.

*Keywords*

*C*-Mannosylation; human RNase 2; Man1α-Trp

## Introduction

Modification of Trp7 in human RNase 2 by the *C*-glycosidic attachment of an α-D-mannopyranosyl residue to the C2 atom of the indole ring was observed[3,4]. In 1998, Krieg *et al*. identified by site-directed mutagenesis the sequence Trp-X-X-Trp, as the recognition motif for *C*-mannosylation, in which Trp oriented towards the N-terminus becomes mannosylated. This sequence has been identified in 336 mammalian proteins, suggesting that *C*-glycosides could be part of the structure of a significant number of proteins. For example, *C*-mannosylation has been identified in proteins such as interleukin-12[5], the terminal four components of human complement system C6, C7, C8α, C8β, and C9[6], human platelet thrombospondin-1[7], properdin[8], recombinant erythropoietin receptors[9], mucins MUC5AC and MUC5B[10]. Exceptions to the Trp-X-X-Trp consensus sequence have been found. For instance, thrombospondin type 1 repeats are *C*-mannosylated on Trp residues without a Trp at position +3[11]. It has been described that *C*-mannosylation occurs intracellularly before secretion of the protein and can be carried out by a variety of mammalian cell cultures[12]. This process is catalyzed by a microsomal transferase according to the biosynthetic pathway Man → GDP-Man → DolP-Man → ($C^2$Man)-Trp[13].

Non-secretory ribonuclease 2 found in human urine is an enzyme involved in the digestion of RNA. RNase 2 contains 134 amino acids, has five *N*-glycosylation sites and one *C*-mannosylation site. It has been shown by NMR spectroscopy that the orientation around the *C*-linkage occupied by the mannose residue in the native protein is different from that in denatured form. Moreover, the pyranose ring is not rigid in the hexapeptide $FTW^{Man}AQW^{1,2}$ and adopts several conformations on the NMR time scale. Our first objective was to study this new type of *C*-linkage by molecular modeling and to determine how the pyranose $^4C_1$ conformation of the mannose residue could be destabilized. To gain insight into the influence of the polypeptide chain on the conformation of the *C*-linked α-D-mannopyranosyl moiety, further NMR studies were carried out on digested glycopeptides of different chain length and amino acid composition.

NMR and molecular modeling studies were performed to investigate in which way the three-dimensional structure of RNase 2 could be responsible for the different orientation of *C*-mannose in native and denatured protein. Since RNase has the same amino acid

sequence as eosinophil-derived neurotoxin (EDN)[14], the three-dimensional structure of recombinant EDN (rEDN from *Escherichia coli*), as determined by X-ray crystallography[15], was used to model the *C*-linkage between mannose and Trp. The short distances between the neighboring amino acid protons and those of the α-D-mannopyranosyl residue, as observed by molecular modeling, were finally compared with the NMR data on native RNAse 2.

**Materials and Methods**

*Samples purification*

RNase 2 (E.C. 3.1.27.5) was purified from male human urine as previously described by Hofsteenge *et al*[3]. Glycopeptides from the N-terminal region of RNase were prepared by digestion of reduced and carboxymethylated protein with the protease from *Staphylococcus aureus* (2% w/w; 18 h), thermolysin (3% w/w; 18 h), elastase (5% w/w; 4 h), or aminopeptidase M (10 units/nmol of peptide; 2 h). All digestions were performed in 50 mM $NH_4HCO_3$, pH 7.8, at 37°C. Subsequently, glycopeptides were purified by reverse phase HPLC[16].

*NMR spectroscopy*

NMR spectra were recorded with a Bruker AMX-500 or AMX-600 spectrometer (Bijvoet Center, NMR Spectroscopy, Utrecht University, The Netherlands), and a Varian UnityPlus 750 MHz spectrometer (SON NMR Large Scale Facility, Utrecht University). Native RNase 2 was dissolved in 90% (v/v) $H_2O/D_2O$, 0.1 M NaCl, 1 mM $NaN_3$, pH 5.1. NOESY and TOCSY $^1$H NMR spectra were recorded at 300, 315 and 320K. 2D NOESY spectra[17] were recorded with a mixing time of 100 ms, with 350 increments (in the $t_1$ dimension) of 2K data points. Water resonance was suppressed by irradiating at low power during the relaxation delay and during the mixing time. In addition, a magnetisation purging sine-bell-shaped pulsed field gradient (PFG) was applied. 2D TOCSY spectra[18] were recorded with a clean MLEV-17 spin lock sequence with a duration of 10, 50, or 80 ms. Spectra were recorded with 440 increments of 2K data points each. As for NOESY experiments, water resonance was suppressed by a low power irradiation applied during the relaxation delay, and a magnetisation purging sine-bell-shaped pulsed field gradient (PFG) was included. The temperature settings of the

instrument were decreased by 3 K to compensate for the rise in sample temperature caused by the rf power of the spin-lock sequence. In this way, the chemical shift changes as a function of sample temperature changes were nulled. For all 2D experiments, quadrature detection was achieved using the State-TPPI method[19].

Peptides were dissolved in 5 mM potassium phosphate, pH 5.4 in $D_2O$ (99.96 atom% D, Isotec, USA). Spectra were recorded at a probe temperature of 300 K. Chemical shifts are expressed in ppm relative to internal acetone ($^1H$ $\delta$ 2.225; $^{13}C$ $\delta$ 32.910). Suppression of the water signal was achieved by a selective WEFT sequence[20]. 1D $^1H$-NMR spectra of 8K or 16K complex data points were collected. 2D spectra were acquired with 256-512 increments of 2048 data points. Quadrature detection in the $t_1$ dimension was achieved by either the time-proportional phase increment (TPPI) method[21] or the States-TPPI method. 2D TOCSY experiments were recorded using a MLEV 17 mixing sequence of 20, 50 or 60 ms[22,23] preceded by a trim pulse of 2.5 ms. Typically, TOCSY spectra were recorded with a mixing time of 10, 50, or 100 ms with the spin-lock field strength adjusted for a 90° pulse-length of 29-30 μs. 2D ROESY spectra were obtained with a spin-lock pulse length of 100 ms, 300 ms, 750 ms, or 1.2 s. The spin-lock field strength was in accordance with a 90° pulse of 100-120 μs. The frequency offset was initially placed on the HOD resonance and switched to about 5.7 ppm just before application of the spin-lock pulse, thereby reducing the Hartmann-Hahn transfer during the ROESY mixing time[24]. NMR data sets were processed using ProSpectND software (Bijvoet Center, University of Utrecht) or NMRPipe[25].

*Molecular modeling of ($C^2$-α-D-Man-)Trp*.

Molecular modeling studies on ($C^2$-α-D-Man-) Trp were performed using the INSIGHTII and DISCOVER molecular modeling packages (MSI/BIOYM) running on a Silicon Graphics work station. For simulations in vacuo, force fields CVFF, CFF91 (MSI/BIOSYM) and AMBER[26,27] were used, with a dielectric constant of 4 with a distance dependency. The dynamics trajectories were recorded at 300 K during 1 ns. The system was first minimized and then heated and equilibrated during 27.5 ps, increasing the temperature from 50 K to 300 K with the following steps: 0.5 ps at 50 K, 1 ps at 100 K, 1 ps at 150 K, 2 ps at 200 K, 3 ps at 250 K and 20 ps at 300 K for the equilibration phase. Three molecular dynamics simulations were carried out with each force field with

the following starting conformations of the α-D-mannopyranose ring: $^1C_4$, $^4C_1$ and $^1S_3$[28]. The GROMOS force field[29], optimized for carbohydrates[30], and CFF91 were used for the dynamics simulations in water of ($C^2$-α-D-Man-)Trp in the $^1S_3$ conformation. The dynamics simulation with GROMOS was run at 300 K during 500 ps after minimization. ($C^2$-α-D-Man-)Trp was placed in a truncated octahedral periodic box containing 404 water molecules. The SPC model was used to describe the water molecules[31]. The dynamics simulation with CFF91 was run at 300 K during 260 ps in a box of water of 25 Å containing 630 water molecules. Periodic boundary conditions were applied. Water was first minimized with ($C^2$-α-D-Man-)Trp fixed and then the entire system was minimized. In all force fields the linkage between the mannose and the indole group was treated as unknown and estimated. In all calculations, ($C^2$-α-D-Man-)Trp was oriented with a small distance between H1'--Hβ,β', H1'--Hα, and H2'--HN1, as described by NMR for the peptide FTW$^{Man}$AQW[1]. All possible ring conformations for mannopyranose have been generated with INSIGHTII. For each conformation specific distances have been measured and coupling constants $J_{i,i+1}$ calculated using generalized Karplus-equations[32]. The following electronegativity factors have been used: 1.3 for oxygen, 0.4 for carbon and 0.85 for nitrogen.

*Molecular dynamics of rEDN-Trp*

Studies were performed using the INSIGHTII and DISCOVER molecular modeling software (MSI/BIOSYM) running on a Silicon Graphics work station. The X-ray structure of rEDN was used as the starting point for molecular modeling, then a mannosyl residue was linked to the C2 atom of the indole ring of Trp7 of rEDN. The monosaccharide residue was oriented to display small distances between H1'--HN1 and H2'--Hβ, as predicted by NMR[2]. Different conformations of the mannose pyranose ring were modeled in the protein: $^1C_4$, $^4C_1$ and $^1S_3$. The CFF91 force field (MSI/BIOSYM) was used, with a dielectric constant of 4 with a distance dependency. The side chains of rEDN were first minimized with the iterative conjugate gradient algorithm for 500 iterations or until the energy gradient fell below 0.1 Kcal/Å. Then, the whole protein was subjected to further energy minimization to reduce the energy gradient to 0.05 Kcal/Å. Dynamics simulations with explicit water were carried out on rEDN without mannose and on rEDN with a $^1C_4$ mannose linked to Trp7. The two sulfate anions present in the crystal structure were also

included in the simulation. A sphere of 32 Å diameter of water molecules was generated around His15, containing 3744 water molecules for the protein without mannose and 3740 with mannose. The dynamics trajectories were recorded at 300 K during 500 ps. Restrains were imposed on the water molecules to be allocated in a 32 Å sphere. Before starting the dynamics simulation, all water molecules were minimized with the steepest descent algorithm for 200 iterations and the protein fixed. Then, the water and the protein were minimized with the iterative conjugate gradient algorithm, and terminated after 500 iterations or when the energy gradient fell below 0.1 Kcal/Å. The system was heated and equilibrated during 27.5 ps, by increasing the temperature from 50 K to 300 K with the following steps: 0.5 ps at 50 K, 1 ps at 100 K, 1 ps at 150 K, 2 ps at 200 K, 3 ps at 250 K and 20 ps at 300 K for the equilibration phase.

**Results and Discussion**

The complete NMR assignment of the $C^2$-α-D-mannopyranosyl-L-tryptophan moiety of the C-glycopeptide FTW$^{Man}$AQW obtained from human RNase 2 has been described previously and was confirmed by analysis of the ($C^2$-α-D-Man-)Trp compound obtained by total synthesis[33]. The atom designation of ($C^2$-α-D-Man-)Trp is presented in Figure 1.

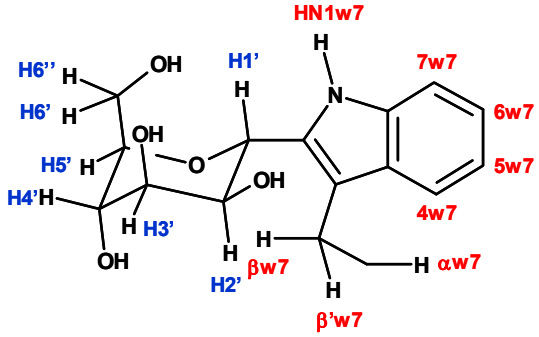


**Figure 1**: α-D-Mannopyranosyl moiety linked to the indole ring of Trp7 in a $^1C_4$-chair conformation. The depicted conformation is only shown as clarification of the text, since the α-D-mannopyranosyl residue is not present in a single conformation (see text).

NMR data obtained for the isolated ($C^2$-α-D-Man-)Trp moiety proved that its mannose is oriented with a small distance between H1'--Hβ,β', H1'--Hα, and H2'--HN1, as has been described already for the peptide FTW$^{Man}$AQW. NMR data previously recorded

were not compatible with a single ring conformation and hence predicted flexibility of the pyranose ring of the mannose residue. Therefore, molecular dynamics calculations for ($C^2$-α-D-Man-)Trp in vacuo were recorded starting from $^4C_1$, $^1C_4$, and $^1S_3$ conformations (Table 1).

**Table 1**: Simulation in vacuum starting from $^4C_1$, $^1C_4$ and $^1S_3$ conformations

| Starting conformation | $^4C_1$ | | | $^1C_4$ | | |
|---|---|---|---|---|---|---|
| Force field | AMBER | CVFF | CFF91 | AMBER | CVFF | CFF91 |
| Trajectory | 1.0 ns | 1.0 ns | 1.0 ns | 1.0 ns | 1.0 ns | 1.0 ns |
| Transition at time | 20 ps | 15 ps | - | - | - | - |
| New conformation | $^1C_4$ | $^1C_4$ | $^4C_1$ | $^1C_4$ | $^1C_4$ | $^1C_4$ |
| After transition | Stable | Stable | Stable | Stable | Stable | Stable |

| Starting conformation | $^1S_3$ | | |
|---|---|---|---|
| Force field | AMBER | CVFF | CFF91 |
| Trajectory | 1.0 ns | 1.0 ns | 1.0 ns |
| Transition at time | -- | 1 ps | 5 ps |
| New conformation | $^1S_3$, $^{1,4}B$ | $^1C_4$ | $^4C_1$ |
| After transition | Not stable | Stable | Stable |

The AMBER and CVFF force fields gave identical results: the $^1C_4$ chair conformation is the most stable conformation, and transition from the $^4C_1$ conformation happens during the first 20 ps of the dynamic simulation. Starting from the $^1S_3$ conformation, the CVFF force field showed transition to the $^1C_4$ conformation during the first 1 ps of simulation, CFF91 to the $^4C_1$ during 5 ps, while AMBER was not able to detect any stable conformation. Molecular dynamics simulations were performed also with explicit water, starting with mannose in the $^1S_3$ conformation. When CFF91 was applied, the pyranose ring stayed in the $^1S_3$ conformation for the whole simulation (Table 2). With GROMOS, transition to a $^1C_4$ chair was observed after 40 ps of simulation. Since there are no specific parameters in molecular modeling for this type of *C*-glycosylation, in all applied force fields the linkage between the mannose and the indole group was considered to be

unknown and estimated. When GROMOS was used, the *C*-linkage was treated as an aromatic carbon linked to $CH_2$.

**Table 2**: Simulation in water starting from a $^1S_3$ conformation

| Force fields | GROMOS | CFF91 |
|---|---|---|
| Trajectory | 500 ps | 240 ps |
| Transition at time | 40 ps | - |
| New conformation | $^1C_4$ | No transition |
| After transition | Stable | - |

To compare molecular modeling calculations with NMR data, all possible conformations of the pyranose ring were generated with INSIGHTII. For each conformation specific distances were measured and coupling constants calculated (Table 3), then compared with experimental NMR data. Since no NOE signals could be detected between H1' and H4' of the mannosyl residue, all conformations presenting a short distance between H1'-H4' could be excluded, in particular $^{1,4}B$, $^1S_5$ and $^1S_3$. The strong NOE signal between H1' and H6' of the mannosyl residue allowed elimination of $^{2,5}B$ and $^0S_2$, while the experimental value $J_{1',2'}$= 8.2 Hz precluded all conformations with a small H1'/H2' coupling constant ($^4C_1$, $^{0,3}B$, $B_{0,3}$, $B_{1,4}$, $^{2,5}B$, $^3S_1$, $^5S_1$, $^2S_0$). The best agreement with the experimental NOE data was obtained for the $^1C_4$ chair conformation, which nevertheless presented a $J_{3',4'}$ value quite different from the experimental one of 5.3 Hz for ($C^2$-α-D-Man-)Trp, 2.8 Hz for $^1C_4$). Therefore, it was concluded that the *C*-linked mannopyranosyl residue must exist in an ensemble of conformations, among which $^1C_4$ seems to be the most represented. Molecular dynamics simulations that seem to favor the $^1C_4$ conformation confirm this assumption. The instability of the normally preferred $^4C_1$ conformation is in this case probably due to the preference of the rigid Trp ring to adopt an equatorial position that minimizes steric interactions.

**Table 3**: Calculation of $J_{i,i+1}$ coupling constants an of NOE contacts' intensities for the pyranose ring of Manα1-Trp from Human RNase $U_s$.

| | $J_{i,i+1}$ | | | |
|---|---|---|---|---|
| | H1'/H2' | H2'/H3' | H3'/H4' | H4'/H5' |
| Manα1-Trp | 8.2 | 3.2 | 5.3 | 3.4 |
| $^4C_1$ | 1.4 | 3.2 | 8.0 | 8.5 |
| $^1C_4$ | 7.7 | 3.1 | 2.8 | 1.2 |
| $^{0,3}B$ | 3.5 | 3.2 | 2.5 | 3.1 |
| $B_{0,3}$ | 2.8 | 2.9 | 8.1 | 3.7 |
| $^{1,4}B$ | 7.9 | 6.7 | 8.6 | 8.5 |
| $B_{1,4}$ | 1.3 | 6.7 | 2.2 | 1.1 |
| $^{2,5}B$ | 1.4 | 3.7 | 1.4 | 1.2 |
| $B_{2,5}$ | 7.7 | 3.1 | 1.8 | 8.5 |
| $^1S_5$ | 7.7 | 5.4 | 6.0 | 8.3 |
| $^0S_2$ | 6.7 | 2.1 | 0.8 | 7.2 |
| $^3S_1$ | 2.3 | 4.4 | 3.4 | 1.6 |
| $^5S_1$ | 2.0 | 5.2 | 0.9 | 1.5 |
| $^2S_0$ | 1.4 | 2.2 | 6.6 | 1.9 |
| $^1S_3$ | 5.4 | 3.8 | 8.9 | 7.2 |

| | Distances (Å) | | | | |
|---|---|---|---|---|---|
| | H3'-H5' | H1'-H6' | H4'-H6'' | H2'-H3' | H1'-H4' |
| Manα1-Trp | (NOE)W[a] | (NOE)S | (NOE)M | (NOE)S | - |
| $^4C_1$ | 2.6 | 4.4 | 2.5 | 2.4 | 4 |
| $^1C_4$ | 4.4 | 2.4 | 2.6 | 2.4 | 4.0 |
| $^{0,3}B$ | 3.5 | 4.5 | 2.4 | 2.3 | 4.6 |
| $B_{0,3}$ | 3.2 | 2.5 | 2.5 | 2.4 | 3.4 |
| $^{1,4}B$ | 2.3 | 3.1 | 2.9 | 2.2 | 1.9 |
| $B_{1,4}$ | 4.2 | 4.1 | 2.5 | 2.2 | 4.8 |
| $^{2,5}B$ | 4.1 | 2.9 | 2.4 | 2.9 | 4.7 |
| $B_{2,5}$ | 3.3 | 4.5 | 2.5 | 2.4 | 3.2 |
| $^1S_5$ | 2.7 | 3.8 | 2.7 | 2.3 | 2.3 |
| $^0S_2$ | 3.7 | 4.6 | 2.4 | 2.4 | 4.1 |
| $^3S_1$ | 4.2 | 4.4 | 2.4 | 2.3 | 4.7 |
| $^5S_1$ | 4.2 | 4.1 | 2.7 | 2.3 | 4.8 |
| $^2S_0$ | 3.5 | 2.6 | 2.4 | 2.5 | 4.0 |
| $^1S_3$ | 2.7 | 2.3 | 2.4 | 2.3 | 2.4 |

[a]NOE intensities were estimated from cross-peak volumes in 2D-NOESY spectra recorded with a mixing time of 100 ms[24]. NOE intensities were determined as a percentage of the summed ROE and diagonal-peak intensities in a $\omega_2$-column of the appropriate line width and were classified as weak (w, less than 5%), medium (m, 6-10%), or strong (s, more than 10%).

To detect whether the ($C^2$-α-D-Man-)Trp conformation could be influenced by the presence of neighboring amino acids, or whether the presence of the *C*-linked mannose could reduce the flexibility of the amino acid region linked to it, peptides with different chain length were isolated form human RNase 2 and characterized by $^1$H NMR. Chemical shifts and $J_{i,i+1}$ coupling constants are reported in Table 4.

**Table 4:** $^1$H chemical shifts (ppm) and homonuclear vicinal $^1$H-$^1$H coupling constants (Hz) of the *C*-glycosylated amino acid residues, measured at 300K.

| | $W_{Man}$[a] | | $W^{Man}AQW$[a] | | $FTW^{Man}AQW$[a] | | $SSSW^{Man}SEW$[b] | | $MSPW^{Man}SEW$[c] |
|---|---|---|---|---|---|---|---|---|---|
| | $\delta_H$ | $J_{i,i+1}$ | $\delta_H$ | $J_{i,i+1}$ | $\delta_H$ | $J_{i,i+1}$ | $\delta_H$ | $J_{i,i+1}$ | $\delta_H$ |
| H1’ | 5.17 | 8.2 | 5.14 | 8.2 | 5.22 | 7.8 | 5.18 | 7.5 | 5.18 |
| H2’ | 4.42 | 3.2 | 4.40 | 3.1 | 4.42 | 3.2 | 4.44 | 3.0 | 4.44 |
| H3’ | 4.11 | 5.3 | 4.08 | 5.4 | 4.09 | 5.5 | 4.00 | 9.1[d] | 4.07 |
| H4’ | 3.95 | 3.4 | 3.94 | 3.8 | 3.96 | 3.8 | 3.93 | | 3.94 |
| H5’ | 3.89 | 8.7 | 3.84 | 8.2 | 3.87 | 8.3 | 3.83 | 8.3 | 3.82 |
| H6’ | 4.25 | | 4.18 | | 4.21 | | 4.18 | | 4.18 |
| H6’’ | 3.73 | | 3.75 | | 3.77 | | - | | - |
| H4 | 7.65 | | 7.57 | | 7.67 | | 7.65 | | 7.53 |
| H5 | 7.13 | | 7.12 | | 7.14 | | 7.14 | | 7.11 |
| H6 | 7.22 | | 7.21 | | 7.20 | | 7.20 | | 7.20 |
| H7 | 7.44 | | 7.44 | | 7.41 | | 7.42 | | 7.42 |

[a] Digested peptides from human RNase $U_s$
[b] 316β-322β chymotryptic peptide from human interleukin 12. Values taken from Doucey *et al.* (1999)[5]
[c] 24-38 tryptic peptide ($MSPW^{Man}SEWSQCDPCLR$) from C9 of human complement system. Values taken from Hofsteenge *et al.* (1999)[6]
[d] $J_{3',4'}+J_{4',5'}$

Searching for structural details of the small peptides responsible for the peculiar *C*-mannose conformation, NMR values for ($C^2$-α-D-Man-)Trp in the RNase 2 peptides were compared with the chymotryptic peptide $SSSW^{Man}SEW$ isolated from human interleukin 12[5] and the tryptic peptide $MSPW^{Man}SEWSQCDPCLR$ isolated from the terminal component C9 of the human complement system[6]. Although the analyzed fragments possess different amino acid sequences, they closely resemble each other with respect to chemical shifts, NOEs (data not shown) and coupling constants. $^1$H NMR-spectroscopic

analysis revealed no evidence for long-range connectivities and secondary structure, arguing against a remarkable stabilization of the analyzed peptides. Moreover, no neighboring amino acid side chains seem to be engaged in interaction with the *C*-mannose, as indicated by the lack of NOEs. All investigated peptides are presumably disordered, and their primary structure does not influence the conformation of the ($C^2$-α-D-Man-)Trp moiety. The J-couplings of the mannosyl residue do not match with one single conformation (see Table 3), therefore the mannose ring can be supposed to have a dynamic structure in all these peptides.

Previously, NMR measurements on RNase 2 showed that the mannose residue adopts different orientations around its *C*-linkage in the native and denatured protein. In the native protein Man H2' is in close proximity of Trp Hβ, Trp Hα, and Man H1' is close to Trp N1H. However, in the denatured protein rotation around the Trp $C^2$-Man C1' bond brings Man H2' close to Trp N1H, and Man H1' close to Trp Hβ and Trp Hα, analogously to what detected for the peptides isolated from RNase 2. $^1$H chemical shifts for the *C*-mannopyranosyl residue in native and denatured RNase 2 are compared in Table 5: values for the denatured protein are close to the ones for digested peptides (see Table 4), while those for the native protein differ significantly for the values of H2' and H6'. Apparently, the three-dimensional structure of the protein affects the conformational features of the *C*-mannopyranosyl residue.

**Table 5**: $^1$H chemical shifts (ppm) at 300K of the C-mannopyranosyl moiety in native and denatured RNase 2.

| | Native | Denatured |
|---|---|---|
| H1' | 5.27 | 5.23 |
| H2' | 4.26 | 4.45 |
| H3' | 4.13 | 4.14 |
| H4' | 3.91 | 3.99 |
| H5' | n.d. | 3.98 |
| H6' | 4.55 | 4.27 |
| H6'' | 3.74 | 3.76 |

To identify the contacts between mannose and the amino acids of the native protein, molecular modeling was employed. Assuming that RNase 2 has a similar three-

dimensional structure as EDN, the X-ray structure of recombinant EDN was used as model for RNase. No strong steric conflicts were met when linking an α-D-mannopyranose unit to C2 of Trp7. The *C*-linkage was oriented with short distances between Man H2'-Trp Hβ and Man H1'-Trp N1H, as derived from NMR studies. Minimization of Manα1-rEDN was performed with the *C*-mannopyranosyl residue in the $^4C_1$, $^1C_4$, and $^1S_3$ conformations. $^1C_4$ and $^1S_3$ have similar orientation and generate the same type of hydrophobic interactions (Figures 2A): H2'--Me Val128, H3'--Me Val128, H3'--Hβ Asp112, H5'--Hβ Asp115, H5'--Hβ Thr6, H6'--Hβ Asp115. Hydrogen bonds with OH2'--OD1 Asp112 and O5'--NH Trp7 were also identified. $^4C_1$ generates instead less hydrophobic contacts (Figure 2B) and cannot justify small distances between Man H1'-Trp NH1 and Man H2'-Trp $C^{\beta}$Hs without strong steric conflicts between the mannose residue and Trp. Therefore, this conformation was considered to have a low probability to exist. Molecular dynamics simulations of the protein were carried out with the mannose residue in the $^1C_4$ conformation, in order to evaluate the flexibility of rEDN around the mannose residue. The *C*-mannopyranosyl $^1C_4$ conformation was stable during the entire simulation, and the small distances between Man H1'-Trp NH1 and Man H2'-Trp $C^{\beta}$Hs were conserved.

The orientation of the mannose residue and the amino acids after 300 ps of dynamics simulation are presented in Figure 3.

The protein conformation is relatively stable during the dynamics simulation. The loop 114-120, which is close to the mannose residue, moves at the beginning of the simulation, as well as the three N-terminal amino acids (Figure 4). The mannose residue follows the loop while the backbone residues Thr6, Trp7 and Val 128 keep the same conformation. Mannose H4' establishes a new hydrophobic contact with Hβ Asp115, but loses the one with H5' (Figure 3); all the other hydrophobic contacts are preserved. The hydrogen bond network observed after 300 ps is the following: OH2'--OD2 Asp112, OH4--OD1 Asp119 OH6'--OD1 Asp115 and O5'--NH Trp7. To conclude, the mannose residue seems to interact with the loop residues 115-123, the end of the β strands Met105-Arg114 and the beginning of the β strands Pro124-Ile134. These interactions stabilize not only to the mannose residue and Trp7 in a specific orientation, but also the N-terminal loop of the protein. This feature could be proved by comparison with the same molecular dynamics simulation on rEDN lacking the *C*-mannosyl residue. In rEDN the loop 114-120 moves at

the same extent as rEDN-Man. However, the N-terminal loop is much more flexibile when mannose is not present, and Trp7 assumes a different conformation (Figure 5).

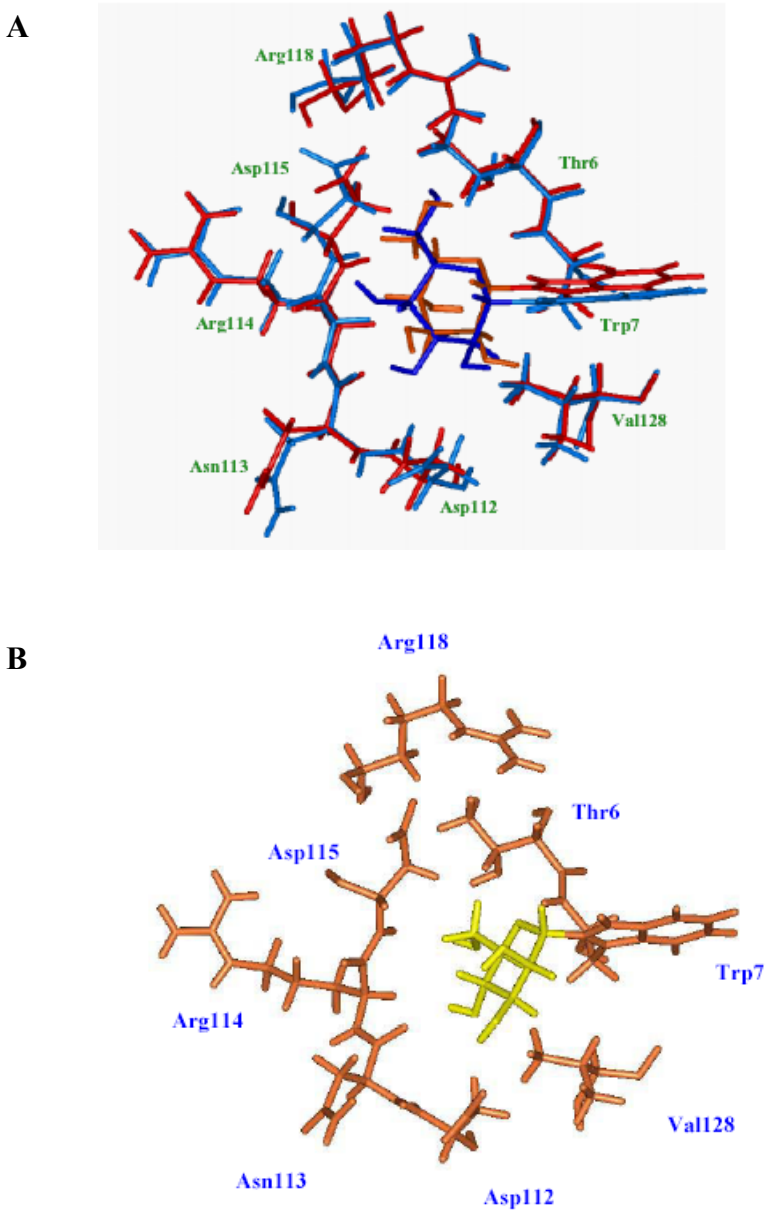


**Figure 2**: Hydrophobic interactions between rEDN and the *C*-linked α-D-mannopyranose in **A**: $^{1}C_{4}$ (red), $^{1}S_{3}$ (blue), **B**: $^{4}C_{1}$ conformations.

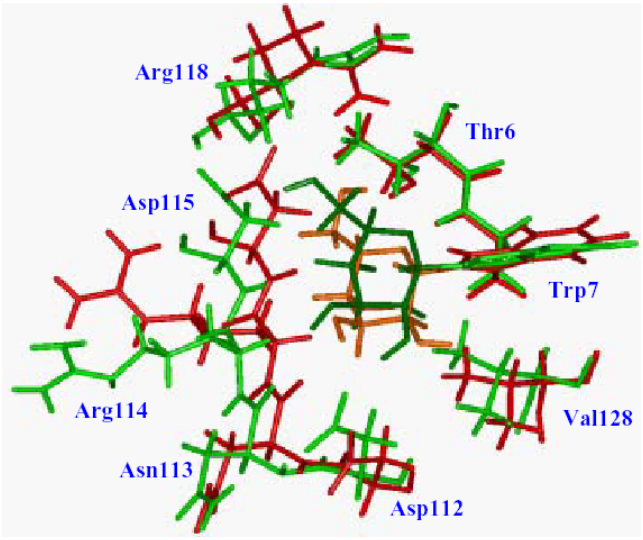


**Figure 3**: Hydrophobic interactions between the *C*-linked α-D-mannopyranose and rEDN in the starting conformation (red), and after 300 ps of dynamic simulation (green).

The protein conformation is relatively stable during the dynamics simulation. The loop 114-120, which is close to the mannose residue, moves at the beginning of the simulation, as well as the three N-terminal amino acids (Figure 4). The mannose residue follows the loop while the backbone residues Thr6, Trp7 and Val 128 keep the same conformation. Mannose H4' establishes a new hydrophobic contact with Hβ Asp115, but loses the one with H5' (Figure 3); all the other hydrophobic contacts are preserved. The hydrogen bond network observed after 300 ps is the following: OH2'--OD2 Asp112, OH4--OD1 Asp119 OH6'--OD1 Asp115 and O5'--NH Trp7. To conclude, the mannose residue seems to interact with the loop residues 115-123, the end of the β strands Met105-Arg114 and the beginning of the β strands Pro124-Ile134. These interactions stabilize not only to the mannose residue and Trp7 in a specific orientation, but also the N-terminal loop of the protein. This feature could be proved by comparison with the same molecular dynamics simulation on rEDN lacking the *C*-mannosyl residue. In rEDN the loop 114-120 moves at the same extent as rEDN-Man. However, the N-terminal loop is much more flexibile when mannose is not present, and Trp7 assumes a different conformation (Figure 5).

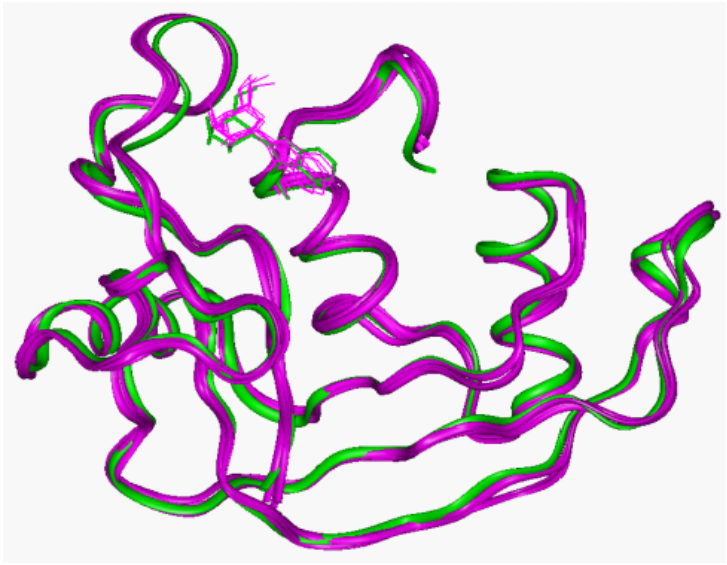

**Figure 4**: Superposition of the starting conformation (green) of rEDN-Man and five conformers (violet) during the dynamics simulation at 100, 200, 300, 400 and 500 ps, respectively. Only the backbone was used for the fit.

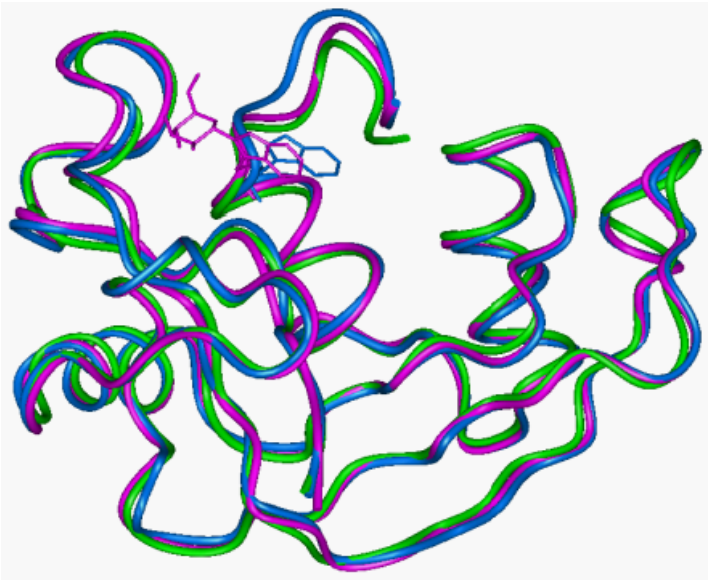

**Figure 5**: Superposition of the X-ray structure (green) of rEDN with the structures of the conformers with *C*-linked mannose (pink) and without (blue) obtained after 200 ps of dynamics simulations.

Conformations predicted by molecular modeling found confirmation in the NMR data recorded on RNase 2. In NOESY spectra, an intense NOE between mannose H1' and H6' indicates that the hydroxymethyl group is not in the usual equatorial orientation, which is typical of the $^4C_1$ conformation, but in the axial orientation presented by the $^1C_4$ chair. NOE signals confirmed also the interactions H3'--Me Val128 and H3'--Hb Asp112. Contacts between H4'-- Hb Asp115 and H5'--Hb Thr6 could not be unambiguously identified, due to signal overlapping in the NOESY spectra.

**Conclusions**

So far, the function of *C*-mannosylation has not been fully elucidated. Ihara *et al.*[34] reported increased expression of *C*-mannosylation in the aortic vessels of diabetic Zucker rats. Their results indicate that *C*-mannosylation is increased in specific tissues or cells under hyperglycemic conditions, suggesting a pathological role for the increased *C*-mannosylation in the development of diabetic complications. For some proteins, such as properdin and TSR modules, it has been hypothesized that the presence of ($C^2$-α-D-Man-)Trp moieties may facilitate adhesion phenomena. Hartmann and Hofsteenge[8] supposed that the 14 mannose residues linked to properdin could be exposed at the surface of the protein thanks to their hydrophilic character, and therefore mediate properdin interaction with the multivalent mannose-binding lectin present in serum. Affinity studies performed by Nishikawa *et al.*[35] demonstrated that although synthesized α-*C*-Man-Trp is not recognized by conventional mannose-binding lectins such as ConA and MBL-C, it nevertheless binds to several proteins present in blood serum.

In TSR modules the occurrence of more than one ($C^2$-α-D-Man-)Trp residue poses steric constraints on protein backbone conformations. The polypeptide chain cannot adopt a helical conformation and the Trp residues that become *C*-mannosylated are oriented so that their polar atoms are exposed and available for potential ligand binding[36]. Although direct involvement of *C*-mannose in adhesion phenomena has not been demonstrated, it is interesting to notice that the W-X-X-W motif and the neighboring sequence CSVTC in TSR modules of TSP have been implicated in adhesive processes with a number of cells[37], in protein-protein[38-40] and protein-glycosaminoglycan interactions[41]. In order to analyze

the biological functions of α-*C*-Man-Trp, efficient strategies have recently been developed to synthesize α-*C*-Man-Trp and its glucose and galactose analogues[42].

For RNase 2 the accessibility of the mannose residue is quite poor, only the face H1 OH3 and OH6 is accessible from the outside (Figure 3). Moreover, for RNase 2 and EDN, the presence of *C*-mannose seems not to be related directly to any specific biological function. Comparing enzymatic activity of recombinant RNase from *E. coli* with *C*-mannosylated RNase 2 no significant differences could be pointed out[43]. Similarly, *C*-mannose does not seem to be essential for the neurotoxic activity of EDN, since also the related RNase eosinophil cationic protein, which contains an arginine at position 7 instead of ($C^2$-α-D-Man-)Trp, is equally toxic[44]. *C*-linked mannose may therefore exert a structural function. ($C^2$-α-D-Man-)Trp is located in the terminal α-helix of RNase 2. NMR and molecular modeling studies demonstrated that mannose interacts with the large insertion loop constituted by the amino acid residues from Asp115 to Tyr123. The three dimensional structure of rEDN has been compared with that of bovine pancreatic RNase A, which lacks the ($C^2$-α-D-Man-)Trp moiety[15]. While the α helices and the β strands are almost identical in the two proteins, the N-terminal loop and the large insertion loop are absent in RNase A. It can be concluded that the main role of the mannose is to stabilize the N-terminal loop of the protein by interaction with the large insertion loop. This hypothesis finds confirmation in the behavior of other glycoproteins, such as the proteinase inhibitor PMP-C. In this case the fucose residue linked to Thr9 causes a decrease in the number of dynamic fluctuations of the molecule[45].

Since it was shown that *C*-mannosylation is a post-translational modification that can only take place before folding of the protein has been completed[12,13], it can be supposed ($C^2$-α-D-Man-)Trp to affect the folding and dynamics of RNase through protein-carbohydrate interactions.

**Acknowledgements**

This work has been supported financially by the CARENET 2 European network (HPRN-CT-2000-000001). We would like to thank Dr. S. Meunier for helping us in processing the NMR data, Dr. S. Mosimann and M. James for the communication of the three-dimensional structure of rEDN.

**References**

[1] de Beer T, Vliegenthart JFG, Löffler A, Hofsteenge J. The hexopyranosyl residue that is *C*-glycosidically linked to the side chain of tryptophan-7 in human RNase $U_s$ is α-mannopyranose. *Biochemistry* **1995**, *34*, 11785-11789.

[2] Löffler A, Doucey M-A, Jansson AM, Müller DR, de Beer T, Hess D, Meldal M, Richter WJ, Vliegenthart JFG, Hofsteenge J. Spectroscopic and protein chemical analyses demonstrate the presence of C-mannosylated tryptophan in intact human RNase 2 and its isoforms. *Biochemistry* **1996**, *35*, 12005-12014.

[3] Hofsteenge J, Müller DR, de Beer T, Löffler A, Richter WJ, Vliegenthart JFG. New type of linkage between a carbohydrate and a protein: *C*-glycosylation of a specific tryptophan residue in human RNase $U_s$. *Biochemistry* **1994**, *33*, 13524-13530.

[4] Krieg J, Hartmann S, Vicentini A, Gläsner W, Hess D, Hofsteenge J. Recognition signal for C-mannosylation of Trp-7 in RNase 2 consists of sequence Trp-x-x-Trp. *Mol. Biol. Cell.* **1998,** *9*, 301-309.

[5] Doucey M-A, Hess D, Blommers MJ, Hofsteenge J. Recombinant human interleukin-12 is the second example of a C-mannosylated protein. *Glycobiology* **1999**, *9*, 435-441.

[6] Hofsteenge J, Blommers M, Hess D, Furmanek A, Miroshnichenko O. The four terminal components of the complement system are *C*-mannosylated on multiple tryptophan residues. *J. Biol. Chem.* **1999**, *274*, 32786-32794.

[7] Hofsteenge J, Huwiler KG, Macek B, Hess D, Lawler J, Mosher DF, Peter-Katalinic J. *C*-Mannosylation and *O*-fucosylation of the thrombospondin type 1 module. *J. Biol. Chem.* **2001**, *276*, 6485-6498.

[8] Hartmann S, Hofsteenge J. Properdin, the positive regulator of complement, is highly *C*-mannosylated. *J. Biol. Chem.* **2000**, *275*, 28569-28574.

[9] Furmanek A, Hess D, Rogniaux H, Hofsteenge J. The WSAWS motif is C-hexosylated in a soluble form of the erythropoietin receptor. *Biochemistry* **2003,** *42,* 8452-8458.

[10] Perez-Vilar J, Randell SH, Boucher RC. C-Mannosylation of MUC5AC and MUC5B Cys subdomains. *Glycobiology* **2004**, *14*, 325-337.

[11] Gonzales de Peredo A, Klein D, Macek B, Hess D, Peter-Katalinic J, Hofsteenge J. Mannosylation and O-fucosylation of thrombospondin type 1 repeats. *Mol. Cell. Proteomics* **2002**, *1*, 11-18.

[12] Krieg J, Gläsner W, Vicentini A, Doucey M-A, Löffler A, Hess D, Hofsteenge J. C-Mannosylation of human RNase 2 is an intracellular process performed by a variety of cultured cells. *J. Biol. Chem.* **1997**, *272*, 26687-26692.

[13] Doucey M-A, Hess D, Cacan R, Hofsteenge J. Protein *C*-mannosylation is enzyme-catalysed and uses dolichyl-phosphate-mannose as a precursor. *Mol. Biol. Cell* **1998**, *9*, 291-300.

[14] Hamann KJ, Barker RL, Loegering DA, Pease LR, Gleich GJ. Sequence of human eosinophil-derived neurotoxin cDNA: identity of deduced amino acid sequence with human nonsecretory ribonucleases. *Gene* **1989**, *83*, 161-167.

[15] Mosimann SC, Newton DL, Youle RJ, James MNG. X-ray crystallographic structure of recombinant eosinophil-derived neurotoxin at 1.83 Å resolution. *J. Mol. Biol.* **1996**, *260*, 540-552.

[16] Hofsteenge J, Servis C, Stone SR. Studies on the interaction of ribonuclease inhibitor with pancreatic ribonuclease involving differential labeling of cysteinyl residues. *J. Biol. Chem.* **1991**, *266*, 24198-24204.

[17] Jeener J, Meier BH, Bachmann P, Ernst RR. Investigation of exchange processes by two-dimensional NMR spectroscopy. *J. Chem. Phys.* **1979**, *71*, 4546-4553.

[18] Griesinger C, Otting G, Wüthrich K, Ernst RR. Clean Tocsy for H-1 spin system-identification in macromolecules. *J. Am. Chem. Soc.***1988**, *110*, 7870-7872.

[19] Marion D, Ikura M, Tschudin R, Bax A. Rapid recording of 2D NMR spectra without phase cycling: application to the study of hydrogen exchange proteins. *J. Magn. Reson.* **1989**, *85*, 393-399.

[20] Hård K, van Zadelhoff G, Moonen P, Kamerling JP, Vliegenthart JFG. The Asn-linked carbohydrate chains of human Tamm-Horsfall glycoprotein of one male. Novel sulfated and novel *N*-acetylgalactosamine-containing N-linked carbohydrate chains. *Eur. J. Biochem.* **1992**, *209*, 895-915.

[21] Marion D, Wüthrich K. Application of phase sensitive two-dimensional correlated spectroscopy (COSY) for measurements of 1H-1H spin-spin coupling constants in proteins. *Biochem. Biophys. Res. Commun.* **1983**, *113*, 967-974.

[22] Braunschweiler L, Ernst RR. Coherence transfer by isotropic mixing: application to proton correlation spectroscopy. *J. Magn. Reson.* **1983**, *53,* 521-528.

[23] Bax A, Davis DG. Practical aspects of two-dimensional transverse NOE spectroscopy. *J. Magn. Reson.* **1985**, *65*, 207-213.

[24] Leeflang BR, Kroon-Batenburg LMJ. CROSREL: Full relaxation matrix analysis for NOESY and ROESY NMR spectroscopy. *J. Biomol. NMR* **1992**, *2*, 495-518.

[25] Delaglio F, Grzesiek S, Vuister GW, Zhu G, Pfeifer J, Bax A. NMRPipe: a multidimensional spectral processing system based on UNIX pipes. *J. Biomol. NMR* **1995**, *6*, 277-293.

[26] Weiner SJ, Kollman PA, Nguyen DT, Case DA. An all atom force field for simulations of proteins and nucleic acids. *J. Comput. Chem*. **1986**, *7*, 230-252.

[27] Homans SW. A molecular mechanical force field for the conformational analysis of oligosaccharides: comparison of theoretical and crystal structures of Manα1-3Manβ1-4GlcNAc. *Biochemistry*, **1990**, *29*, 9110-9118.

[28] IUPAC-IUB Joint Commission on Biochemical Nomenclature (JCBN). Conformational nomenclature for five and six-membered ring forms of monosaccharides and their derivatives. Recommendations 1980. *Eur. J. Biochem.* **1980**, *111*, 295-298.

[29] van Gunsteren WF, Berendsen HJ. On the fluctuation-dissipation theorem for interacting brownian particles. *Molec. Phys.* 1982*, 47,* 721-723.

[30] Spieser SAH, van Kuik JA, Kroon-Batenburg LMJ, Kroon J. Improved carbohydrate force field for GROMOS: ring and hydroxymethyl group conformations and exo-anomeric effect. *Carbohydr. Res.* **1999**, *322,* 264-273.

[31] Berendsen HJC, Postma JPM, van Gunsteren WF, Hermans J. (1981) *Intermolecular Forces* (Reidel Publishing, Dordrecht, The Netherlands.

[32] Haasnoot CAG, de Leeuw FAAM, Altona C. The relation between proton-proton NMR coupling constants and substituent electronegativities. I. An empirical generalization of the Karplus equation. *Tetrahedron* **1980**, *36,* 2783-2792.

[33] Manabe S, Ito Y. Total synthesis of novel subclass of glyco-amino acid structure motif: $C^2$-α-D-*C*-mannosylpyranosyl-L-tryptophan. *J. Am. Chem. Soc.* **1999**, *121*, 9754-9755.

[34] Ihara Y, Manabe S, Kanda M, Kawano H, Nakayama T, Sekine I, Kondo T, Ito Y. Increased expression of protein C-mannosylation in the aortic vessels of diabetic Zucker rats. *Glycobiology* **2005**, *15*, 383-392.

[35] Nishikawa T, Kajii S, Sato C, Yasukawa Z, Kitajima K, Isobe M. α-*C*-Mannosyltryptophan is not recognized by conventional mannose-binding lectins. *Bioorg. Med. Chem.* **2004**, *12*, 2343-2348.

[36] Tan K, Duquette M, Liu J-H, Dong Y, Zhang R, Joachimiak A, Lawler J, Wang J-H. Crystal structure of the TSP-1 type 1 repeats: a novel layered fold and its biological implication. *J. Cell. Biol.* **2002**, *159*, 373-382.

[37] Prater CA, Plotkin J, Jaye D, Frazier WA. The properdin-like type I repeats of human thrombospondin contain a cell attachment site. *J. Cell. Biol.* **1991**, *112*, 1031-1040.

[38] Li WX, Howard RJ, Leung LL. Identification of SVTCG in thrombospondin as the conformation-dependent, high affinity binding site for its receptor, CD36. *J. Biol. Chem.* **1993**, *268*, 16179-16184.

[39] Dawson DW, Pearce SF, Zhong R, Silverstein RL, Frazier WA, Bouck NP. CD36 mediates the in vitro inhibitory effects of thrombospondin-1 on endothelial cells. *J. Cell. Biol.* **1997**, *138*, 707-717.

[40] Crombie R, Silverstein RL, MacLow C, Pearce SF, Nachman RL, Laurence J. Identification of a CD36-related thrombospondin 1-binding domain in HIV-1 envelope glycoprotein gp120: relationship to HIV-1-specific inhibitory factors in human saliva. *J. Exp. Med.* **1998**, *187*, 25-35.

[41] Guo NH, Krutzsch HC, Negre E, Vogel T, Blake DA, Roberts DD. Heparin- and sulfatide-binding peptides from the type I repeats of human thrombospondin promote melanoma cell adhesion. *Proc. Natl. Acad. Sci. U.S.A.* **1992**, *89*, 3040-3044.

[42] Nishikawa T, Koide Y, Kanakubo A, Yoshimura H, Isobe M. Synthesis of β-analogues of *C*-mannosyltryptophan, a novel *C*-glycosylamino acid found in proteins. *Org. Biomol. Chem.* **2006**, *4*, 1268-1277.

[43] Furmanek A, Hofsteenge J. Protein C-mannosylation: Facts and questions. *Acta Biochimica Polonica* **2000**, *47***,** 781-789.

[44] Snyder MR, Gleich GJ. *Ribonucleases, Structures and Functions*, in D'Alessio G, Riordan JF, eds (Academic Press, Inc., New York), **1997**, 425-444.

[45] Mer G, Hietter H, Lefevre J-F. Stabilization of proteins by glycosylation examined by NMR analysis of a fucosylated proteinase inhibitor. *Nat. Struct. Biol*. **1996**, *3*, 45-53.

# 5

# SPR studies of carbohydrate-protein interactions: signal enhancement of low-molecular-mass analytes by organoplatinum(II)-labeling

Daniela Beccati[1], Koen M. Halkes[1], Guido D. Batema[2], Gabriela Guillena[2], Adriana Carvalho de Souza[1], Gerard van Koten[2], Johannis P. Kamerling[1]

[1]*Bijvoet Center, Department of Bio-Organic Chemistry, Utrecht University, Padualaan 8, 3584 CH Utrecht, The Netherlands*

[2]*Debye Institute, Department of Metal-Mediated Synthesis, Utrecht University, Padualaan 8, 3584 CH Utrecht, The Netherlands*

Published in *ChemBioChem* **2005**, *6*, 1196-1203

**Abstract**

The relatively insensitive surface plasmon resonance (SPR) signal detection of low-molecular-mass analytes that bind with weak affinity to a protein - for example, carbohydrate-lectin binding - is hampering the use of biosensors in interaction studies. In this investigation, low-molecular-mass carbohydrates have been labeled with an organoplatinum(II) complex of the type [PtCl(NCN-R)]. The attachment of this complex increased the SPR response tremendously and allowed the detection of binding events between monosaccharides and lectins at very low analyte concentrations. The platinum atom inside the organoplatinum(II) complex was shown to be essential for the SPR-signal enhancement. The organoplatinum(II) complex did not influence the specificity of the biological interaction, but both the signal enhancement and the different binding character of labeled compounds when compared with unlabeled ones makes the method unsuitable for the direct calculation of biologically relevant kinetic parameters. However, the labeling procedure is expected to be of high relevance for qualitative binding studies and relative affinity ranking of small molecules (not restricted only to carbohydrates) to receptors, a process of immense interest in pharmaceutical research.

*Keywords*

Surface plasmon resonance spectroscopy; organoplatinum(II)-labeling; signal enhancement; carbohydrates; lectin.

## Introduction

Introduced in the early 1990s, biosensors based on surface plasmon resonance (SPR) have become a well-established tool for studying biomolecular interactions in real time[1,2]. Major applications have been reported, not only for protein-protein interactions, including in conjunction with mass spectrometry, but also in SPR studies on nucleic acid-protein, carbohydrate-protein, and carbohydrate-carbohydrate interactions[3-6].

Qualitative SPR applications range from orphan-ligand and small-analyte screening to epitope mapping and complex assembly studies, whereas quantitative experiments include concentration measurements of active molecules in solution, evaluation of competition/inhibition events, and determination of rate and affinity constants. Nevertheless, since the SPR response is proportional to the accumulation of mass on the sensor surface, a serious constraint imposed by this technique concerns the dimension of the molecules to be employed as analytes[7].

In recent years, several groups have focused on SPR as an emerging technique to detect protein-carbohydrate interactions[8-20], key steps in many biological events[21,22]. SPR studies of these biological events are hampered by the low availability of high-molecular-mass oligosaccharides and by the weakness of protein-carbohydrate interactions. To overcome these problems, more accessible low-molecular-mass carbohydrate epitopes are multivalently presented to the lectin to increase both their binding affinity and overall mass (thereby enhancing the SPR response). Thus, glycan epitopes can either be immobilized on the surface of a sensorchip[23] or, when used as analytes, conjugated to carrier proteins[24-26] or, in the case of carbohydrate-carbohydrate interactions, clustered on gold glyconanoparticles[27].

Although recent improvements in signal-to-noise ratio have made it possible to measure the binding of monovalently presented low-molecular-mass analytes directly[28], relevant control surfaces for blank subtraction and high surface concentrations of active immobilized ligands are needed. This is often difficult to achieve, and mass transport limitations and rebinding events may complicate interaction analysis at such high ligand densities[29]. Moreover, to obtain sufficient SPR signal for the weak-affinity binding of a carbohydrate to a protein with analytes of molecular mass < 1000 Da, high analyte concentrations (up to the millimolar range) are required[15,30-34]. Under these conditions, the

contribution from the bulk refractive index to the specific response becomes significant, with an apparent loss in specific binding.

This study presents a method that allows facile qualitative SPR detection of low-molecular-mass carbohydrate epitopes at low concentrations with a Biacore 2000 instrument. In our experimental set-up, low-molecular-mass carbohydrates (mono- and disaccharides) are labeled with an organoplatinum(II) complex. These compounds, when allowed to flow at very low analyte concentrations (0.5 – 20 μM range) across suitable lectin surfaces, give rise to intense SPR signals. The crucial role of the platinum atom for this SPR signal enhancement is discussed.

**Material and Methods**

Surface plasmon resonance studies were carried out on a Biacore 2000 instrument, with CM5 sensor chips and Biaevaluation 3.0 software (Pharmacia Biosensor AB, Uppsala, Sweden). *N*-Hydroxysuccinimide was purchased from Merck (NJ, USA), *N*-ethyl-*N*′-(dimethylaminopropyl)carbodiimide and ethanolamine from Sigma (St. Louis, USA), cysteamine hydrochloride and *N*-ethylmorpholine from Fluka (Buchs, Switzerland), and *O*-benzotriazol-1-yl-*N*,*N*,*N*′,*N*′-tetramethyluronium tetrafluoroborate (TBTU) from NovaBiochem (Breda, The Netherlands). C-18 Extract-Clean columns were purchased from Alltech (Breda, The Netherlands) and Dowex 50 Wx2 ($H^+$, 200-400 mesh) from Fluka (Buchs, Switzerland). *Ricinus communis* agglutinin from castor bean ($RCA_{120}$) and concanavalin A lectin from *Canavalia ensiformis* (ConA) were supplied by Sigma (St. Louis, USA). Compounds **1**[35] and **6**[36] were synthesized by procedures similar to those used for their iodide and bromide analogues, respectively. Compounds **8** and **10** were synthesized as described earlier[37].

Reactions were monitored by TLC on silica gel 60 ($F_{254}$, Merck); after examination under UV light, compounds were visualized by heating with methanolic $H_2SO_4$ (10% v/v), orcinol (2 mg/mL) in methanolic $H_2SO_4$ (20%, v/v), or ninhydrin (1.5 mg/mL) in BuOH-$H_2O$-HOAc (38:1.75:0.25, v/v). Vacuum line column chromatography (VLC) was performed on silica gel (Merck 60, 0.040-0.063 mm). UV-irradiation for synthetic purposes was performed in quartz vials at 254 nm with a grid tube lamp (VL-50 C, 50 W, Vilber Lourmat). Organic solvents were removed under reduced pressure at 30-50°C on a water bath. $^1$H NMR spectra were recorded at 300 K with a Bruker AMX 500 (500 MHz)

spectrometer; $\delta_H$ values are given in ppm relative to the signal for internal $Me_4Si$ ($\delta_H$ = 0, $CDCl_3$) or internal acetone ($\delta_H$ = 2.22, $D_2O$). Two-dimensional $^1H$-$^1H$ TOCSY (mixing time 7 ms) spectra were recorded at 300 K with a Bruker AMX 500 spectrometer. Exact masses were measured by matrix-assisted laser desorption ionization time-of-flight mass spectrometry using a Voyager-DE Pro (Applied Biosystems) instrument in the reflector mode at a resolution of 5000 FWHM. α-Cyano-4-hydroxycinnamic acid (Fluka Chemie GmbH, Buchs, Switzerland) in $H_2O$ (5 mg/mL) was used as a matrix. A ladder of maltose oligosaccharides (G3-G13) was added as internal standard.

*[PtCl(NCN)]-3-(amidoethylthio)propyl β-lactoside* (**2**)

Cysteamine hydrochloride (29.7 mg, 0.262 mmol) was added to a solution of allyl β-lactoside (100 mg, 0.262 mmol) in water (3 mL). The mixture was transferred to a quartz vial and irradiated with UV light for 2 h, after which TLC analysis (dichloromethane-methanol 8:2, v/v) showed the formation of a new spot on the baseline and some remaining allyl β-lactoside. The mixture was applied to a Dowex 50 Wx2 ($H^+$) column (50 mm x 6 mm), and after the elution of contaminants with water, 3-(aminoethyl thio) propyl β-lactoside was eluted with aq. ammonia (6%). The product was lyophilized twice from water, and was directly used in the next reaction step. A solution of **1** (17.5 mg, 31.3 μmol) in tetrahydrofuran (0.3 mL) was added to a solution of 3-(aminoethylthio)propyl β-lactoside (10 mg, 20.8 μmol) in aq. $NaHCO_3$ (0.25 M)-acetonitrile (1:1, v/v; 0.6 mL), and the mixture was agitated gently overnight. After concentration *in vacuo*, the residue was dissolved in water (15 mL), washed with dichloromethane (3 x 15 mL), and the aqueous layer was concentrated to a volume of approximately 3 mL, and then loaded on a C-18 Extract-Clean column. The remaining 3-(aminoethylthio)propyl β-lactoside was eluted with water (15 mL) and **2** with methanol (10 mL). After concentration *in vacuo*, followed by lyophilization from water, **2** was obtained as a white solid (11.0 mg, 59%). $\delta_H$ (500 MHz; $D_2O$) = 1.93 (m, 2 H, $OCH_2CH_2CH_2S$), 2.73 (bt, 2 H, $OCH_2CH_2CH_2S$), 2.80 (bt, 2 H, $SCH_2CH_2ND$), 3.02 and 3.14 (2 s, each 6 H, 2 $CH_2N(CH_3)_2$), 3.28 (dd, 1 H, $J_{1,2}$ = 7.9 Hz, $J_{2,3}$ = 8.1 Hz, H-2), 3.48 (m, 1 H, H-5), 3.66 (m, 1 H, H-5'), 3.72 and 3.89 (2 m, each 1 H, $OCH_2CH_2CH_2S$), 3.73 (dd, 1 H, $J_{5',6a'}$ = 4.5 Hz, $J_{6a',6b'}$ = 11.4 Hz, H-6a'), 3.80 (dd, 1 H, $J_{5',6b'}$ = 7.7 Hz, H-6b'), 3.84 (dd, 1 H, $J_{5,6b}$ = 4.6 Hz, $J_{6a,6b}$ = 12.3 Hz, H-6b), 3.87 (bd, 1 H, $J_{3',4'}$ = 2.4 Hz, $J_{4',5'}$ < 1 Hz, H-4'), 3.93 (dd, 1 H, $J_{5,6a}$ = 2.2 Hz, H-6a), 4.15 and 4.16 (2

s, each 2 H, 2 C$H_2$N($CH_3$)$_2$), 4.36 (d, 1 H, H-1), 4.42 (d, 1 H, $J_{1',2'}$ = 6.4 Hz, H-1'), 7.32 and 7.34 (2 s, each 1 H, 2 x C$H_{arom}$). High-resolution MS data of $C_{30}H_{50}{}^{35}ClN_3O_{12}{}^{195}PtS$ (M, 906.245): $[M + H - HCl]^+$ found 871.273, calculated 871.276.

*[PtCl(NCN)]-3-(amidoethylthio)propyl β-D-galactopyranoside* (**3**)

Cysteamine hydrochloride (32.5 mg, 0.286 mmol) was added to a solution of allyl β-D-galactopyranoside (63 mg, 0.286 mmol) in water (3 mL). The mixture was transferred to a quartz vial and irradiated with UV-light for 2 h, after which TLC analysis (dichloromethane-methanol 85:15, v/v) showed the formation of a new spot on the baseline and some remaining allyl β-D-galactopyranoside. The mixture was applied to a Dowex 50 Wx2 ($H^+$) column (50 mm x 6 mm), and after the elution of contaminants with water, 3-(aminoethylthio)propyl β-D-galactopyranoside was eluted with aq. ammonia (6%). The product was lyophilized twice from water, and directly used in the next reaction step. A solution of **1** (17.7 mg, 31.5 μmol) in tetrahydrofuran (0.3 mL) was added to a solution of 3-(aminoethylthio)propyl β-D-galactopyranoside (7 mg, 21.0 μmol) in aq. $NaHCO_3$ (0.25 M)-acetonitrile (1:1, v/v; 0.6 mL), and the mixture was agitated gently overnight. After concentration *in vacuo*, the residue was dissolved in water (15 mL), washed with dichloromethane (3 x 15 mL), and the aqueous layer was concentrated to a volume of approximately 3 mL, and then loaded on a C-18 Extract-Clean column. The remaining 3-(aminoethylthio)propyl β-D-galactopyranoside was eluted with water (15 mL) and **3** with methanol (10 mL). After concentration *in vacuo*, followed by lyophilization from water, **3** was obtained as a light yellow solid (10.7 mg, 72%). $\delta_H$ (500 MHz; $D_2O$) = 1.91 (m, 2 H, $OCH_2CH_2CH_2S$), 2.71 (bt, 2 H, $OCH_2CH_2CH_2S$), 2.83 (bt, 2 H, $SCH_2CH_2ND$), 2.90 (bs, 12 H, 2 $CH_2N(CH_3)_2$), 3.26 and 3.92 (2 m, each 1 H, $OCH_2CH_2CH_2S$), 3.50 (dd, 1 H, $J_{1,2}$ = 7.7 Hz, $J_{2,3}$ = 9.7 Hz, H-2), 3.59 (m, 2 H, $SCH_2CH_2ND$), 3.63 (dd, 1 H, $J_{3,4}$ = 3.5 Hz, H-3), 3.91 (bd, 1 H, $J_{4,5}$ < 1 Hz, H-4), 4.19 (bs, 4 H, 2 C$H_2$N($CH_3$)$_2$), 4.40 (d, 1 H, H-1), 7.41 (bs, 2 H, C$H_{arom}$). High-resolution MS data of $C_{24}H_{40}{}^{35}ClN_3O_7{}^{195}PtS$ (M, 744.192): $[M + H - HCl]^+$ found 709.229, calculated 709.224.

*[PtCl(NCN)]-3-(amidoethylthio)propyl α-D-mannopyranoside* (**4**)

Cysteamine hydrochloride (25.7 mg, 0.227 mmol) was added to a solution of allyl α-D-mannopyranoside (50 mg, 0.227 mmol) in water (3 mL). The mixture was transferred to a quartz vial and irradiated with UV-light for 2 h, after which TLC analysis (dichloromethane-methanol 85:15, v/v) showed the formation of a new spot on the baseline and some remaining starting allyl α-D-mannopyranoside. The mixture was applied to a Dowex 50 Wx2 ($H^+$) column (50 mm x 6 mm), and after the elution of contaminants with water, 3-(aminoethylthio)propyl α-D-mannopyranoside was eluted with aq. ammonia (6%). The product was lyophilized twice from water, and directly used in the next reaction step. A solution of **1** (25.5 mg, 45.5 μmol) in tetrahydrofuran (0.3 mL) was added to a solution of 3-(aminoethylthio)propyl α-D-mannopyranoside (10 mg, 30.3 μmol) in aq. $NaHCO_3$ (0.25 M)-acetonitrile (1:1, v/v; 0.6 mL), and the mixture was agitated gently overnight. After concentration *in vacuo*, the residue was dissolved in water (15 mL), washed with dichloromethane (3 x 15 mL), and the aqueous layer was concentrated to a volume of approximately 3 mL, and then loaded on a C-18 Extract-Clean column. The remaining 3-(aminoethylthio)propyl α-D-mannopyranoside was eluted with water (15 mL) and **4** with methanol (10 mL). After concentration *in vacuo*, followed by lyophilization from water, **4** was obtained as a white solid (9.9 mg, 46%). $\delta_H$ (500 MHz; $D_2O$) = 1.91 (m, 2 H, $OCH_2CH_2CH_2S$), 2.69 (bt, 2 H, $OCH_2CH_2CH_2S$), 2.82 (bt, 2 H, $SCH_2CH_2ND$), 2.99 (bs, 12 H, 2 $CH_2N(CH_3)_2$), 3.59 and 3.80 (2 m, each 1 H, $OCH_2CH_2CH_2S$), 3.61 (bt, 2 H, $SCH_2CH_2ND$), 3.89 (bd, 1 H, $J_{1,2} < 1$ Hz, $J_{2,3} = 3.2$ Hz, H-2), 4.18 (bs, 4 H, 2 $CH_2N(CH_3)_2$), 4.82 (bs, 1 H, H-1), 7.31 (s, 2 H, $CH_{arom}$). High-resolution MS data of $C_{24}H_{40}{}^{35}ClN_3O_7{}^{195}PtS$ (M, 744.192): $[M + H - HCl]^+$ found 709.222, calculated 709.224.

*[PtCl(NCN)]-3-(amidoethylthio)propyl β-D-glucopyranoside* (**5**)

Cysteamine hydrochloride (20.7 mg, 0.182 mmol) was added to a solution of allyl β-D-glucopyranoside (40 mg, 0.182 mmol) in water (3 mL). The mixture was transferred to a quartz vial and irradiated with UV-light for 2 h, after which TLC analysis (dichloromethane-methanol 85:15, v/v) showed the formation of a new spot on the baseline and some remaining allyl β-D-glucopyranoside. The mixture was applied to a Dowex 50 Wx2 ($H^+$) column (50 mm x 6 mm), and after the elution of contaminants with

water, 3-(aminoethylthio)propyl β-D-glucopyranoside was eluted with aq. ammonia (6%). The product was lyophilized twice from water, and directly used in the next reaction step. A solution of **1** (28.1 mg, 50.0 μmol) in tetrahydrofuran (0.3 mL) was added to a solution of 3-(aminoethylthio)propyl β-D-glucopyranoside (11 mg, 33.3 μmol) in aq. $NaHCO_3$ (0.25 M)-acetonitrile (1:1, v/v; 0.6 mL), and the mixture was agitated gently overnight. After concentration *in vacuo*, the residue was dissolved in water (15 mL), washed with dichloromethane (3 x 15 mL), and the aqueous layer was concentrated to a volume of approximately 3 mL, and then loaded on a C-18 Extract-Clean column. The remaining 3-(aminoethylthio)propyl β-D-glucopyranoside was eluted with water (15 mL) and **5** with methanol (10 mL). After concentration *in vacuo*, followed by lyophilization from water, **5** was obtained as a white solid (16.1 mg, 68%). $\delta_H$ (500 MHz; $D_2O$) = 1.93 (m, 2 H, $OCH_2CH_2CH_2S$), 2.72 (bt, 2 H, $OCH_2CH_2CH_2S$), 2.78 (bt, 2 H, $SCH_2CH_2ND$), 3.02 and 3.14 (2 s, each 6 H, 2 $CH_2N(CH_3)_2$), 3.21 (dd, 1 H, $J_{1,2}$ = 7.9 Hz, $J_{2,3}$ = 9.1 Hz, H-2), 3.42 (bt, 1 H, H-3), 3.34 (m, 2 H, H-4 and H-5), 3.56 (t, 2 H, $SCH_2CH_2ND$), 3.72 (m, 1 H, H-6b), 3.72 and 3.99 (2 m, each 1 H, $OCH_2CH_2CH_2S$), 3.88 (dd, 1 H, $J_{5,6a}$ = 1.3 Hz, $J_{6a,6b}$ = 12.1 Hz, H-6a), 4.14 and 4.15 (2 s, each 2 H, 2 $CH_2N(CH_3)_2$), 4.33 (d, 1 H, H-1), 7.32 and 7.33 (2 s, each 1 H, 2 $CH_{arom}$). High-resolution MS data of $C_{24}H_{40}{}^{35}ClN_3O_7{}^{195}PtS$ (M, 744.192): $[M + H - HCl]^+$ found 709.228, calculated 709.224.

*[PtCl(NCN)]-valine-β-lactosylamide (7)*

A solution of **6** (59.1 mg, 111 μmol) in dry dimethylformamide (1 mL), preactivated for 5 min with TBTU (34.7 mg, 107 μmol) and *N*-ethylmorpholine (21.2 μL, 185 μmol) was added to a solution of β-lactosylamine[38] (12 mg, 37.0 μmol) in dimethylformamide-dimethyl sulfoxide (1:1, v/v; 500 μL). The mixture was stirred overnight, and then concentrated *in vacuo* and coconcentrated with toluene (4 x 10 mL). A solution of the residue in $H_2O$ (20 mL) was washed with dichloromethane (3 x 15 mL), and was then concentrated to a volume of approximately 3 mL and loaded onto a C-18 Extract-Clean column. Side products and salts were eluted with water (15 mL), and **7** with methanol (10 mL). After concentration *in vacuo*, followed by lyophilization from water, **7** was obtained as a slightly yellow solid (10.1 mg, 32%). $\delta_H$ (500 MHz; $D_2O$) = 0.93 (d, 3 H, $J_{H\beta,H\gamma a}$ = 6.8 Hz, $CH_3$-γa), 0.96 (d, 3 H, $J_{H\beta,H\gamma b}$ = 7.0 Hz, $CH_3$-γb), 2.00 (m, 1 H, H-β), 2.76 (bs, 12 H, 2 $CH_2N(CH_3)_2$), 3.21 (bs, 1 H, H-α), 3.47 (bt, 1 H, H-2), 3.56 (dd, 1 H, $J_{1',2'}$ = 7.8 Hz, $J_{2',3'}$

= 9.9 Hz, H-2'), 3.93 (bd, 1 H, $J_{3',4'}$ = 3.4 Hz, $J_{4',5'}$ < 1 Hz, H-4'), 4.24 (s, 4 H, 2 C$H_2$N(C$H_3$)$_2$), 4.47 (d, 1 H, H-1'), 5.06 (d, 1 H, $J_{1,2}$ = 9.2 Hz, H-1), 6.98 (s, 2 H, 2 C$H_{arom}$). High-resolution MS data of $C_{30}H_{51}{}^{35}ClN_4O_{11}{}^{195}Pt$ (M, 873.289): $[M + H - HCl]^+$ found 838.324, calculated 838.320.

*[Br(NCN)]-3-(amidoethylthio)propyl β-lactoside* (**9**)

A solution of **8** (29.2 mg, 93.9 μmol) in dry dimethylformamide (1 mL), pre-activated for 5 min with TBTU (29.1 mg, 90.8 μmol) and *N*-ethylmorpholine (17.9 μL, 156 μmol) was added to a solution of 3-(amino-ethylthio)propyl β-lactoside (15 mg, 31.3 μmol) in dry dimethylformamide (1 mL). The mixture was stirred overnight, and was then concentrated *in vacuo* and coconcentrated with toluene (4 x 10 mL). The product was purified by VLC (dichloromethane-methanol-triethylamine 98:1.5:0.5 → 95:4:1→ 90:9:1, v/v) to afford **9** as an amorphous white solid (12.4 mg, 54%). $\delta_H$ (500 MHz; $D_2O$) = 1.91 (m, 2 H, OCH$_2$C$H_2$CH$_2$S), 2.29 (s, 12 H, 2 CH$_2$N(C$H_3$)$_2$), 2.71 (bt, 2 H, OCH$_2$CH$_2$C$H_2$S), 2.84 (bt, 2 H, SC$H_2$CH$_2$ND), 3.26 (dd, 1 H, $J_{1,2}$ = 8.0 Hz, $J_{2,3}$ = 9.3 Hz, H-2), 3.54 (dd, 1 H, $J_{1',2'}$ = 7.8 Hz, $J_{2',3'}$ = 9.9 Hz, H-2'), 3.66 (dd, 1 H, $J_{3',4'}$ = 3.3 Hz, H-3'), 3.73 (s, 4 H, 2 C$H_2$N(CH$_3$)$_2$), 3.74 and 3.95 (2 m, each 1 H, OC$H_2$CH$_2$CH$_2$S), 3.92 (bd, 1 H, $J_{4',5'}$ < 1 Hz, H-4'), 4.42 (d, 1 H, H-1), 4.43 (d, 1 H, H-1'), 7.68 (bs, 2 H, C$H_{arom}$). High-resolution MS data of $C_{30}H_{50}{}^{79}BrN_3O_{12}S$ (M, 755.230): $[M + H]^+$ found 756.237, calculated 756.238.

*[Cl(NCN)]-3-(amidoethylthio)propyl β-lactoside* (**11**)

A solution of **10** (25.0 mg, 93.9 μmol) in dry dimethylformamide (1 mL), pre-activated for 5 min with TBTU (29.1 mg, 90.8 μmol) and *N*-ethylmorpholine (17.9 μL, 156 μmol) was added to a solution of 3-(aminoethylthio)propyl β-lactoside (15 mg, 31.3 μmol) in dry dimethylformamide (1 mL). The mixture was stirred overnight, and was then concentrated *in vacuo* and coconcentrated with toluene (4 x 10 mL). The product was purified by VLC (dichloromethane-methanol-triethylamine 98:1.5:0.5 → 95:4:1→ 90:9:1, v/v) to afford **11** as a white amorphous solid (8.9 mg, 41%). $\delta_H$ (500 MHz; $D_2O$) = 1.94 (m, 2 H, OCH$_2$C$H_2$CH$_2$S), 2.35 (s, 12 H, 2 CH$_2$N(C$H_3$)$_2$), 2.75 (bt, 2 H, OCH$_2$CH$_2$C$H_2$S), 2.88 (bt, 2 H, SC$H_2$CH$_2$ND), 3.31 (dd, 1 H, $J_{1,2}$ = 8.1 Hz, $J_{2,3}$ = 9.3 Hz, H-2), 3.58 (dd, 1 H, $J_{1',2'}$ = 7.7 Hz, $J_{2',3'}$ = 9.9 Hz, H-2'), 3.69 (dd, 1 H, $J_{3',4'}$ = 3.3 Hz, H-3'), 3.79 (s, 4 H, 2 C$H_2$N(CH$_3$)$_2$), 3.75 and 4.00 (2 m, each 1 H, OC$H_2$CH$_2$CH$_2$S), 3.96 (bd, 1 H, $J_{4',5'}$ < 1 Hz,

H-4'), 4.47 (d, 2 H; H1 and H-1'), 7.77 (bs, 2 H, C$H_{arom}$). High-resolution MS data of $C_{30}H_{50}{}^{35}ClN_3O_{12}S$ (M, 711.280): $[M + H]^+$ found 712.290, calculated 712.288.

*Benzoyl-3-(amidoethylthio)propyl β-lactoside* (**12**)

Benzoyl chloride (29.2 μL, 208.4 μmol) was slowly added at 0°C to a solution of 3-(aminoethylthio)propyl β-lactoside (20 mg, 41.6 μmol) in dry pyridine (4 mL). After 2 h, when TLC analysis (dichloromethane-methanol 9:1, v/v) showed the formation of a faster moving spot ($R_f$ 0.23), the mixture was concentrated and then coconcentrated with toluene (4 x 10 mL). The product was purified by VLC (dichloromethane-methanol 99:1 → 95:5, v/v) to yield **12** as a white solid (20.2 mg, 89%). $\delta_H$ (500 MHz; $D_2O$) = 1.92 (m, 2 H, $OCH_2CH_2CH_2S$), 2.71 (bt, 2 H, $OCH_2CH_2CH_2S$), 2.85 (bt, 2 H, $SCH_2CH_2ND$), 3.28 (dd, 1 H, $J_{1,2}$ = 8.1 Hz, $J_{2,3}$ = 9.5 Hz, H-2), 3.54 (dd, 1 H, $J_{1',2'}$ = 7.8 Hz, $J_{2',3'}$ = 9.9 Hz, H-2'), 3.61 (bt, 2 H, $SCH_2CH_2ND$), 3.63 (dd, 1 H, $J_{3,4}$ = 9.5 Hz, H-3), 3.66 (dd, 1 H, $J_{3',4'}$ = 3.3 Hz, H-3'), 3.77 and 3.98 (2 m, each 1 H, $OCH_2CH_2CH_2S$), 3.92 (bd, 1 H, $J_{4',5'}$ < 1 Hz, H-4'), 4.43 (d, 1 H, H-1'), 4.44 (d, 1 H, H-1), 7.53, 7.61, and 7.77 (3 m, 2 H, 1 H, and 2 H, 5 C$H_{arom}$). High-resolution MS data of $C_{24}H_{37}NO_{12}S$ (M, 563.204): $[M + Na]^+$ found 586.189, calculated 586.193.

*Preparation of sensor surfaces*

CM5 sensor surfaces were equilibrated with Tris-HCl buffered saline (pH 7.5, 10 mM), containing NaCl (150 mM), $CaCl_2$ (2 mM), and $MgCl_2$ (2 mM), and were then activated with a 10 min pulse of a mixture (1:1, v/v) of *N*-hydroxysuccinimide (0.05 M) and *N*-ethyl-*N'*-(dimethylaminopropyl) carbodiimide (0.2 M), at a flow rate of 5 μL/min. ConA lectin was attached to channels 1 and 2 by two injections of 7 min (200 μg/mL in 10 mM sodium acetate buffer, pH 4.8; ~ 11,000 response units (RUs) each); remaining *N*-hydroxysuccinimide esters were blocked by a 10-min pulse of ethanolamine hydrochloride (1.0 M, pH 8.5). In a similar way, ~ 11,500 RU of $RCA_{120}$ lectin were immobilized to channels 3 and 4. To measure the level of nonspecific binding and to serve as blank channels for mathematical data treatment, ConA bound to channel 2 and $RCA_{120}$ bound to channel 4 were denatured by a 8 min injection of guanidinium chloride (6 M, pH 1.0), followed by a 4 min injection of SDS (0.5%).

*SPR detection of saccharides*

Free and derivatized saccharides, dissolved at various concentrations (see Results) in Tris-HCl buffered saline (10 mM, pH 7.5), containing NaCl (150 mM), $CaCl_2$ (2 mM), and $MgCl_2$ (2 mM), were allowed to flow across the lectin surfaces for 5 min at a flow rate of 5 μL/min, and were allowed to dissociate for 8 min. To restore the response level to zero, a regenerating solution (20 μL) was used. To this end, several regenerating solutions were screened for their effectiveness towards the release of PtCl(NCN-R)-labeled oligosaccharides. The best results were obtained with a mixture of methyl α-D-mannopyranoside (25 μM; ConA) and methyl β-D-galactopyranoside (25 μM; $RCA_{120}$) in Tris-HCl buffer (pH 7.5).

**Results**

*PtCl(NCN-R)-labeling ensures higher sensitivity in SPR detection*

$RCA_{120}$ (specific for galactose/lactose) and ConA (specific for mannose and displaying a weak binding affinity for glucose) were chosen as model carbohydrate-binding proteins for SPR analysis of the interactions between low-molecular-mass saccharides and immobilized lectins. Each lectin was immobilized on two channels of a CM5 sensor chip (~ 11,000 RU for dimeric ConA; ~ 11,500 RU for $RCA_{120}$), and one channel of each lectin was denatured to serve as a blank surface. Firstly, the mono- and disaccharides D-mannose, D-glucose, D-galactose, methyl α-D-mannopyranoside, methyl β-D-galactopyranoside, and lactose were tested for their SPR responses on the lectin surfaces. The same series of free mono- and disaccharides were then labeled with the organoplatinum(II) complex of the type [PtCl-(NCN-R)] with the aid of the activated ester **1** (**2–5**, Figure 1) and allowed to flow over the same lectin surfaces (NCN-R is an abbreviation for the terdentate, monoanionic, 4-substituted 2,6-bis(dimethylamino methylene) phenyl "pincer" ligand[36,39]).

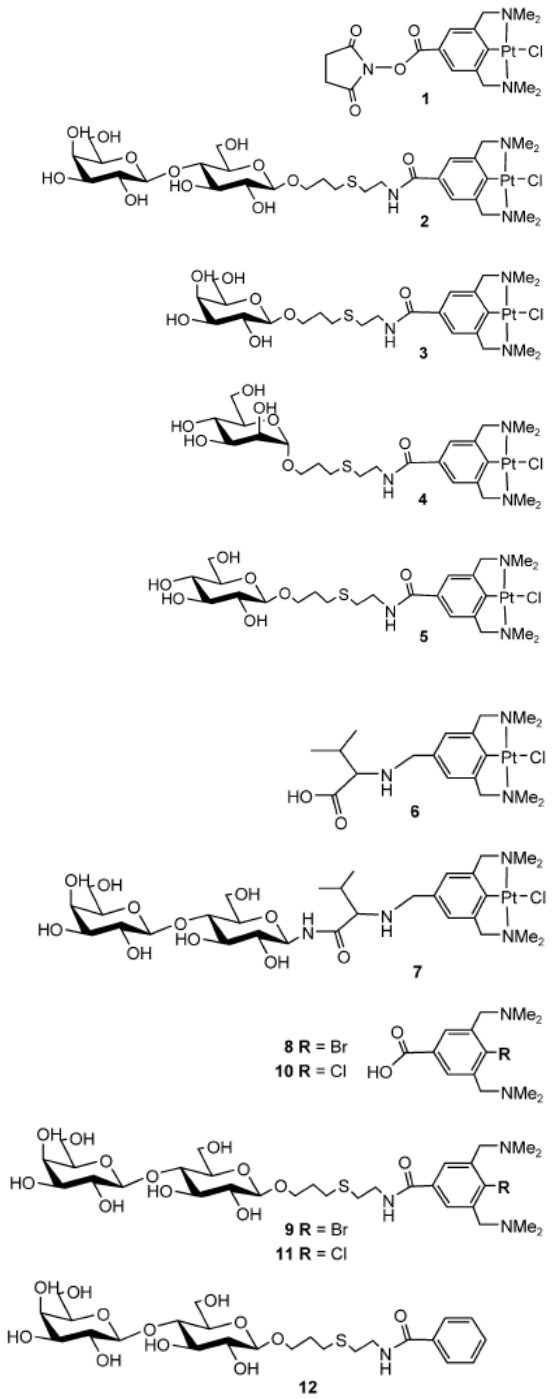


**Figure 1**: Synthesized compounds **1-12** used in this study (see Materials and Methods).

Despite their well-known specificity for these lectins, none of the free saccharides or methyl glycopyranosides showed any detectable binding either to ConA or to $RCA_{120}$ in the 1 – 600 μM concentration range. In contrast, lactose labeled with the organoplatinum(II) complex PtCl(NCN-R) (**2**), injected at 9 μM concentration over $RCA_{120,}$ produced a strong SPR signal (Figure 2). To examine whether such a high response could be attributed to specific binding, compound **2** (9 μM) was also injected simultaneously onto denatured $RCA_{120}$, ConA, and denatured ConA. As depicted in Figure 2, only the active $RCA_{120}$ surface gave a strong SPR signal, while the responses on the other surfaces were comparable to one another and very low. Similar sensorgrams, demonstrating the signal-enhancing properties of the organoplatinum(II) complex, were obtained for galactose derivative **3** on the $RCA_{120}$ surface (90 RU at 2.5 μM after blank subtraction), and for mannose derivative **4** and glucose derivative **5** on the ConA surface (50 and 10 RU at 2.5 μM after blank subtraction, respectively).

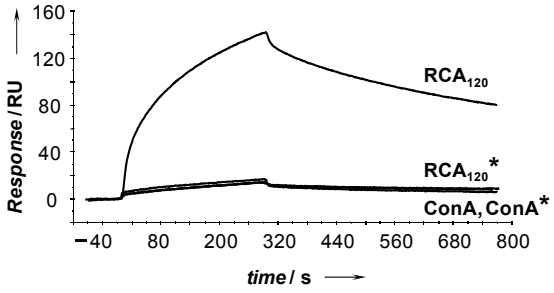


**Figure 2**: Sensorgrams of PtCl(NCN-R)-labeled lactose **2** (9 μM) flowing across $RCA_{120}$, denatured $RCA_{120}$*, ConA, and denatured ConA*. An asterisk denotes a denatured component.

Figure 3a shows the concentration-dependent overlay plot for **2** (1.1–17.5 μM), injected over $RCA_{120}$. The question of whether the length of the linker between the saccharide and the organoplatinum(II) complex would influence the signal-enhancing qualities of the complex or prevent the biomolecular interaction was also investigated. For this purpose, compound **7** was synthesized and analyzed by SPR. As illustrated in the sensorgram in Figure 3b, a signal-enhancing SPR response similar to that observed for **2** (Figure 3a) was seen; this establishes that the binding of **7** to $RCA_{120}$ was not disturbed by the close proximity of the organoplatinum(II) complex to the carbohydrate.

Subsequently, the binding affinities of free and PtCl(NCN-R)-labeled lactose **2** on $RCA_{120}$ were compared in a competition experiment. Increasing amounts of free lactose were added to a 7.5 μM solution of **2**, and the resulting sensorgrams were measured. The SPR data presented in Figure 3c show that the response decreased progressively with increasing free lactose concentration, resulting in a reduction to half of the original RU for an equimolar free lactose/compound **2** solution. This result demonstrates clearly that PtCl(NCN-R)-labeled lactose competes effectively with free lactose for the same lectin binding site.

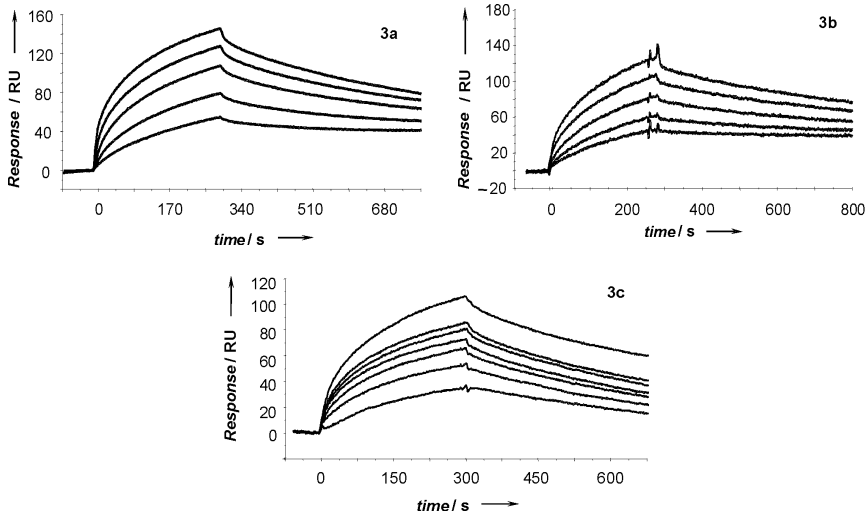


**Figure 3**: a) Concentration-dependent binding of **2** to $RCA_{120}$. Concentrations from bottom to top: 1.1, 2.2, 4.4, 8.75, 17.5 μM. b) Concentration-dependent binding of **7** to $RCA_{120}$. Concentrations from bottom to top: 1.25, 2.5, 5, 10, 20 μM. c) Competition assay between free lactose and PtCl(NCN-R)-labeled lactose **2**. Increasing amounts of free lactose were progressively added to a 7.5 μM solution of **2** (top curve; from top to bottom curve, free lactose concentrations: 0, 0.5, 1, 2, 4, 8, 16 μM).

*Unraveling the characteristics of the organoplatinum(II) complex*

To investigate the influence of the different structural components of the organoplatinum(II) complex PtCl(NCN-R) on the signal-enhancing phenomenon, the lactose derivatives **9**, **11**, and **12** were synthesized. The modifications relative to **2** involved the removal of the platinum atom (**9** and **11**) and the removal of both the platinum atom and the pincer arms to yield an unsubstituted phenyl moiety (**12**). Free lactose and compounds **2**, **9**, **11**, and **12** (1.25 – 40 μM) were allowed to flow across the

$RCA_{120}$ surfaces to yield, after blank subtraction, the sensorgrams depicted in Figure 4a-e. The strongest response is clearly that associated with the organoplatinum(II)-containing compound **2** (60-160 RU, Figure 4b). The sensorgrams of compounds **9**, **11**, and **12** (Figure 4c-e) show that the intensity of the SPR signal decreased dramatically whenever the aglycon did not contain a platinum atom.

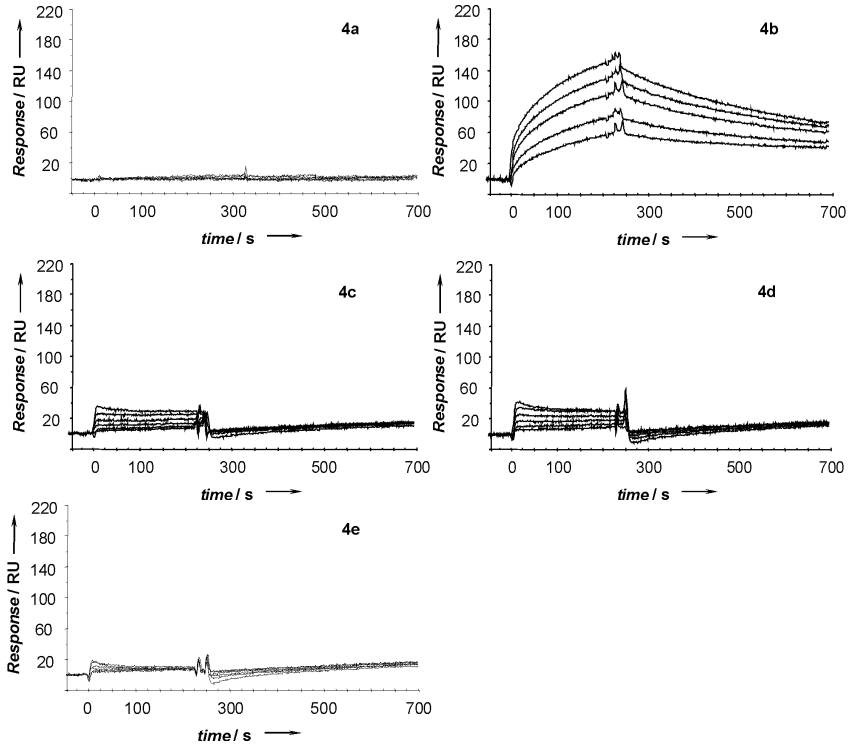


**Figure 4:** Sensorgrams of lactose variants with different aglycon structures. All binding curves have been corrected for nonspecific binding ($RCA_{120}$-$RCA_{120}$*). a) Free lactose. b) Compound **2**. c) Compound **11**. d) Compound **9**. e) Compound **12**. Concentrations: 40–1.25 μM (top to bottom).

As would be expected, the platinum-free compounds presented low signals that increased linearly according to their molecular masses. In the chosen concentration range the RU values are close to zero for free lactose (MW=342), 2-7 RU for **12** (MW=563), and 5-40 RU for **11** and **9** (MW=711/713 and 755/757, respectively). Hence, it appears that the response shown by **2** (60 – 160 RU) cannot be explained simply by the increase in molecular mass of **2** (MW=906/908). This observation is further supported by comparison

of the SPR responses (at 1 μM concentration) of PtCl(NCN-R)-labeled galactose **3** and Br(NCN-R)-labeled lactose **9**, possessing close molecular masses (MW=745 *vs* 755/757), but differing in the presence or absence of the platinum atom. Even though lactose has a higher affinity for $RCA_{120}$ than galactose[40], the lack of the platinum atom in **9** causes a significant drop in RU relative to **3** (Figure 5).

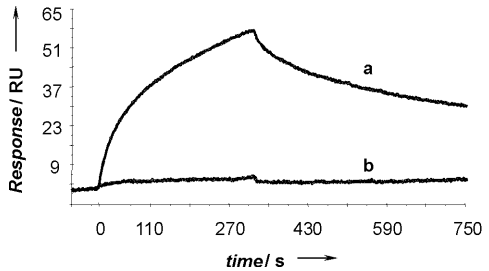


**Figure 5:** Relative response (RU) versus time for the binding responses of: a) PtCl(NCN-R)-labeled galactose **3** (MW=745) and b) Br(NCN-R)-labeled lactose **9** (MW=755/757) flowing across immobilized $RCA_{120}$ at 1μM concentration.

A curve relating the RU values at 26 μM concentration for lactose, **2, 9, 11**, and **12** with their respective molecular masses (Figure 6) reveals that the PtCl(NCN-R)-labeled lactose **2** and the PtCl(NCN-R)-labeled galactose **3** not only deviate from the linear trend presented by **9**, **11**, and **12**, but also give responses corresponding to higher-molecular-mass compounds.

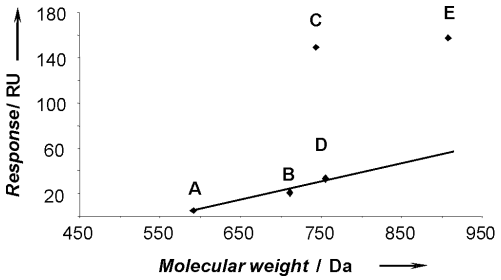


**Figure 6**: Molecular mass versus SPR response at 26 μM concentration for: A) compound **12**, B) compound **11**, C) compound **3**, D) compound **9**, and E) compound **2**.

*Evaluation of the reference surface*

To investigate whether denatured lectins could be considered suitable reference surfaces, compound **2** was allowed to flow across $RCA_{120}$, denatured $RCA_{120}$, ConA, and denatured ConA for 50 min at 8 μM concentration. Inspection of the sensorgrams

presented in Figure 7 reveals that the SPR response on active $RCA_{120}$ during the first 5 min of association differed significantly from those observed on denatured $RCA_{120}$, ConA, and denatured ConA, due to specific binding on this surface. With prolonged injection times, similar linear increases are observed for all the four curves, suggesting nonspecific binding of **2** on each of the sensorchip surfaces. Since both active and denatured surface present the same trend, subtraction of reference channels from the active lectin surface could be usable to correct for nonspecific binding, refractive index changes and detector drift. The contribution of these phenomena to the measured SPR response could be further minimized by use of low analyte concentrations (0.5-20 μM) and short injection times (3-5 min).

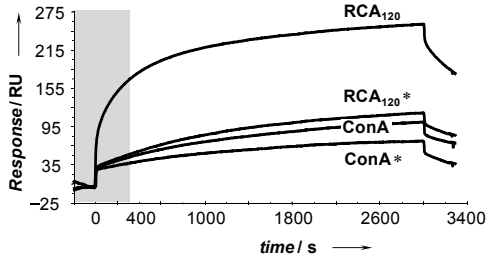


**Figure 7:** Sensorgrams of PtCl(NCN-R)-labeled lactose **2** (8 μM) flowing across $RCA_{120}$, denatured $RCA_{120}$*, Con A, and denatured Con A*. Injection time: 50 min. The shaded part indicates the injection time usually considered in Biacore analysis

**Discussion and Conclusions**

SPR is an optical phenomenon that is generated at a noble metal-coated interface (a 10 nm gold film in Biacore biosensors) between two media of different refractive index (RI), by a beam of monochromatic, plane-polarized light. Under conditions of total internal reflection, an evanescent wave will penetrate into the medium of lower RI, causing free electrons in the metal layer to oscillate, resulting in the generation of the so-called surface plasmon waves. These plasmons can be resonantly excited only at a well-defined angle of incidence, and can be monitored in the reflected light since a reduction in its intensity occurs at that angle. The SPR of the system is very sensitive to variations in the refractive index of the media adjacent to the metal layer. For a given number of ligand sites, the response increases linearly with the mass bound to the sensor surface, as the RI changes are stronger for high-molecular-mass analytes[41].

Oligosaccharides binding to immobilized proteins are not easily detected, due to their low molecular masses and weak binding affinities, so labeling procedures are often required.

In this study it has been shown that attachment of an organoplatinum(II)-containing aglycon of the PtCl(NCN-R) type to a saccharide produces a strong SPR signal enhancement, allowing binding studies of low-molecular-mass saccharides to lectins at very low analyte concentration: monosaccharide analytes containing such an aglycon give rise to intense SPR signals even at 1.25 μM concentration. The PtCl(NCN-R)-labeled saccharides are completely water-soluble, do not aggregate in the buffer solutions conventionally used in SPR experiments, and can be stored for long periods. Competition experiments between free saccharides and their organoplatinum(II)-containing analogues have demonstrated that the labeling does not affect the specificity of the biomolecular interaction. In addition, the binding experiments with organoplatinum(II)-labeled glucose and mannose over the Con A surface show that the relative affinity order of unlabeled glucose and mannose is preserved. The presence of a shorter spacer than the 3-(amidoethylthio)propyl spacer between saccharide and organoplatinum(II) complex gave the same lectin binding profile. This demonstrates that although the organoplatinum(II) complex is in close proximity to the binding site of the lectin, it does not influence the binding of the analyte to it.

Since this signal-enhancing property cannot be explained simply in terms of the molecular mass increase of the carbohydrate, a possible explanation has to be inferred from the SPR phenomenon itself. The observation that the platinum atom is essential for conferring signal-enhancing properties to the aromatic aglycon, raises the possibility that the nobel metal atom may cause more complex effects than simply inducing bulk changes in the RI close to the gold layer[42]. Introductory experiments, performed in our group, with compounds in which the Pt atom is replaced by a Pd atom have shown the same signal-enhancing effect (data not shown). A significant interaction between the platinum electrons and the evanescent wave produced in the proximity of the sensorchip surface is believed to be responsible for the observed phenomenon.

The inaccuracy involved in relating the response of PtCl(NCN-R)-labeled saccharides directly to their molecular masses may cause overestimation of calculated thermodynamical parameters, such as their affinity constants toward lectins. Exploratory kinetic binding studies indicate that, as a consequence of the signal enhancement, values

calculated for the PtCl(NCN-R)-labeled lactose/$RCA_{120}$ interaction ($K_D$ = 2 μM) are between 10 to 30 times higher than values previously determined for the lactose/$RCA_{120}$ interaction by isothermal titration calorimetry[40] or equilibrium dialysis calculation[43,44]. Discrepancies in $K_D$ values can also be observed between the PtCl(NCN-R)-labeled mannose/ConA affinity measured by SPR ($K_D$ = 0.6 μM) and values obtained from titration microcalorimetry[45], fluorescence anisotropy[45] and SPR[19,46] for the methyl α-D-mannopyranoside/ConA interaction. In addition, careful inspection of the SPR sensorgrams of organoplatinum(II)-labeled lactose and unlabeled lactose derivatives (e.g., **9** or **11**) shows that both the association with and dissociation from the lectin are slower for the organoplatinum(II)-labeled compound. The discussed limitations associated with the use of the organoplatinum(II) label make quantitative SPR binding studies unfeasible.

To conclude, labeling low-molecular-mass saccharides with the PtCl(NCN-R) aglycon ensures high SPR responses. The organoplatinum(II) complex is therefore an excellent label for the qualitative detection of binding events taking place on the gold surface of the biosensor. Although the signal enhancement causes overestimation of the calculated affinities, specificity and affinity ranking between compounds are preserved. Therefore, relative values, more than absolute ones, can furnish a clear picture of the different affinities of labeled oligosaccharides for the tested proteins. We envision that this labeling procedure could be applicable to establishing the carbohydrate-binding specificity of unknown lectins with biosensors, a method traditionally hampered by the low availability of high-molecular-mass oligosaccharides. More generally, qualitative binding studies of synthetic or isolated small molecules to receptors, and their relative affinity ranking, by organoplatinum(II) labeling of analytes has become a possibility. SPR screening of organoplatinum(II)-labeled plant/animal extracts or chemical libraries (e.g., peptide, carbohydrate, DNA, or heterocycles) allows the identification of biologically active lead compounds, a process of immense importance in pharmaceutical research.

**Acknowledgements**

This research was supported through a European Community Marie Curie Training Site Grant (HPMT-CT-2000-00045) for D.B. The financial support of the Academic Biomedical Center, Utrecht University (Expertise Center for Carbohydrate Analysis and Synthesis) is gratefully acknowledged (J.P.K. and K.M.H.).

**References**

[1] Rich RL, Myszka DG. Advances in surface plasmon resonance biosensor analysis. *Curr. Opin. Biotechnol*. **2000**, *11*, 54-61.

[2] Green RJ, Frazier RA, Shakesheff KM, Davies MC, Roberts CJ, Tendler SJB. Surface plasmon resonance analysis of dynamic biological interactions with biomaterials. *Biomaterials* **2000**, *21*, 1823-1835.

[3] Rich RL, Myszka DG. Survey of the 1999 surface plasmon resonance biosensor literature. *J. Mol. Recognit*. **2000**, *13*, 388-407.

[4] Rich RL, Myszka DG. Survey of the year 2000 commercial optical biosensor literature. *J. Mol. Recognit.* **2001**, *14*, 273-294.

[5] Rich RL, Myszka DG. Survey of the year 2001 commercial optical biosensor literature. *J. Mol. Recognit.* **2002**, *15*, 352-376.

[6] Rich RL, Myszka DG. A survey of the year 2002 commercial optical biosensor literature. *J. Mol. Recognit.* **2003**, *16*, 351-382.

[7] Stenberg E, Persson B, Roos H, Urbaniczky C. Quantitative determination of surface concentration of protein with surface plasmon resonance using radiolabeled proteins. *J. Colloid Interface Sci*. **1991**, *143*, 513-526.

[8] Shinohara Y, Kim F, Shimizu M, Goto M, Tosu M, Hasegawa Y. Kinetic measurement of the interaction between an oligosaccharide and lectins by a biosensor based on surface plasmon resonance. *Eur. J. Biochem*. **1994**, *223*, 189-194.

[9] Hutchinson AM. Characterization of glycoprotein oligosaccharides using surface plasmon resonance. *Anal. Biochem.* **1994**, *220*, 303-307.

[10] Yamamoto K, Ishida C, Shinohara Y, Hasegawa Y, Konami Y, Osawa T, Irimura T. Interaction of immobilized recombinant mouse C-type macrophage lectin with glycopeptides and oligosaccharides. *Biochemistry* **1994**, *33*, 8159-8166.

[11] Adler P, Wood SJ, Lee YC, Lee RT, Petri WA Jr, Schnaar RL. High affinity binding of the Entamoeba histolytica lectin to polyvalent N-acetylgalactosaminides. *J. Biol. Chem.* **1995**, *270*, 5164-5171.

[12] Holmskov U, Fischer PB, Rothmann A, Højrup P. Affinity and kinetic analysis of the bovine plasma C-type lectin collectin-43 (CL-43) interacting with mannan. *FEBS Lett.* **1996**, *393*, 314-316.

[13] Blikstad I, Fägerstam LG, Bhikhabhai R, Lindblom H. Detection and characterization of oligosaccharides in column effluents using surface plasmon resonance. *Anal. Biochem.* **1996**, *233*, 42-49.

[14] Haseley SR, Talaga P, Kamerling JP, Vliegenthart JFG. Characterization of the carbohydrate binding specificity and kinetic parameters of lectins by using surface plasmon resonance. *Anal. Biochem.* **1999**, *274*, 203-210.

[15] Haselhorst T, Weimar T, Peters T. Molecular recognition of sialyl Lewis(x) and related saccharides by two lectins. *J. Am. Chem. Soc.* **2001**, *123*, 10705-10714.

[16] Goto S, Masuda K, Miura M, Kanazawa K, Sasaki M, Masui M, Shiramizu M, Terada H, Chuman H. Quantitative estimation of interaction between carbohydrates and concanavalin A by surface plasmon resonance biosensor. *Chem. Pharm. Bull*. **2002**, *50*, 445-449.

[17] Ideo H, Seko A, Ohkura T, Matta KL, Yamashita K. High-affinity binding of recombinant human galectin-4 to $SO_3^- \rightarrow$3Galß1$\rightarrow$3GalNAc pyranoside. *Glycobiology* **2002**, *12*, 199-208.

[18] Haseley SR, Kamerling JP, Vliegenthart JFG. Unravelling carbohydrate interactions with biosensors using surface plasmon resonance (SPR) detection. *Topics Curr. Chem.* **2002**, *218*, 93-114.

[19] Smith EA, Thomas WD, Kiessling LL, Corn RM. Surface plasmon resonance imaging studies of protein-carbohydrate interactions. *J. Am. Chem. Soc*. **2003**, *125*, 6140-6148.

[20] Gutiérrez Gallego R, Haseley SR, van Miegem VFL, Vliegenthart JFG, Kamerling JP. Identification of carbohydrates binding to lectins by using surface plasmon resonance in combination with HPLC profiling**.** *Glycobiology* **2004**, *14*, 373-386.

[21] Varki A. Biological roles of oligosaccharides: all of the theories are correct. *Glycobiology* **1993**, *3*, 97-130.

[22] Dwek RA. Glycobiology: toward understanding the function of sugars. *Chem. Rev.* **1996**, *96*, 683-720.

[23] Jungar C, Mandenius C-F. Neoglycoconjugates as affinity ligands in surface plasmon resonance analysis. *Anal. Chim. Acta* **2001**, *449*, 51-58.

[24] Hasegawa Y, Shinohara Y, Sota H. Structure analysis of saccharides using a biosensor based on molecular recognition. *Trends Glycosci. Glycotechnol.* **1997**, *9*, S15-S24.

[25] Zeng X, Nakaaki Y, Murata T, Usui T. Chemoenzymatic synthesis of glycopolypeptides carrying α-Neu5Ac-(2→3)-β-D-Gal-(1→3)-α-D-GalNAc, β-D-Gal-(1→3)-α-D-GalNAc, and related compounds and analysis of their specific interactions with lectins. Arch. Biochem. Biophys. 2000, 383, 28-37.

[26] Frison N, Marceau P, Roche A-C, Monsigny M, Mayer R. Oligolysine-based saccharide clusters: synthesis and specificity. *Biochem. J.* **2002**, *368*, 111-119.

[27] Hernáiz MJ, de la Fuente JM, Barrientos AG, Penadés S. A model system mimicking glycosphingolipid clusters to quantify carbohydrate self-interactions by surface plasmon resonance. *Angew. Chem. Int. Ed*. **2002**, *41*, 1554-1557.

[28] Malmqvist M. BIACORE: an affinity biosensor system for characterization of biomolecular interactions. *Biochem. Soc. Trans.* **1999**, *27*, 335-340.

[29] Duverger E, Frison N, Roche A-C, Monsigny M. Carbohydrate-lectin interactions assessed by surface plasmon resonance. *Biochimie* **2003**, *85*, 167-179.

[30] Ohlson S, Strandh M, Nilshans H. Detection and characterization of weak affinity antibody antigen recognition with biomolecular interaction analysis. *J. Mol. Recognit.* **1997**, *10*, 135-138.

[31] Strandh M, Persson B, Roos H, Ohlson S. Studies of interactions with weak affinities and low-molecular-weight compounds using surface plasmon resonance technology. *J. Mol. Recognit.* **1998**, *11*, 188-190.

[32] Jungar C, Strandh M, Ohlson S, Mandenius C-F. Analysis of carbohydrates using liquid chromatography--surface plasmon resonance immunosensing systems. *Anal. Biochem.* **2000**, *281*, 151-158.

[33] Weimar T, Haase B, Köhli T**.** Low affinity carbohydrate lectin interactions examined with surface plasmon resonance. *J. Carbohydr. Chem.* **2000**, *19*, 1083-1089.

[34] Larsson A, Ohlsson J, Dodson KW, Hultgren SJ, Nilsson U, Kihlberg J. Quantitative studies of the binding of the class II PapG adhesin from uropathogenic *Escherichia coli* to oligosaccharides. *Bioorg. Med. Chem.* **2003**, *11*, 2255-2261.

[35] Suijkerbuijk BMJM, Slagt MQ, Klein Gebbink RJM, Lutz M, Spek AL, van Koten G. Platinum-pincer introduction using active ester chemistry. *Tetrahedron Lett*. **2002**, *43*, 6565-6568.

[36] Albrecht M, Rodríguez G, Schoenmaker J, van Koten G. New peptide labels containing covalently bonded platinum(II) centers as diagnostic biomarkers and biosensors. *Org. Lett.* **2000**, *2*, 3461-3464.

[37] Slagt MQ, Klein Gebbink RJM, Lutz M, Spek AL, van Koten G. Synthetic strategies towards new *para*-functionalised NCN-pincer palladium(II) and platinum(II) complexes. *J. Chem. Soc., Dalton Trans.* **2002**, *13*, 2591-2592.

[38] Likhosherstov LM, Novikova OS, Derevitskaya VA, Kochetkov NK. A new simple synthesis of amino sugar β-D-glycosylamines. *Carbohydr. Res*. **1986**, *146*, C1-C5.

[39] Albrecht M, van Koten G. Platinum group organometallics based on "pincer" complexes: sensors, switches, and catalysts. *Angew. Chem. Int. Ed*. **2001**, *40*, 3750-3781.

[40] Sharma S, Bharadwaj S, Surolia A, Podder SM. Evaluation of the stoichiometry and energetics of carbohydrate binding to *Ricinus communis* agglutinin: a calorimetric study. *Biochem. J.* **1998**, *333*, 539-542.

[41] Schuck P. Use of surface plasmon resonance to probe the equilibrium and dynamic aspects of interactions between biological macromolecules. *Annu. Rev. Biophys. Biomol. Struct.* **1997**, *26*, 541-566.

[42] Kaplan H. Effect of an impurity layer on surface waves**.** *Phys. Rev.* **1962**, *125*, 1271-1276.

[43] Olsnes S, Saltvedt E, Phil A. Isolation and comparison of galactose-binding lectins from *Abrus precatorius* and *Ricinus communis*. *J. Biol. Chem.* **1974**, *249*, 803-810.

[44] Zentz C, Frénoy JP, Bourrillon R. Binding of galactose and lactose to ricin. Equilibrium studies. *Biochim. Biophys. Acta* **1978***, 536,* 18-26.

[45] Weatherman RV, Mortell KH, Chervenak M, Kiessling LL, Toone EJ. Specificity of *C*-glycoside complexation by mannose/glucose specific lectins. *Biochemistry* **1996**, *35*, 3619-3624.

[46] Mann DA, Kanai M, Maly DJ, Kiessling LL. Probing low affinity and multivalent interactions with surface plasmon resonance: Ligands for Concanavalin A**.** *J. Am. Chem. Soc.* **1998**, *120*, 10575-10582.

## Summary

Carbohydrate chains play key roles in living organisms. They are involved in a variety of events such as inflammation, cell-cell recognition, immunological response, fertilization, signal transduction, and protein folding. In biological systems they are present as free saccharides, or as covalently bound entities of glycoconjugates (glycoproteins, glycosaminoglycans, glycolipids, and glycosylphosphatidylinositol anchors). Carbohydrate chains can modify the intrinsic properties of proteins to which they are attached to, for instance, by altering the stability, protease resistance, or quaternary structure. It has been observed that in the same glycoprotein identical types of glycan structures can be responsible for different effects, but also that different glycans can exert similar functions. This finding demonstrates that structure and local molecular environment are decisive factors in determining the functional behavior of glycans.

Novel techniques have been developed in recent years to investigate the structure/function of carbohydrates. 2D nuclear magnetic resonance (NMR) and molecular dynamics (MD) simulation in conjunction with NMR refinement, as well as surface plasmon resonance (SPR), have been employed in this thesis to map structures and biological functions of glycans.

**Chapter 1** gives an overview of the concept of prebiotics, probiotics and synbiotics, with particular emphasis on carbohydrates as possible prebiotics. The present state of knowledge of the physiological effects of pre- and probiotics on the intestinal microflora is described, as well as their possible applications to specific health problems. Significant results obtained in recent clinical studies are also reported.

In **Chapter 2** the studies carried out in the framework of the European Union project "Novel Food Additives and bio-active components from milk for innovative engineering (NOFA)" are reported. To overcome the major bottleneck of obtaining naturally occurring oligosaccharides in sufficient amounts to perform structural characterization and biological testing, an improved protocol to isolate large quantities of lactose-free oligosaccharide fractions from non-human milk was developed. Major components from goat colostrum were isolated and structurally characterized by high-pH anion-exchange chromatography, MALDI-TOF mass spectrometry, and NMR spectroscopy. Bacterial adhesion studies with isolated acidic oligosaccharide fractions showed a significant

inhibition of the adherence of faecal *Salmonella fyris* B8132 to cultured intestinal epithelial cells. However, for faecal *Escherichia coli* 0119 no detectable inhibitory effect was found.

Since oligosaccharides present in human milk have proved to be beneficial for human health by promoting the growth of bifidobacteria and lactobacilli in the large intestine and preventing adhesion of pathogenic agents to intestinal epithelial cells, one of the main goals of the NOFA project was to enrich milk isolates with selected oligosaccharides, considered as prebiotics. As demonstrated in Chapter 2, naturally occurring galacto-oligosaccharides can be isolated in large amounts from skimmed goat milk (or colostrum) oligosaccharide pools, when incorporating a β-galactosidase (*E. coli*) digestion in the isolation protocol. Analysis of the generated oligosaccharides and control of the process are important in the development of applications of enzymatic lactose hydrolysis on a technical scale.

In **Chapter 3** the isolation of tri- and tetrasaccharides from goat milk after enzymatic lactose hydrolysis with *E. coli* β-galactosidase, and their structural analysis by methylation analysis, mass spectrometry, and NMR spectroscopy, is described.

After analyzing the structure and function of free oligosaccharides, in **Chapter 4** our research was focused on covalently bound oligosaccharides. In an attempt to understand the biological significance of a recently discovered form of glycosylation, *i.e. C*-mannosylation, the conformation of Man1α-Trp in human RNase 2 was investigated. NMR experiments and molecular modeling calculations for ($C^2$-α-D-Man-)Trp demonstrated that the *C*-linked mannopyranosyl residue exists in an ensemble of conformations, among which $^1C_4$ is the most represented. For isolated glycopeptides, NMR showed no evidence for long-range connectivities and secondary structure, arguing against a stabilization of the analyzed glycopeptides, due to the *C*-linked mannopyranosyl residue. For native RNase 2, molecular modeling studies and NMR data revealed that the mannopyranosyl residue interacts with the loop residues Asp115-123 of RNase 2, the end of the β strands Met105-Arg114 and the beginning of the β strands Pro124-Ile134. These interactions stabilize not only to the mannose residue and Trp7 in a specific orientation, but also the N-terminal loop of the protein.

**Chapter 5** focuses on the feasibility of the emerging technique surface plasmon resonance (SPR) to detect oligosaccharide-protein interactions. Introduced in the early

1990s, biosensors based on SPR have become a well-established tool for studying biomolecular interactions in real time. Nevertheless, a serious constraint imposed by this technique concerns the dimension of the molecules to be employed as analytes. To this end we developed an organoplatinum(II) label to increase the SPR response of low-molecular-mass analytes. Hence, we demonstrated to be able to detect binding events between monosaccharides and lectins even at very low analyte concentrations. The organoplatinum(II) complex did not influence the interaction, and platinum(II) was shown to be essential for the SPR signal enhancement.

## Samenvatting

Koolhydraatketens (glycanen) spelen een belangrijke rol in levende organismen. Ze zijn betrokken bij vele biologische processen zoals ontstekingen, cel - cel herkenning, immunologische reacties, bevruchting, signaaltransductie en eiwitvouwing. In biologische systemen komen ze voor als vrije suikers, of als covalent gebonden eenheden van glycoconjugaten: glycanen (glycoproteïnen, glycosaminoglycanen, glycolipiden, glycosylphosphatidylinositol ankers). Glycanen kunnen de eigenschappen van eiwitten waaraan ze zijn gebonden veranderen, bijvoorbeeld door het wijzigen van de stabiliteit, de resistentie tegen proteases of de quaternaire structuur. Er is aangetoond dat in één glycoproteïne dezelfde glycaanstructuren verantwoordelijk kunnen zijn voor verschillende effecten, maar ook dat verschillende glycanen dezelfde functies kunnen uitoefenen. Deze bevindingen tonen aan dat structuur en lokale moleculaire omgeving bepalende factoren zijn voor de functie van glycanen. In de afgelopen jaren zijn er nieuwe technieken ontwikkeld om de structuur en functie van glycanen te onderzoeken. 2D Nuclear magnetic resonance (NMR) spectroscopie en moleculaire dynamica (MD) simulaties in combinatie met NMR, als mede surface plasmon resonance (SPR) zijn gebruikt in dit proefschrift om structuren en biologische functies van glycanen in kaart te brengen.

**Hoofdstuk 1** geeft een overzicht van het concept van prebiotica, probiotica en synbiotica, met de nadruk op koolhydraten als mogelijke prebiotica. De huidige kennis van de fysiologische effecten van pre- en probiotica op de darmflora is beschreven, en de mogelijke toepassingen op het gebied van bepaalde gezondheidsaandoeningen. Ook staan de resultaten van recente klinische studies hierin vermeld.

In **Hoofdstuk 2** staan de studies beschreven die zijn uitgevoerd in het kader van het EU project “Novel Food Additives and bio-active components from milk for innovative engineering (NOFA)”. In deze studies is gewerkt aan het verkrijgen van voldoende grote hoeveelheden natuurlijke oligosachariden die nodig zijn voor structuuropheldering en biologische testen. Een verbeterd protocol is ontwikkeld om grote hoeveelheden lactose-vrije oligosachariden te isoleren uit niet-humane melk. Belangrijke oligosachariden van geiten colostrum werden geïsoleerd en gekarakteriseerd met anionenwisselingschromatografie, MALDI-TOF massaspectrometrie en NMR spectroscopie. Studies naar hechting van bacteriën aan geïsoleerde zure oligosachariden

toonden een significante inhibitie van hechting van feces *Salmonella fyris* B8132 aan gekweekte darmepitheelcellen. Voor feces *Escherichia coli* 0119 werd echter geen remmend effect waargenomen.

Aangezien oligosachariden in humane melk bevorderend zijn voor de gezondheid doordat ze de groei van bifidobacteriën en lactobacillen in de dikke darm stimuleren en pathogene substanties beletten aan de epitheelcellen van de darm te hechten, is één van de belangrijkste doelen van het NOFA project geweest de melk te verrijken met geselecteerde oligosachariden, die worden beschouwd als prebiotica. Zoals beschreven in Hoofdstuk 2, kunnen natuurlijke galacto-sachariden in grote hoeveelheden worden geïsoleerd uit magere geitenmelk (of colostrum), wanneer er een β-galactosidase (*E. coli*) digestie wordt uitgevoerd in het protocol. Analyse van de gegenereerde oligosachariden en de controle van het proces zijn belangrijk in de opschaling van enzymatische lactose hydrolyse naar productieniveau.

In **Hoofdstuk 3** wordt de isolatie van tri- en tetrasachariden uit geitenmelk na een enzymatische lactose hydrolyse met *E. coli* β-galactosidase beschreven. De structuuranalyse van deze sachariden werd uitgevoerd door middel van methyleringsanalyse, massaspectrometrie en NMR spectroscopie.

Na het analyseren van structuren en functies van ongebonden sachariden, lag de nadruk van het onderzoek in **Hoofdstuk 4** op sachariden die covalent gebonden zijn. In een poging de wetenschappelijke relevantie te verklaren van een recent aangetoonde vorm van glycosylering, namelijk *C*-mannosylering, werd de conformatie van Man1α-Trp in humaan RNase 2 nader onderzocht. NMR experimenten en moleculaire berekeningen aan ($C^2$-α-D-Man-)Trp hebben aangetoond dat het C-gebonden mannopyranosyl residu in een ensemble van confirmaties aanwezig is, waarin de $^1C_4$ conformatie dominant is. Voor geïsoleerde glycopeptiden hebben NMR studies geen bewijs geleverd voor het bestaan van interacties tussen mannose en de peptide keten op grote afstand van de plaats van glycosylering noch voor secundaire structuren. Dit suggereert dat er geen stabilisatie in de ruimtelijke structuur van de geanalyseerde glycopeptiden plaatsvindt door de aanwezigheid van C-gebonden mannopyranosyl residuen. Voor natief RNase 2 hebben moleculaire modelling studies en NMR data aangetoond dat het mannopyranosyl residu een wisselwerking aangaat met de lus residuen Asp115-123, het einde van de β strengen Met105-Arg114 en het begin van de β strengen Pro124-Ile134. Deze wisselwerkingen

zorgen niet alleen voor de stabilisatie van het mannose residu en Trp7 in een bepaalde oriëntatie, maar ook voor de N-terminale lus van het eiwit.

De focus van **Hoofdstuk 5** ligt op het onderzoeken van de mogelijkheden van surface plasmon resonance (SPR) voor de detectie van interacties tussen oligosachariden en eiwitten. Na hun introductie in het begin van de jaren 90, hebben biosensoren gebaseerd op SPR hun toepassing gevonden in het bestuderen van real-time biomoleculaire interacties. Een belangrijke beperking van deze techniek heeft betrekking op de moleculaire massa's van de te analyseren ligande moleculen. Vastgesteld kon worden dat aanhechting van een organoplatinum(II) label de SPR respons van een laag-moleculair koolhydraat ligande aanzienlijk vergroot. Deze techniek maakt het mogelijk monosacharide-lectine interacties bij lage concentraties monosacharaide aan te tonen. Het organoplatinum(II) complex had geen invloed op de interactie en voor platinum(II) is aangetoond dat deze essentieel is voor het vergroten van het SPR signaal.

## Sommario

I carboidrati giocano un ruolo essenziale nella vita degli organismi viventi, essendo coinvolti in svariati fenomeni quali infiammazione, riconoscimento cellulare, risposta immunologica, fertilizzazione, traduzione dei segnali, folding di proteine. Nei sistemi biologici i carboidrati possono essere presenti come zuccheri liberi oppure quali entitá covalentemente legate, come nel caso dei glicoconiugati (glicoproteine, glicosamminoglicani, glicolipidi, ancore glicosil-fosfatidil-inositolo). I carboidrati possono alterare le proprietá intrinseche delle proteine a cui sono legati modificandone la stabilitá, la resistenza alle proteasi, la struttura quaternaria. E' stato dimostrato che la medesima struttura glicosidica puó esercitare effetti diversi nella stessa glicoproteina, ma anche che glicani diversi possono essere responsabili per la stessa funzione. Questa scoperta dimostra chiaramente che sia la struttura che l'ambiente molecolare sono fattori fondamentali nel determinare il comportamento funzionale dei glicani.

Lo studio della struttura/funzione dei carboidrati si avvale oggi di tecnologie recentemente sviluppate, quali surface plasmon resonance (SPR), simulazioni di dinamica molecolare (MD) supportate da dati NMR, risonanza magnetica nucleare bidimensionale (NMR). Le tecniche summenzionate sono state impiegate in questa tesi allo scopo di determinare la struttura e la funzione biologica dei carboidrati.

Il **Capitolo 1** presenta una panoramica sul concetto di prebiotici, probiotici e simbiotici, con particolare interesse per i carboidrati quali possibili prebiotici. Vengono descritte le conoscenze attuali degli effetti fisiologici dei pre- e probiotici sulla microflora intestinale e le loro possibili applicazioni nella cura di specifici disturbi. Sono riportati inoltre alcuni tra i risultati piú significativi ottenuti nei recenti studi clinici.

Nel **Capitolo 2** descrive la ricerca eseguita nel contesto del progetto della Comunitá Europea: "Novel Food Additives and bio-active components from milk for innovative engineering (NOFA)". Per superare l'ostacolo di purificare gli oligosaccaridi naturalmente presenti nel latte animale in quantitá sufficienti per poter effettuare caratterizzazioni strutturali e test biologici, e' stato messo a punto un protocollo che permette di isolare grosse quantitá di frazioni oligosaccaridiche prive di lattosio. I componenti principali del colostro caprino sono stati cosi' isolati e caratterizzati strutturalmente tramite high-pH anion-exchange chromatography, spettrometria di massa MALDI-TOF, spettroscopia

NMR. Le frazioni di oligosaccaridiche acide isolate sono state impiegate in studi di adesione batterica verso cellule intestinali epiteliali coltivate. E' stata dimostrata un'inibizione significativa dell'aderenza di *Salmonella fyris* B8132 fecale ad opera di oligosaccaridi acidi, mentre nessun effetto inibitorio quantificabile e' stato osservato nel caso di *Escherichia coli* 0119 fecale.

Dato il positivo effetto dimostrato dagli oligosaccaridi presenti nel latte umano nel promuovere la crescita di bifidobatteri e lattobacilli nell'intestino crasso e nel prevenire l'adesione di agenti patogeni alle cellule intestinali, uno degli scopi pricipali del progetto NOFA consisteva nell'arricchire le fomulazioni lattee con oligosaccaridi selezionati, considerati come probiotici. Come dimostrato nel Capitolo 2, i galatto-oligosaccaridi naturali possono essere ottenuti in grandi quantitá da miscele di oligosaccaridi da latte (o colostro) caprino scremato introducendo una digestione enzimatica ad opera di β-galattosidasi nel protocollo di isolamento. L'analisi degli oligosaccaridi generati e un attento controllo di processo sono importanti nello sviluppo delle applicazioni dell'idrolisi enzimatica del lattosio su larga scala.

Nel **Capitolo 3** viene descritto l'isolamento di tri- e tetrasaccaridi da latte caprino dopo l'idrolisi enzimatica del lattosio ad opera di *E. coli* β-galattosidasi. Le strutture ottenute sono caratterizzate via methylation analysis, spettrometria di massa, spettroscopia NMR.

Dopo aver analizzato la struttura e la funzione degli oligosaccaridi liberi, il **Capitolo 4** verte su oligosaccaridi covalentemente legati. Nel tentativo di comprendere il significato biologico di una forma di glicosilazione recentemente scoperta, la *C*-mannosilazione, la conformazione del Man1α-Trp nella RNase 2 umana é stata analizzata. Esperimenti NMR e calcoli di modellistica molecolare per ($C^2$-α-D-Man-)Trp dimostrano che il residuo *C*-mannopiranosidico esiste in un insieme di conformazioni, tre le quali la $^1C_4$ é la maggiormente rappresentata. Nel caso di glicopeptidi isolati, studi NMR non hanno mostrato l'esistenza di connettivitá a lungo raggio o di strutture secondarie, negando la stabilizzazione dei glicopeptidi analizzati ad opera del residuo *C*-mannopiranosidico. Per l'RNase nativa, studi di NMR e modellistica molecolare hanno rivelato che il residuo mannopiranosio interagisce con i residui Asp115-123 del loop dell'RNase 2, con la parte terminale del β strands Met105-Arg114 e con la parte iniziale del β strand Pro124-Ile134.

Queste interazioni stabilizzano non solo il residuo mannosidico e il Trp7 in un'orientazione specifica, ma anche il loop N-terminale della proteina.

Il **Capitolo 5** investiga la possibilitá di utizzare una tecnica recentemente sviluppata, la surface plasmon resonance (SPR), per analizzare le interazioni tra proteine e oligosaccaridi. Introdotti nei primi anni 90, i biosensori basati sull'SPR sono diventati uno strumento affermato per studiare le interazioni biologiche in tempo reale. Tuttavia, una seria limitazione imposta da questa tecnica consiste nelle dimensioni delle molecole da impiegare come analiti. A questo scopo e' stato sviluppato un marker con organoplatino(II) che permette di aumentare il segnale SPR degli analiti a basso peso molecolare. Viene dimostrato come sia possibile monitorare eventi di legame tra lettine e monosaccaridi, anche a concentrazioni molto basse di analita. Il complesso organoplatino(II) non influenza l'interazione biologica e l'atomo di platino risulta essenziale per ottenere un significativo aumento del segnale.

## Curriculum Vitae

Daniela Beccati was born on November 5th 1971, in Milan, Italy. She graduated in organic chemistry in 1997 from Universita' Statale di Milano, with a thesis on "Cathodic reduction of halogenosugars: a novel approach to the synthesis of modified disaccharides".

In July 1997 she obtained a Research Scholarship at the Scientific Institute for Chemical and Biochemical Research 'G. Ronzoni' in Milan, where she worked in the framework of the European network project "NOFA, Novel food additives and bioactive components from milk for innovative engineering".

She joined the Department of Bio-Organic Chemistry (Bijvoet Center, Utrecht University) in 2001, where she performed her PhD under the supervision of Prof. Dr. J.P. Kamerling and Prof. Dr. J.F.G. Vliegenthart. She completed her thesis while working as assistant researcher at 'G. Ronzoni' Institute of Milan, where she focused on characterisation of glycosaminoglycans and polysaccharides by NMR.

She is currently employed as a scientist in the Analytics Research Department of Momenta Pharmaceuticals, Boston, US.

## Publication

Beccati D, Halkes KM, Batema GD, Guillena G, Carvalho de Souza A, van Koten G, Kamerling JP. SPR studies of carbohydrate-protein interactions: signal enhancement of low-molecular-mass analytes by organoplatinum(II)-labeling. *Chembiochem.* **2005**, *6*, 1196-1203.

Levy-Adam F, Abboud-Jarrous G, Guerrini M, Beccati D, Vlodavsky I, Ilan N. Identification and characterization of heparin/heparan sulfate binding domains of the endoglycosidase heparanase. *J. Biol. Chem.* **2005**, *280*, 20457-66.

Guerrini M, Guglieri S, Beccati D, Torri G, Viskov C, Mourier P. Conformational transitions induced in heparin octasaccharides by binding with antithrombin III. *Biochem. J.* **2006**, *399*, 191-198.

Guerrini M*, Beccati D*, Shriver Z*, Naggi A, Viswanathan K, Bisio A, Capila I, Lansing JC, Guglieri S, Fraser B, Al-Hakim A, Gunay NS, Zhang Z, Robinson L, Buhse L, Nasr M, Woodcock J, Langer R, Venkataraman G, Linhardt RJ, Casu B, Torri G, Sasisekharan R. Oversulfated chondroitin sulfate is a contaminant in heparin associated with adverse clinical events. *Nat. Biotechnol.* **2008**, *26*, 669-675.
(*These authors contributed equally to this work.)

Beccati D, Casset F, Leeflang BR, Hofsteenge J, Vliegenthart JFG. Conformation analysis of the *C*-linkage Man1α-Trp in human RNase 2. Manuscript in preparation.

**Acknowledgements**

I am deeply grateful to my promoters Prof. J.P. Kamerling and Prof. J.F.G. Vliegenthart for giving me the wonderful opportunity to study in the Bio-Organic Chemistry Department. I really admire your scientific knowledge and I have greatly appreciated your guidance throughout all these years. Thank you for your enthusiasm and patience, and for never giving up advising me, in spite of the distance.

Part of my thesis could not have been completed without the collaboration with Ronzoni Institute. I would like to heartily thank Prof. B. Casu for his precious guidance through the initial steps of my research, for the fruitful scientific discussions, for always believing in my work, for the all the help and warmth every time I went back to Italy.

Thank you to Dr. Torri and Dr. Naggi for giving me the great opportunity to work at the European Union project NOFA and to study abroad.

Also, I would like to express my gratitude to Prof. Coppa and Dr. Zampini for the fruitful collaboration and for welcoming me in their city and their labs.

Moreover, I would like to acknowledge Prof G. van Koten and his team of the Department of Metal-Mediated Synthesis for their research with the organoplatinum(II) complex.

I would like to thank all my colleagues from the BOC for the fantastic three years we spent together: Vincent, thank you for all your help and for trying all my culinary experiments; Philippe, thank you for the long evenings at the Polstillon for dealing with my obsessions for Italian coffee and shopping; Angela, I always remember your wonderful cooking and the crazy late nights out; Sean, when are we going to a Gothic party again? Veronique, I remember the fantastic time we had in Grenoble (I still have the pictures) and the Thursday nights in the city; Christian, I really enjoyed our daily coffee routine and the chats over an Italian espresso; Guus, thank you for the drinks at JP and for fixing my first flat tire (and thank you to Sean, Philippe, Vincent, Roberto…. for fixing all the many others!); Gerrit, thank you for your kindness and for understanding my Southern Europe spirit, Simon, thank you for your help with the Biacore; Hiromi, we had so much fun painting my bike; Kate, with you the term ‘miserable’ acquires new sense! Koen, sorry you had to listen to my complains about the Dutch weather and food; Adriana, I really admire your positive attitude; Lizette, thank you for letting me eat your seafood in Grenoble; Nick, thank you for all your funny crazy stories; JP, it was very interesting to

discuss with you about Dutch writers; Lisa, hope you are keeping up your rocker attitude; Justyna, it's a pity that you joined the BOC only when I was already leaving; Manon, thank you for driving me around to visit the Dutch castles; Emmy, thank you for not considering me "too old" to hung out with; Theodora, thank you for all the help with the documents for the thesis; Mayken, it was so nice to meet you in Utrecht again; Bas, thank you for teaching me NMR and for your help; Albert, I will never forget your kindness.

Thank you to the BOC volleyball team for welcoming me to be part of it - Bart, Marjie, Chantal, Claire, Sjiors, Eelco, Sean - I had a fantastic time!

A special thank goes to the colleagues of the NMR Department of Utrecht University: Simona, thank you for being there whenever I needed a friend; Roberto, I wish I could try again your exploded banana; Rainer, thank you so much for helping me setting up NMR experiments and for your friendship; Danny and Nico, you visited me in Milan - now I expect both of you in Boston! Cyril, thank you for inviting me to your great parties, Monique, thank you for never complaining about me chatting with Simona in Italian in your office; Mike, thank you for adopting us, Roberto's friend, as yours; Eugene, thank you for never letting me pay for my beer.

And thank you to all my friends who made me feel at home in Holland: Maria, your Nutella ice-cream is to die for! Wim, sharing frustrations has never been so fun; Roman, I would never have imagined Russian and Italian culture to be so close; Maki, do you still cook your Bolognese sauce? Yanet, your enthusiasm is contagious; Mitia, I hope your vampire phase is over; Julien, thank you for all the CDs; Jim, did you finally build the laser sword?

A great thank you to my friends back home: to Manuela, for her support throughout the years, and for organizing my holidays; Marta, for the laughs, the drinks and the Spanish slang; Luisa, for welcoming me in her family; Karen, for reminding me to never give up; Antonella, for being a friend rather than a boss; Marco, for all the teaching and friendship; Cesare, for the wonderful pictures and the aperitivi at Matricola; Sara, for always being willing to help me; Alessandra, for sharing confidences and drinks.

And finally, I am deeply grateful to my family, to my parents Paola and Antonio, and to my brother Lorenzo. Thank you for supporting me throughout all those years, always understanding, always willing to help, and always cheering me up in the difficult moments. None of this would have been possible without you!

**Notes**